SN130

ADDITIONAL SUPPORT FOR THE TDK / MABL

COMPUTER PROGRAM

FINAL REPORT

Contract NAS8-39048

P 100

19 March 1993

Authors:

G.R. Nickerson
S.S. Dunn

TABLE OF CONTENTS

LIST OF FIGURES

LIST OF TABLES

NOMENCLATURE

Alphanumeric:

c_i i th chemical species

H   total enthalpy

N   total number of chemical species

P   pressure

Pr   Prandtl number

r   distance from the nozzle center line

s   length along the boundary layer path

u   velocity along s

v   velocity normal to s

x   distance parallel to the nozzle center line

y   distance measured normal to s

Greek:

α mixing fraction; =0 for primary flow, =1 for secondary flow

δ boundary layer thickness

ε eddy viscosity

μ dynamic viscosity

ρ gas density

ω chemical species production/dissipation term

Subscripts:

$b\ell$ boundary layer

core   primary flow

e   boundary layer edge

gg   gas generator exhaust (secondary flow)

inj   injectant (secondary flow)

trans   transpired fluid (secondary flow)

T   turbulent

w   wall

Superscripts:

j   j=0 for planar symmetry and j-1 for axisymmetric

′   fluctuating with time

Abbreviations:

DROPMIX	computer code for injector performance prediction
MABL	Mass Addition Boundary Layer module of TDK
MABL-E	MABL with equilibrium chemistry
MABL-F	MABL with chemical compositions frozen at the stagnation value
MABL-K	MABL with finite rate chemical kinetics
P.D.E.	partial differential equations
PNS	Parabolized Navier Stokes
SCAP	Spray Combustion Analysis Program
SOW	Statement of Work
SSME	Space Shuttle Main Engine
STME	Space Transportation Main Engine
TDE	TDK with equilibrium chemistry
TDK	Two Dimensional nozzle analysis code with chemical kinetics
VIPER	Viscous Interaction Performance Evaluation Routine computer code

1.0 INTRODUCTION

An advanced version of the Two-Dimensional Kinetics (TDK)[1] computer program was developed under contract NAS8-36863 and released to the propulsion community in early 1989. Exposure of the code to this community indicated a need for improvements in certain areas.

In particular, the TDK code needed to be adapted to the special requirements imposed by the Space Transportation Main Engine (STME) development program. This engine utilizes injection of the gas generator exhaust into the primary nozzle by means of a set of slots. The subsequent mixing of this secondary stream with the primary stream with finite rate chemical reaction can have a major impact on the engine performance and the thermal protection of the nozzle wall. In attempting to calculate this reacting boundary layer problem, the Mass Addition Boundary Layer (MABL) module of TDK was found to be deficient in several respects. For example, when finite rate chemistry was used to determine gas properties, (MABL-K option) the program run times became excessive because extremely small step sizes were required to maintain numerical stability. A robust solution algorithm was required so that the MABL-K option could be viable as a rocket propulsion industry design tool. Solving this problem was a primary goal of the Phase I work effort under Contract NAS8-39048. Phase I was conducted between 1 August 1991 and 31 December 1991. The Statement of Work (SOW) for Phase I is shown in Table 1.

Towards the end of the Phase I effort it became apparent that much labor could be saved if the TDK code was made more compatible with the analysis tools being used for calculating the STME power cycle, and for calculating distributed energy release efficiency. For this reason a Phase II effort was initiated when funds became available in September 1992. Phase II of the contract was conducted between 16 September 1992 and 19 March 1993. The SOW for Phase II is shown in Table 2.

---

1. Nickerson, G.R., Coats, D.E., Dang, A.L., Dunn, S.S., and Kehtarnavaz, H., *Two-Dimensional Kinetics (TDK) Nozzle Performance Computer Program, Volume I, II, and III*, Software and Engineering Associates, Inc., NAS8-36863, dated 31 March 1989, prepared for George C. Marshall Space Flight Center.

Table 1. Phase I Statement of Work, NAS8-39048

STATEMENT OF WORK

The Two-Dimensional Kinetics (TDK) computer program is a large software package oriented to predict the performance of a liquid rocket thrust chamber. Many options are available for a variety of problems, and several boundary layer modules are coupled with the code. Substantial modifications to the program have been completed recently, and a rigorous documentation set has been prepared to use this analytical capability for the development of projected future engine designs.

The contemplated effort is directed to improve some prediction features, supporting associated design elements in the thrust chamber, to provide support for the code operation on different computer systems, and to resolve difficulties occurring during program execution. The individual tasks are outlined below:

Tasks

1. MABL Restart

   Add a restart capability to the Mass Addition Boundary Layer (MABL) module so that after TDK has been run, MABL can be executed from a saved file using different options.

2. MABL-K Stability

   Develop a robust kinetic algorithm for MABL by applying the method used to make TDK numerically reliable at high chamber pressures.

3. MABL-K with Injection

   Make MABL with kinetics applicable to nozzles with tangential slot injection and transpiration cooling.

4. Technical Support and Documentation

   Technical support of the code will consist of the following activities:

   o Error correction
   o Hot-line response to user problems
   o Program modifications that may be necessary to make the code fully useful
   o Updates to the input preprocessor and postprocessor
   o Additions and improvements to the TDK program documentation, version March 1989.

Table 2. Phase II Statement of Work, NAS8-39048

STATEMENT OF WORK

The Two-Dimensional Kinetics (TDK) computer program is a large software package oriented to predict the performance of a liquid rocket thrust chamber. Many options are available for a variety of problems, and several boundary layer modules are coupled with the code. Substantial modifications to the program have been completed recently, and a rigorous documentation set has been prepared to use this analytical capability for the development of projected future engine designs.

The projected six months effort will support an optimum STME engine design based on the interaction of the performance prediction codes with the power cycle and energy release programs. At present, only the thrust chamber performance is determined with the TDK/MABL code based on provided interface conditions. However, engine component optimization depends strongly on the flow distribution in the selected gas generator cycle approach. To accomplish this goal, the interaction with 'Power Cycle' and energy release codes must be coordinated. Especially, losses from the injection element operation and the boundary layer behavior with flow injection are of interest. The individual tasks are outlined below:

Tasks

1   Provide technical guidance for the program operation (TDK, MABL, BLM, Preprocessor, Processing of Results).

2   Calculate the mass flow in the boundary layer and the associated profiles, including injected mass flows.

3   Activate the shock calculation with the tri-propellant option.

4   Prepare information from TDK program solutions for use in an engine power cycle code (Efficiencies for C and ISP, Mass Fractions, etc.)

5   Support the effort to standardize the energy release method and to implement the respective features into the TDK program. This includes review of the DROPMIX program principles.

6   Prepare a file holding x-y arrays of significant parameters for result visibility, plotting, and optional printout for TDK results along the wall, the center line, the boundary layer edge, profiles normal to the wall, and in the exit plane.

7   Update the preprocessor program, MSFC version, to include all input items related to the latest TDK program changes.

8   Update the existing TDK documentation as required.

9   Quarterly progress reporting and a final report is required.

2.0 SUMMARY OF RESULTS, PHASE I

MABL-K Analysis

The boundary layer equations for compressible turbulent flow including the effects of finite rate chemical kinetics can be derived from the time dependent Navier-Stokes equations using the Reynolds time-averaging procedure and the usual boundary layer order of magnitude assumptions. As presented below, the boundary layer equations are written in a curvilinear coordinate system in which s is the wetted length along the wall and y is measured normal to it (x is axial distance measured along the centerline). A bar over a quantity denotes that it is a time averaged quantity. It has been assumed that the lateral and transverse curvature terms can be neglected. The conservation equations are:

Continuity

$$\frac{\partial}{\partial s} (\rho u r_w^j) + \frac{\partial}{\partial y} \left[(\rho v + \overline{\rho' v'}) r_w^j \right] = 0 \tag{1}$$

Momentum

$$\rho u \frac{\partial u}{\partial s} + (\rho v + \overline{\rho' v'}) \frac{\partial u}{\partial y} = - \frac{dP_e}{ds} + \frac{\partial}{\partial y} (\mu + \rho \varepsilon) \frac{\partial u}{\partial y} \tag{2}$$

Energy

$$\rho u \frac{\partial H}{\partial s} + (\rho v + \overline{\rho' v'}) \frac{\partial H}{\partial y} = \frac{\partial}{\partial y} \left[\left[\frac{u}{Pr} + \frac{\rho \varepsilon}{Pr_T} \right] \frac{\partial H}{\partial y} \right.$$

$$+ \left[\mu \left[1 - \frac{1}{Pr} \right] + \rho \varepsilon \left[1 - \frac{1}{Pr_T} \right] \right] u \frac{\partial u}{\partial y} \right] \tag{3}$$

Species Conservation

$$\rho u \frac{\partial c_i}{\partial s} + (\rho v + \overline{\rho' v'}) \frac{\partial c_i}{\partial y} = \frac{\partial}{\partial y} \left[\left[\frac{\mu}{Pr} + \rho \varepsilon \frac{1}{Pr_T} \right] \frac{\partial c_i}{\partial y} \right] + \omega_i$$

$$i = 1,2,...N \tag{4}$$

where j=0 for 2-D planar flow, j=1 for axisymmetric flow. The quantities μ and Pr, are the dynamic viscosity, and Prandtl number, respectively. The quantities ε and Pr_T are their turbulent counterparts.

Boundary conditions for these P.D.E.'s are applied at the boundary layer edge, and at the wall, as described below.

At the edge, $y = \delta$

Flow conditions here are inviscid and the boundary conditions are obtained using the TDK code, i.e.

$$u = u_e$$
$$H = H_e$$
$$c_i = c_{i_e}$$

In practice the pressure distribution, rather than the edge velocity, is specified and the velocity distribution is found from the pressure gradient by integrating Bernoulli's equation.

At the wall, $y = 0$, the boundary conditions are:

$$u = 0$$
$$\frac{\partial H}{\partial y} = 0 \quad , \quad \text{for adiabatic wall, or}$$
$$T = T_w \quad , \quad \text{for specified wall temperature distribution.}$$

The effects of transpiration cooling are approximated by modifying the wall boundary condition. At the wall

$$u\big|_w = 0 \quad , \quad \varepsilon\big|_w = 0 \quad , \quad \text{and} \quad \omega_i\big|_w = \text{small}$$

so that equation (4) becomes

$$\overset{\text{(wall side)}}{\ \ }\quad\overset{\text{(b.l. side)}}{\ \ }$$
$$(\rho\,v)_w \frac{\partial c_i}{\partial y} = \frac{\mu}{Pr}\frac{\partial}{\partial y}\left[\frac{\partial c_i}{\partial y}\right] .$$

Thus

$$(\rho\,v)_w \, dc_i = \frac{\mu}{Pr}\,d\left[\frac{\partial c_i}{\partial y}\right] .$$

The species concentrations transpired from the wall are $c_{i,trans}$. At the boundary layer side of the wall the species concentrations are $c_{i,w}$. Integration across the wall boundary element gives

$$(c_{i,w} - c_{i,trans}) (\rho\, v)_w = \frac{\mu}{Pr} \frac{\partial c_i}{\partial y}$$

so that

$$\frac{\partial c_i}{\partial y} \bigg|_w = \left[\frac{Pr}{\mu} \right] (\rho\, v)_w (c_{i,w} - c_{i,trans}) \bigg|_w \tag{5}$$

Equation (5) is the boundary condition that is applied for a transpiration cooled wall. The term $(\rho\, v)_w$ is the rate at which mass is transpired across a unit area at the boundary, and this value must not be too large if the method is to work properly. It must be input for each species at each station along the transpiration cooled sections of the wall, i.e.

$$(\rho\, v)_w = \sum_{i=1}^{N} (\rho\, v)_w\, c_{i,trans}.$$

Nozzles that utilize a tangential slot injection scheme can be treated by the MABL analysis if the following assumptions are made:

1. The injectant must be introduced parallel to the nozzle wall (tangential injection). The velocity of the injectant cannot exceed the velocity of the core flow at the point of injection.

2. The pressure of the injected gas must match that of the core flow.

3. The mass flow rate of the injected gas is small (less than ~5%) compared to the total engine mass flow rate.

These assumptions are required for the analysis if it is to be consistent with the thin shear layer approximations. The application of the method is fully described in Appendix B of Reference 1, Volume III.

The difficulty in integrating the kinetic boundary layer equations (1) through (4) results from the source term ω_i appearing in equation (4). This term can be extremely sensitive to the chemical species concentrations, c_i, leading to numerically "stiff" behavior. Thus, an "implicit" PDE integration scheme with some type of active step size control is required.

The method used by MABL-K is first order simple back difference. The method requires the inversion of a large matrix (see Reference 1, Vol. I, Section 6). The coefficients in this matrix include terms of the form

$$\partial \, \omega_i \, / \, \partial \, c_i$$

and these are found analytically, rather than by numerical differencing. Stabilizing the MABL-K algorithm required that the implicit method be rederived to assure its correctness, since any error in the formulation could adversely affect numerical stability. Furthermore, cases were run where the derivative expressions were evaluated by numerical differencing. The matrix coefficients obtained in this manner were compared to the matrix coefficients actually used by the code, i.e. those obtained by formal differentiation.

The MABL-K was reworked from end-to-end in an effort to improve its numerical stability. However, the most fruitful result was achieved by bounding the net change in species concentrations during each integration step. Species integration is of the form

$$c_{i,n+1} = c_{i_n} + \Delta c_{i,n+1}^{(1)}$$

where

$$\sum c_i = 1$$

$$\sum \Delta c_i = 0 \, .$$

The predicted $\Delta c_{i,n+1}^{(1)}$ were bounded so that no individual change exceeded a few percent per step. If one species is affected, then all are affected, since atomic conservation must be maintained.

The modifications discussed above have decreased run times required for the MABL-K module by factors ranging from 2:1 to 10:1, while increasing both the accuracy and the reliability of the calculations.

Figures 1 through 4 show example results obtained using the MABL-K/TDK code to calculate boundary layer properties for the SSME (see Reference 1, Section 11.4 for a discussion of performance calculations for this engine). For the purposes of these calculations an adiabatic wall has been assumed. Edge conditions for the boundary layer were provided by

a two dimensional kinetics (TDK) inviscid calculation. MABL-F, MABL-K, and MABL-E calculations were then carried out and the results compared (the restart option was used; see Table 1, Task 1). The assumptions that differ between the calculations are:

MABL-F   gas in the boundary layer is frozen at the stagnation composition

MABL-K   gas composition is determined by finite rate chemistry (consistent with TDK)

MABL-E   the boundary layer is everywhere in a state of chemical equilibrium (gas composition is not required).

In Figure 1 it can be seen that the adiabatic wall temperature as determined by MABL-K does not track the equilibrium (MABL-E) values. A similar result is found for displacement thickness (see Figure 2). However, the MABL-K predictions for momentum thickness and integrated shear stress do track the equilibrium (MABL-E) values (see Figures 3 and 4). For this case it can be concluded that if wall heat transfer is important, then a MABL-K calculation may be required. However, a MABL-E calculation is adequate for performance prediction.

The MABL-K calculation shown above required less than a minute on an IBM RISC/6000 320H machine. The calculation would have taken over eight minutes on the previous version of the code.

The MABL-K result for adiabatic wall temperature shown in Figure 1 has been verified by repeating this calculation using the VIPER code[2], which provides a PNS computation for the flow field downstream of the nozzle throat.

---

2.   Kawasaki, A.H., Berker, D.R., Coats, D.E., Dunn, S.S., and Nickerson, G.R., *Viscous Interaction Performance Evaluation Routine for Two-Phase Nozzle Flows With Finite Rate Chemistry, VIPER 2.0, Computer User's Manual,* Software & Engineering Associates, Inc., PL-TR-92-3053, January 1993 prepared for Phillips Laboratory.
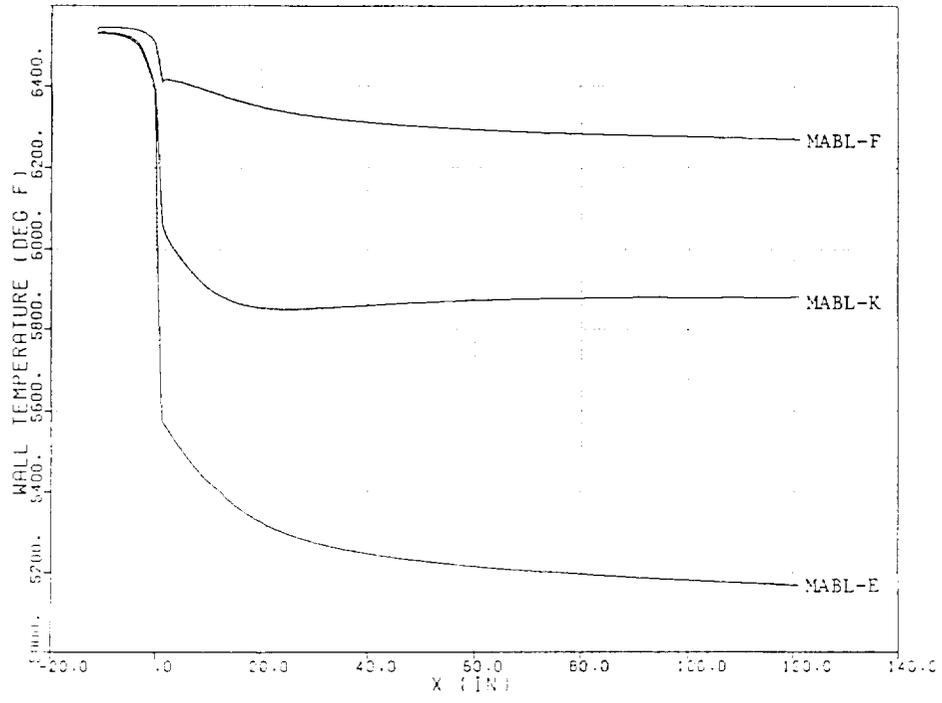
Figure 1. Adiabatic Wall Temperature vs Length. SSME
(Note: all calculations assume the same edge velocity.)
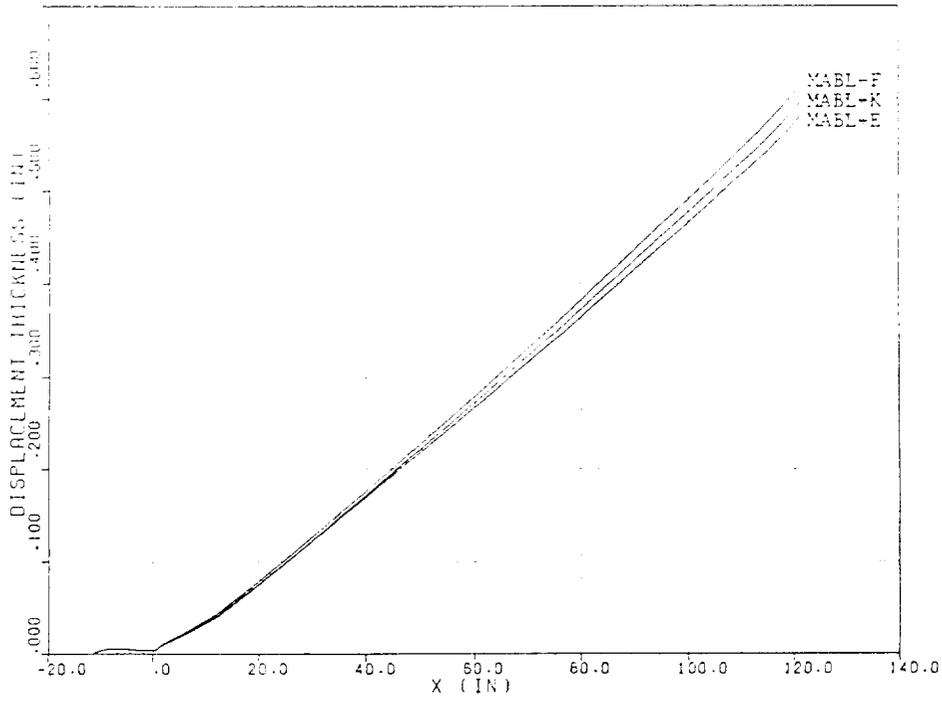
Figure 2. Displacement Thickness, δ^*, vs Length. SSME
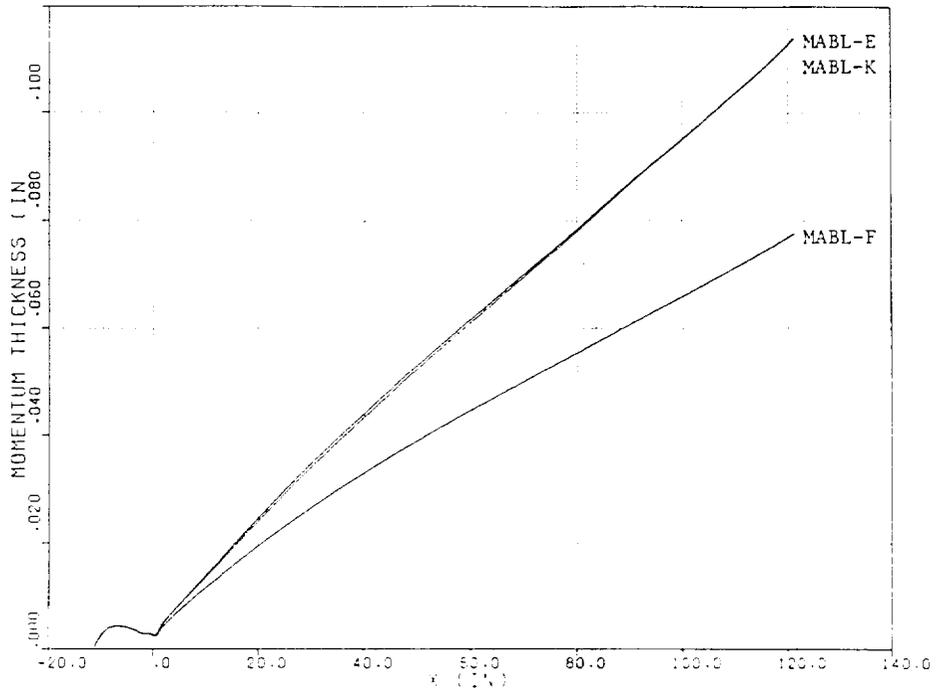
Figure 3. Momentum Thickness, θ, vs Length. SSME
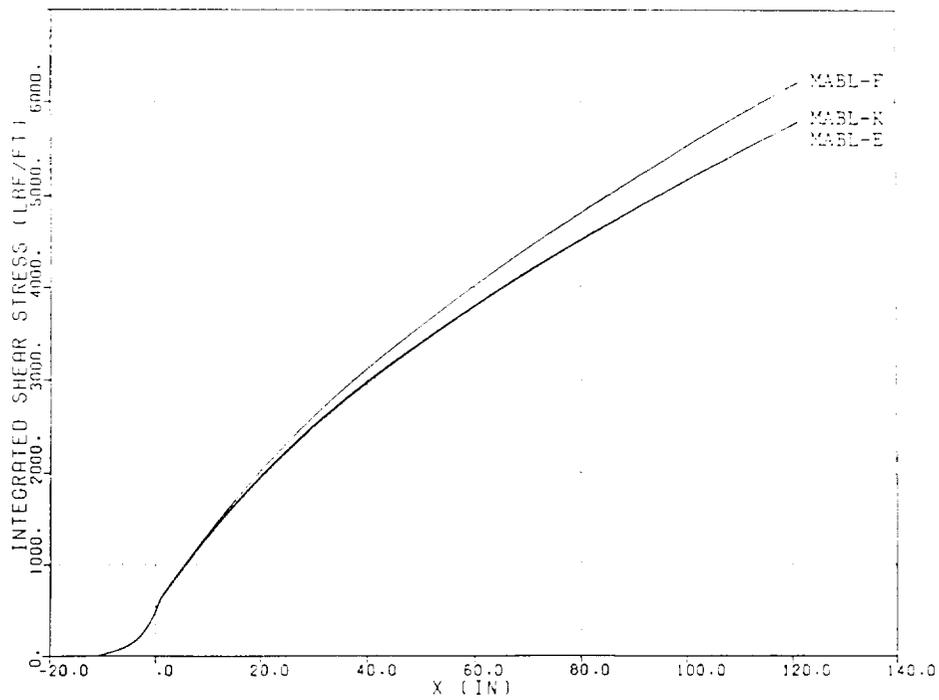
Figure 4. Integrated Wall Shear Stress, τ, vs Length. SSME

3.0 SUMMARY OF RESULTS, PHASE II

A new Users Manual[3] has been prepared that includes modifications to the TDK/MABL code that were carried out under this contract. This document replaces Reference 1, Volume III.

In an effort to coordinate with other computer codes being used to evaluate power cycle behavior, and energy release effects, several auxiliary calculations were added to the TDK/MABL code. Tasks 2 and 4 were included in the SOW for this purpose. The methods used are described below.

In order to calculate the mass flow in the boundary layer and the associated profiles, including injected mass flows, the "mass flow in the boundary" layer was taken as:

$$\dot{m}_{b\ell} = \int_{o}^{\delta} \rho \, u \, 2 \, \pi \, r_e \, dy \tag{6}$$

where δ is that point in the boundary layer where the velocity attains a value that is 99.5% of the edge velocity, U_e, i.e.,

$$y = \delta \quad \text{when} \quad (u/U_e) = .995 \tag{7}$$

The above definition is arbitrary since the boundary layer profiles attain the edge values asymptotically.

---

3.   Nickerson, G.R., Berker, D.R., Coats, D.E., and Dunn, S.S., *Two-Dimensional Kinetics (TDK) Nozzle Performance Computer Program Volume III, Users Manual*, Software and Engineering Associates, Inc., NAS8-39048, dated 31 March 1993, prepared for George C. Marshall Space Flight Center.

If the nozzle is designed with injection ports along the wall, then for binary mixtures (MABL-F and MABL-E) equation (4) is replaced by the following equation:

Mixture Conservation

$$\rho u \frac{\partial \alpha}{\partial s} + (\rho v + \overline{\rho' v'}) \frac{\partial \alpha}{\partial y} = \frac{\partial}{\partial y} \left[\left[\frac{\mu}{Pr} + \rho \varepsilon \frac{1}{Pr_T} \right] \frac{\partial \alpha}{\partial y} \right] \tag{8}$$

Equation (6) can then be written as:

$$\dot{m}_{b\ell} = \int_0^\delta \alpha \rho u \, 2 \pi r_e \, dy + \int_0^\delta (1-\alpha) \rho u \, 2 \pi r_e \, dy \tag{9}$$

Equation (9), above, separates the boundary layer flow into two components; injectant (α=1) and core flow (α=0). It is also required that α=0 at y=δ because the boundary layer must contain all of the injectant.

Thus, the main flow in the boundary layer can contain two components:

$$\dot{m}_{b\ell} = \dot{m}_{gg,b\ell} + \dot{m}_{core,b\ell}$$

When the injection occurs at a discrete position along the nozzle wall, X_{inj}, as is the case with tangential slot injection, then

$$\dot{m}_{gg,b\ell} = 0 \qquad\qquad X < X_{inj}$$

$$\dot{m}_{gg,b\ell} = \dot{m}_{inj} \qquad\qquad X \geq X_{inj}$$

that is

$$\int_0^\delta \alpha \rho u \, 2 \pi r_e \, dy = \dot{m}_{inj} \qquad\qquad X \leq X_{inj} \tag{10}$$

which is a constant value.

The following plot files containing boundary layer profiles are provided at up to 20 specified locations along the nozzle wall (see Reference 3, Vol. II, Section 9.9).

$\dot{m}_{b\ell}$ vs   y   (for MABL-F, MABL-K, and MABL-E options using

equation (6))

$\dot{m}_{gg,b\ell}$ vs   y   (for MABL-F and MABL-E options using equation (10))

where

$0 \le y \le \delta.$

Since α pertains only to binary mixtures (MABL-E and MABL-F options), only the $\dot{m}_{b\ell}$ vs y profiles are provided for kinetic boundary layer (MABL-K) calculations.

A plot file is also provided that gives

$\dot{m}_{b\ell}$ vs   X.

Application to the STME

During the course of the work effort, the TDK/MABL code was used to obtain performance calculations for a number of rocket engines. Four engines in particular were analyzed: 1) the SSME, 2) the P&W 40K thrust level STME test engine, 3) the 583K STME design, and 4) the 650K STME design. Analysis results for this latter engine are presented here to demonstrate this newest version of the TDK/MABL code.

The STME design utilizes a combustion chamber extending to a supersonic expansion ratio of 7:1 where an expansion nozzle is attached. The configuration is shown in Figures 5a and 5b. The nozzle is cooled by gH_2 flowing inside of coolant tubes forming the wall contour. Additional cooling is provided by injection of gas generator gases, consisting of primarily gH_2 from the low mixture ratio reaction. The joint separating the chamber and nozzle is cooled with a small amount of gas generator turbine exhaust that is injected normal to the primary flow without being choked (subsonic film). The remainer of the turbine exhaust is injected parallel to the primary flow as a supersonic film. The mass flow of the supersonic film is approximately five times greater than the subsonic film mass flow. The nozzle injector region is contained in the dashed circle shown in Figure 5a. An enlarged view of this region is shown in Figure 5b.
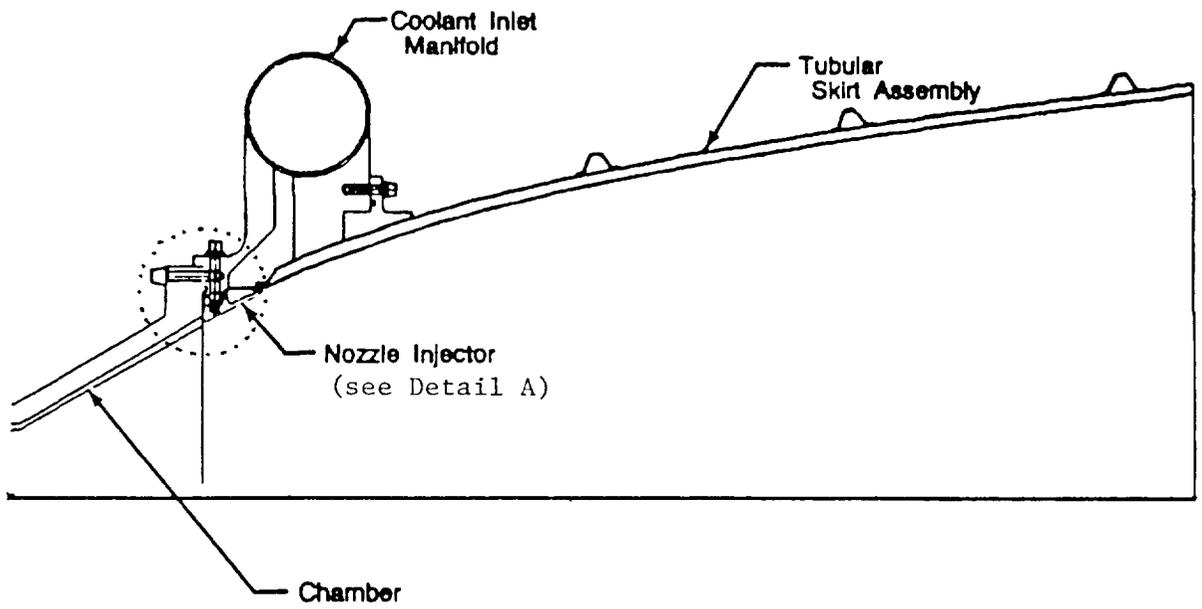
Figure 5a. STME Chamber/Nozzle Configuration
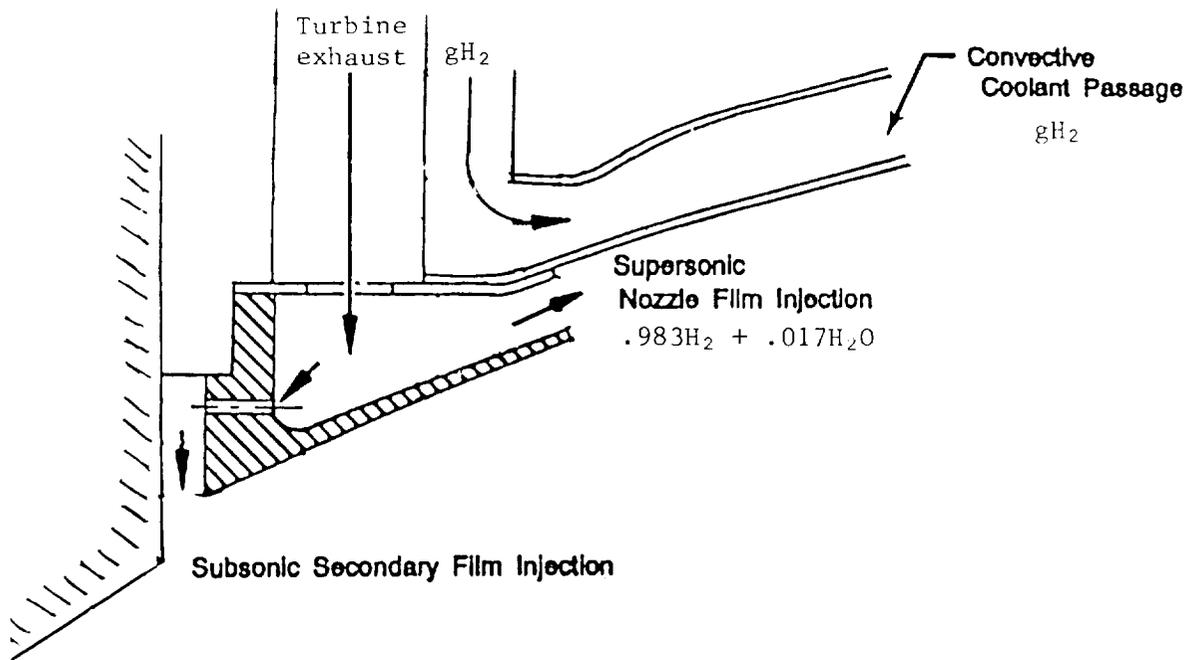
Figure 5b. Detail A: STME Nozzle Injector Region

Input data defining the STME geometry and operating conditions is given in Table 3. The analysis consists of a two dimensional calculation for the thrust chamber core flow, followed by an analysis of the wall boundary layer flow. The TDK code treats the core flow as an inviscid chemically reacting process. A wall boundary layer is calculated by the MABL code using edge conditions supplied by TDK. Since the flow is found to be in a state very near to chemical equilibrium, equilibrium chemistry is assumed; i.e., TDE and MABL-E results were obtained and are presented here.

At the STME chamber/nozzle interface a small amount of turbine exhaust is injected normal to the wall, followed approximately three inches downstream by tangential injection of a larger amount. Slot injection effects are calculated by the boundary layer analysis (MABL). Both slots are treated as tangential injection, since the code has no normal injection capability other than injection by transpiration. Thus, flow injected at the first slot is assumed to be turned parallel to the core flow. Since the injection flow rate at the first slot is low, and occurs behind a rearward facing step, this assumption should give a reasonable approximation of the boundary layer properties.

The TDK/MABL computational procedure requires that the pressure of the injectant be equal to the boundary layer edge pressure at the injection position. Thus, the procedure calculates the injection nozzle expansion ratio that provides the matched edge pressure. The flow from both slots have the same stagnation temperature (see Table 3, TOGG=2*1224 °R in $ODE), but have different stagnation pressures (POGG=77.,204. psi for slots 1 and 2, respectively). The flow is assumed to expand from these values isentropically to match the pressure of the adjacent core flow as calculated by the TDE analysis. Computer print-out showing the results of these expansion calculations is presented in Table 4. Included in this output is the ratio of the mass flow per unit area of the injectant to the mass flow per unit area of the boundary layer edge flow. At the first slot the coolant is injected normal to the edge flow. However, it can be seen that the ratio of injectant to edge mass flow per unit area is only .166, which implies that flow turing effects can be ignored (the analysis requires this).

Table 4 also shows that the edge pressure at injection is 67.26 and 56.75 psi for the first and second injectants, respectively. This give Mach number values after expansion of .447 and 1.489. Hence, the first slot is said to have "subsonic" injection. The second slot expands the film to approximately Mach 1.5, which is believed to provide sufficient margin so that the injectant ports will remain choked. Since it turns out that the primary nozzle mass flow is predicted to be 1482 lbm/sec, the slot mass flows are 7 and 35 lbm/sec, respectively (see Table 3, input item FXMGG=.004697, .023687 in $MABL).

```
TITLE  F/S NLS 650K ENGINE: GG SUBSONIC AND SUPERSONIC INJECTION...2 ZONE
DATA
 $DATA
 ODE = 1, ODK = 0, TDE = 1, MABL = 1, IMABL = 3, MABLE = T,
 ASUP = 7.,43.097, NASUP=2,
 RSI = 6.9,
 XIC(1) = 5.36, NXIC = 1,
  RWTU=0.494, RWTD=.2, RI = 1.598,
  THETA= 29.228, THE=8.312, THETAI=25.42,
  IWALL=4, ITYPE=1,
 ECRAT=2.682,ASUB(1)=2.682, NASUB=1,
 RS(2) =      1.252232, 1.541037, 1.888917, 2.267946,
              2.661167, 3.058127, 3.452169, 3.838668,
              4.214417, 4.576776, 4.924005, 5.254459,
              5.567102, 5.860643, 6.134528, 6.388157,
              6.564863,
 ZS(2) =      0.498084, 0.973261, 1.547740, 2.203318,
              2.935726, 3.742109, 4.620865, 5.571712,
              6.592352, 7.683121, 8.841478,10.067299,
             11.358459,12.715493,14.135952,15.618718,
             16.777452,
 NWS =    18,
 XWGG=2.836, 3.267, NWGG=2, AFWGG=2*1, EQLGG=T,
 NZONES = 2, XM(1) = .925, .075,
 TRI=T, OFCORE= .87827, .83333,
 FFCORE=.12173, .16667,
 GFCORE=2*0,
         OFGG = .47617, FFGG = 0, GFGG = .52383,
 $END
REACTANTS
O 2.                                      100.    -2899.L  100.33O 1.149
H 2.                                      100.    -1963.L   40.33F .0709
H 2.                                      100.    -1963.L   40.33G .0709

NAMELISTS
 $ODE
 RKT = T,
 P = 2250., XP(1) = 2*1, PSIA = T,
 POGG= 77., 204., TOGG=2*1224., DELH=2*52.265,
 $END
 $TRANS
 MP = 150,
 DRMIN = .0005,
 $END
 $MOC
 EXITPL = T,
 NC = -1,
 $END
 $MABL
  DXI=2E-4, NDXI=50, NYI=115, DXLIM(1) = .002,.02,
  LDXLIM=2, XLIM=5,10,
  FXMGG=.004697, .023687,
  ADBATC=0,
  OFC=2, DISTRB=0,
  XCO=-2.58986,
  XCE=2.836,
  ETAC=1,
  NTQW=25,
  XTQW= -1000.,-2.6,-1.8,-1.4,-1.1,-0.6,-0.2,-0.1,
        .05,0.23,0.85,1.3,2.,2.3,2.75,3.24,4.35,5.84,
        7.33,8.82,10.31,11.79,13.28,14.77,15.98,
   TQW = 1100.,1100.,1350.,1300.,1325.,1250.,1350.,1300.,
         950.,650.,850.,800.,650.,600.,1200.,1215.,1197.,1523.,
         1684.,1759.,1793.,1806.,1811.,1803.,1744.,
 ITHKBL = 1,
 $END
```

Table 4. TDE Print-out of Injection Conditions

SLOT	XGG (X/R*)	RGG (R/R*)	POGG (PSI)	TOGG (DEG R)	PGG (PSI)	GG MULTI-SLOT OPTION FOR UPPER WALL TGG (DEG R)	RHOGG (LBM/FT3)	VGG (FT/SEC)	(RHOV)GG /(RHOV)E	MGG	AE/AT	ISP/GG (SEC)	ISP/EXIT (SEC)
1	2.836	2.610	77.00	1224.	67.26	1179.	2.045E-02	2049.	.166	.447	1.459	.00	264.39
2	3.267	2.829	204.00	1224.	56.75	859.	2.368E-02	5839.	.617	1.489	1.171	240.59	281.03

The wall boundary layer, including interaction of the injectant streams with the primary flow, is calculated by the Mass Addition Boundary Layer (MABL) code. Some results obtained from these calculations are presented in Figures 6 through 14. The plotted results shown in these figures are of two types; 1) boundary layer profiles at a given axial locations, and 2) boundary layer parameters such as edge values, wall heat flux, wall shear stress, body displacement, etc. vs axial location.

Figure 6 shows boundary layer profiles for mass flow, α, u/U_e, and temperature at an axial position immediately behind the first slot. The approach boundary layer has been displaced, and a slug of injectant has been inserted between it and the wall, as can be seen in the plot of y/y_e vs α. The plots of y/y_e vs $\dot{m}_{b\ell}$ and $\dot{m}_{gg}$ are obtained using equations (6) and (10). The vertical line terminating the $\dot{m}_{gg}$ profile shows that 7 lbm/sec of turbine exhaust has been injected.

Figure 7 shows these same plots at an axial position immediately behind the second slot. The plot of y/y_e vs α shows a mixing profile for the first injectant that is superimposed on a new slug of injectant from the second slot. The plot of y/y_e vs $\dot{m}_{gg}$ shows that a total of 42 lbm/sec of turbine exhaust has been injected (7 + 35).

Figure 8 shows these same profiles at the nozzle exit, which is 7.8 feet from slot number 2. The plot of y/y_e vs α shows that at the wall ($y/y_e = 0$) approximately 30% of the mass flow is injectant and 70% is entrained edge flow (of course these are reacted to a state of equilibrium since the MABL-E calculation is used here). The calculation indicates that the film stays within four inches of the wall ($y_e = 3.9$ inches).
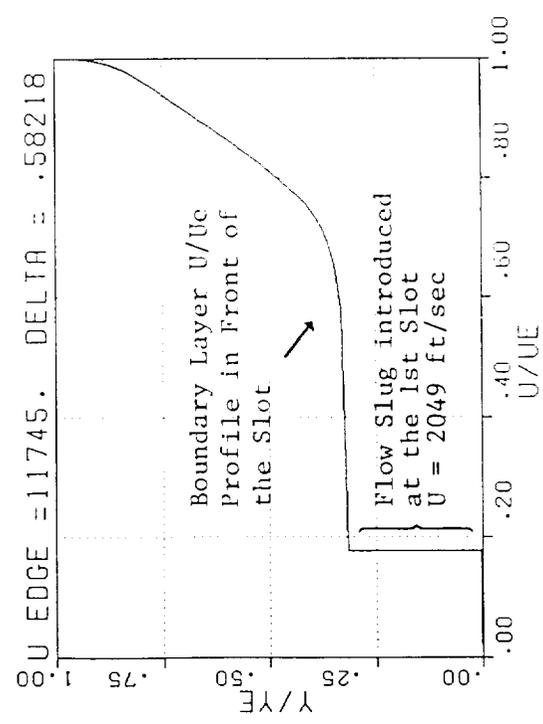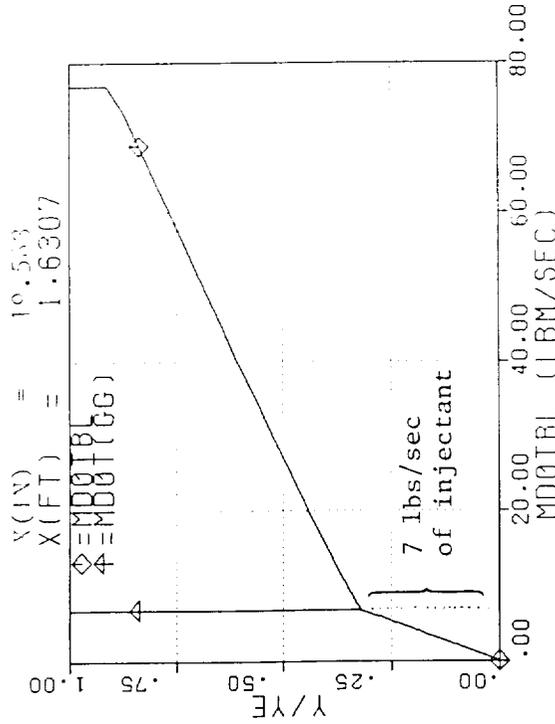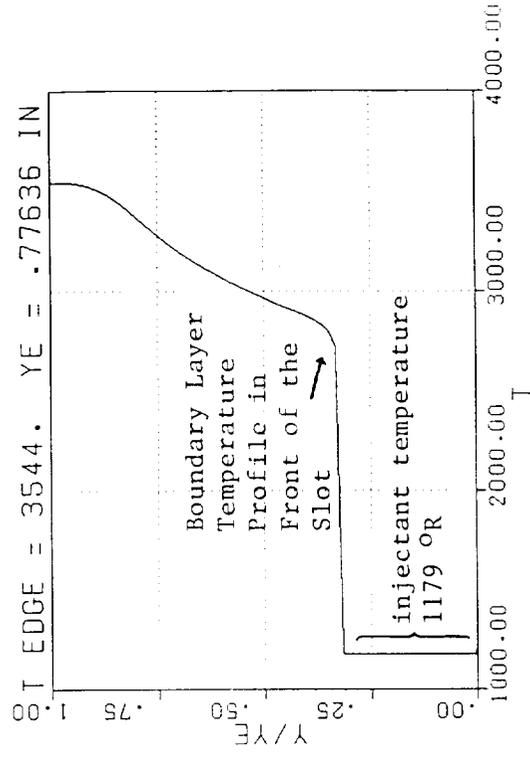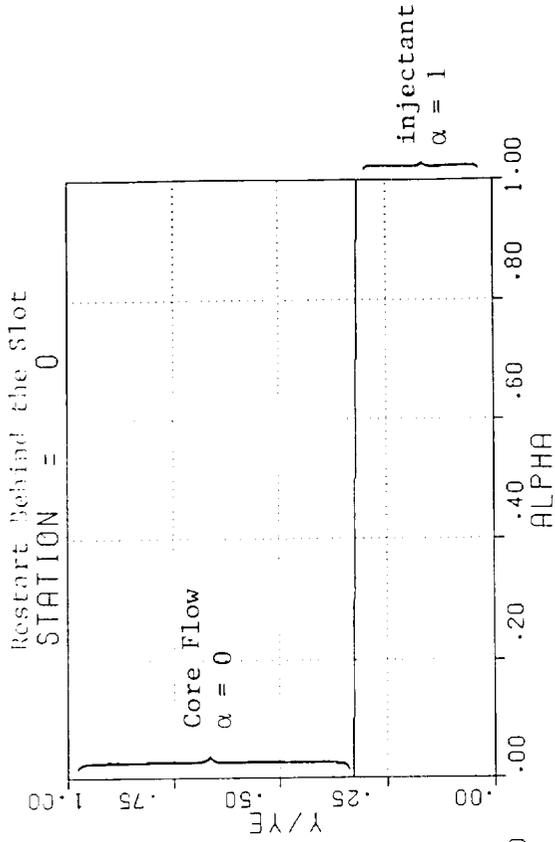
Figure 6. y/y_e vs $\dot{m}_{b\ell}$, $\dot{m}_{gg}$, α, u/U_e, and T behind Slot 1. 650K STME

18

T930345
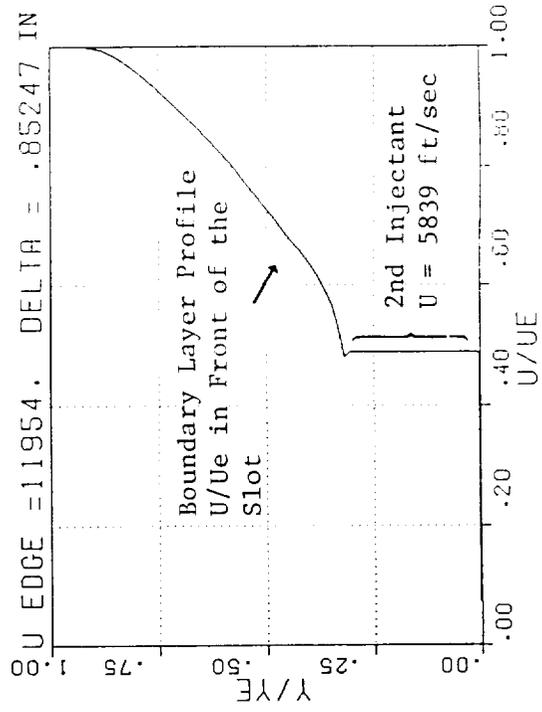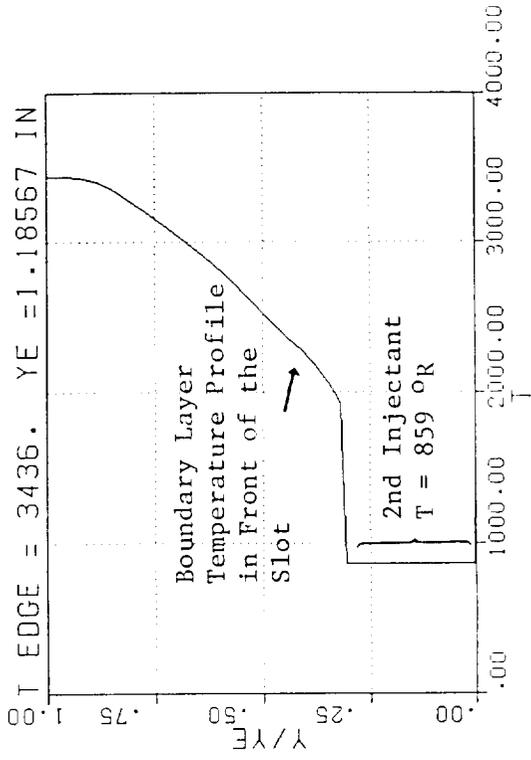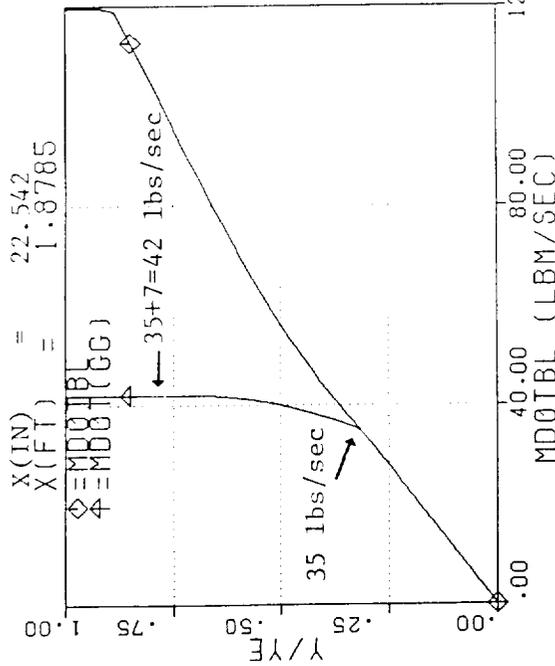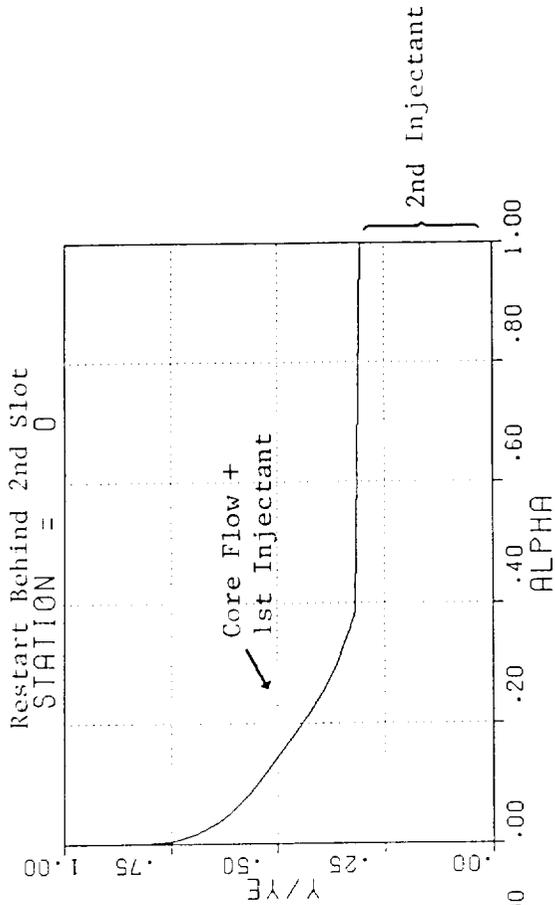
Figure 7. y/y_c vs $\dot{m}_{b\ell}$, $\dot{m}_{gg}$, α, u/U_e, and T behind Slot 2. 650K STME

19
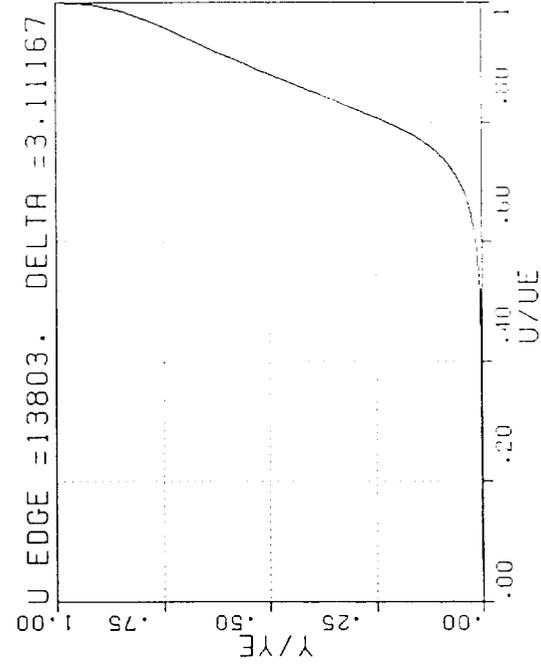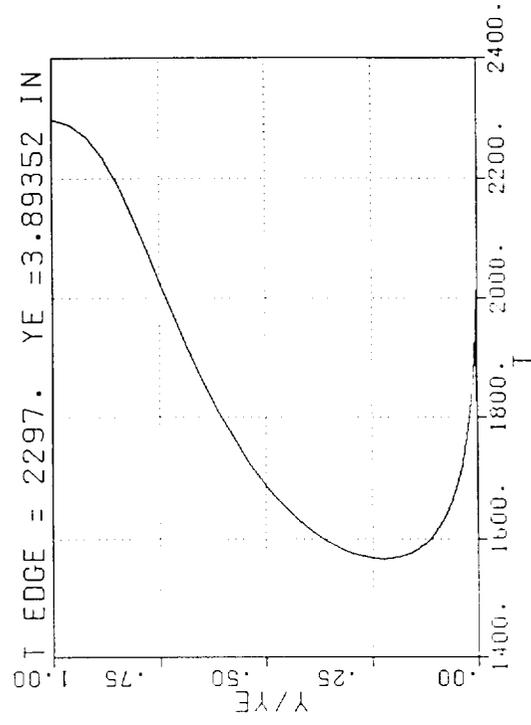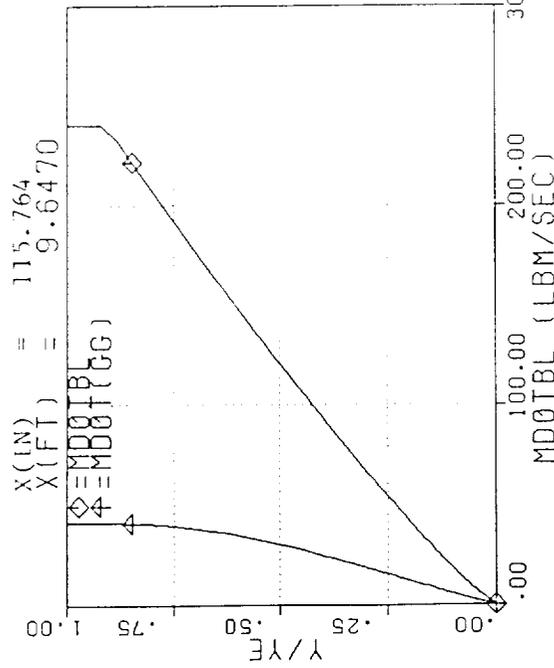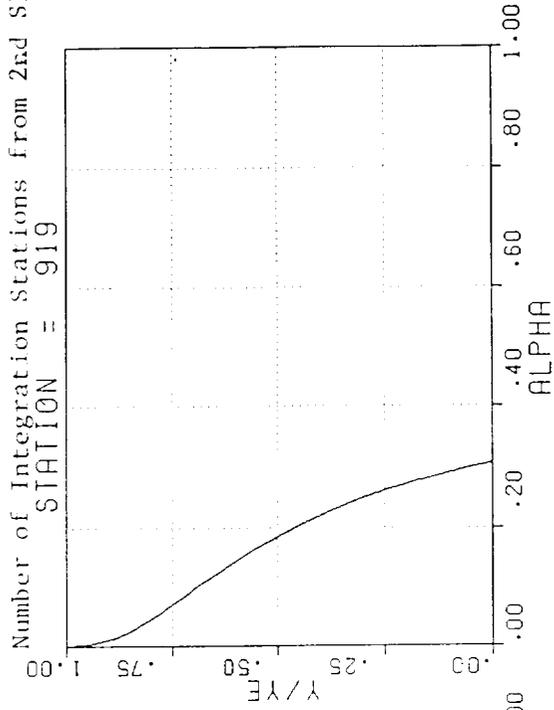
Figure 8. y/y_e vs $\dot{m}_{b\ell}$, $\dot{m}_{gg}$, α, u/U_e, and T at the Nozzle Exit. 650K STME

T930345

20

Figures 9 through 14 are plots of selected boundary layer parameters vs axial position. Figure 9 gives $\dot{m}_{b\ell}$ vs X, and can be compared to the profiles given for this quantity in Figures 6, 7, and 8. The injection positions are seen in Figure 9. Note that at the nozzle exit the boundary layer has entrained 240 out of 1482 lbm/sec, or 16% of the total flow. (42 lbm/sec of this is injectant).

Figures 10 through 14 give the user specified wall temperature, integrated wall surface heat flux, surface integrated wall shear stress, boundary layer thrust decrement, and body displacement vs axial position. The nozzle wall temperatures shown in Figure 10 should be regarded as preliminary, and were obtained by an independent analysis provided to SEA, Inc. by the NASA/MSFC. This is the profile listed in the TDK input, Table 3, arrays XTQW and TQW. Figure 11 shows the predicted wall heat pick-up obtained using the wall temperatures shown in Figure 10. It should be noted that wall temperature variations of a few hundred °F have only a mild effect on this quantity because the adiabatic wall temperature is so high (heat flux is roughly proportional to the difference between the adiabatic wall temperature and the input wall temperature). It can be seen that injection of the relatively cool turbine exhaust is predicted to give a large reduction in wall heating.

Figure 12 shows the surface integrated wall shear stress. Injection of the relatively low velocity turbine exhaust is predicted to give a large reduction in this quantity also, but not so large as the reduction in wall heating. A reduction in wall shear stress provides an increase in thrust, which in this case could be as much as 5000 lbf.

Figure 13 shows the predicted boundary layer loss. In this figure the stream thrust of the primary injectant can be seen as a vertical line at the injection position (X = 22.5 inches), and provides a thrust of ~ 7500 lbf (this is the force component aligned with the nozzle axis). As the injectant expands within the primary flow, it provides additional thrust which fully off-sets drag loss until the X ~ 75 inch position is reached. Because of the injectant, the boundary layer provides a net gain in engine thrust of about 7000 lbf.

Figure 14 shows body displacement. It can be seen that one inch of displacement is sufficient to accommodate the boundary layer and the injectants. Note that the displacement thickness at the nozzle throat is negative due to the large amount of wall cooling taking place there, so that the gas density in the boundary layer is increased significantly. The "body displacement" is required to adjust the potential to the real wall contour.
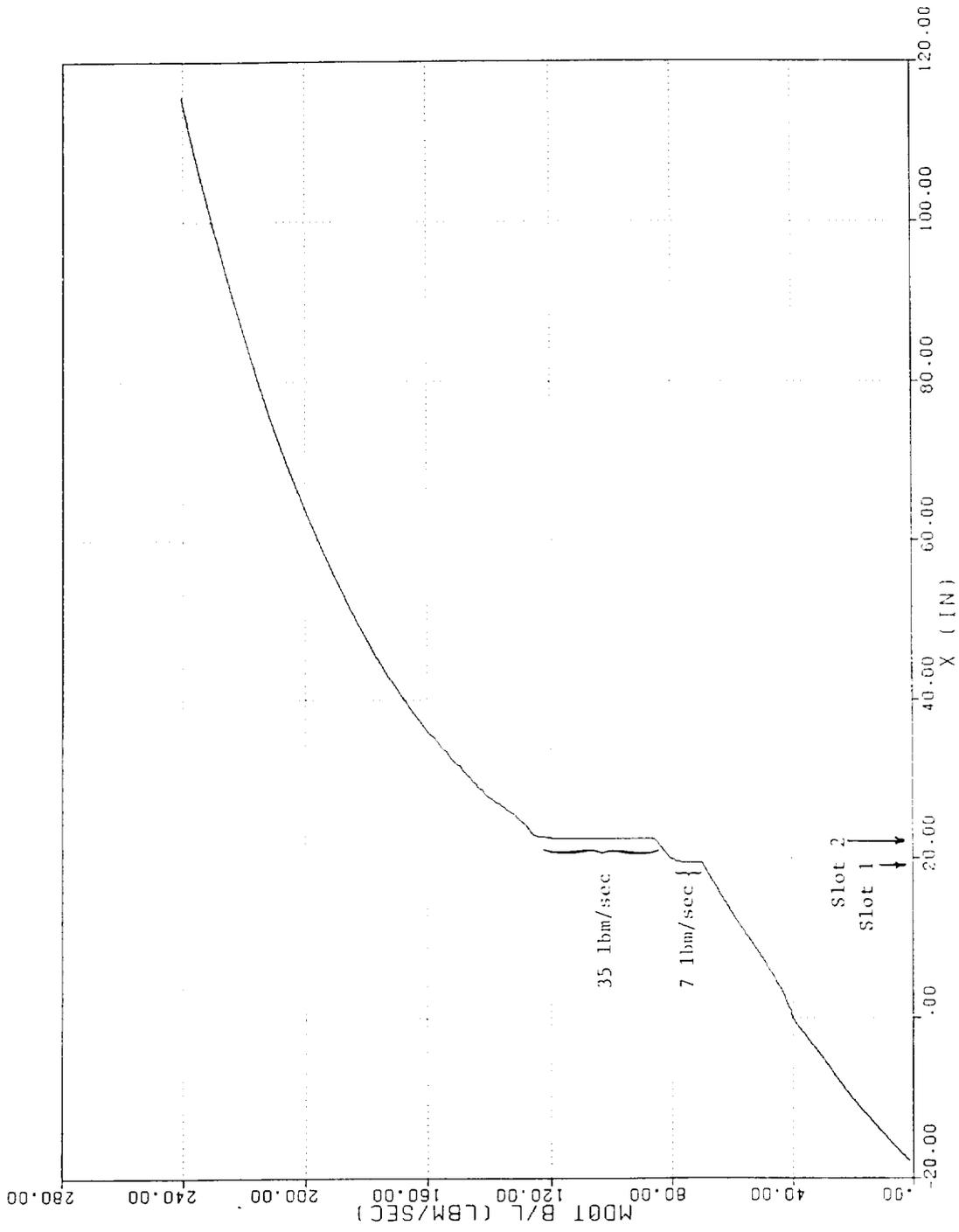
Figure 9. $\dot{m}_{b\ell}$ vs X for the 650K STME

T930345

22
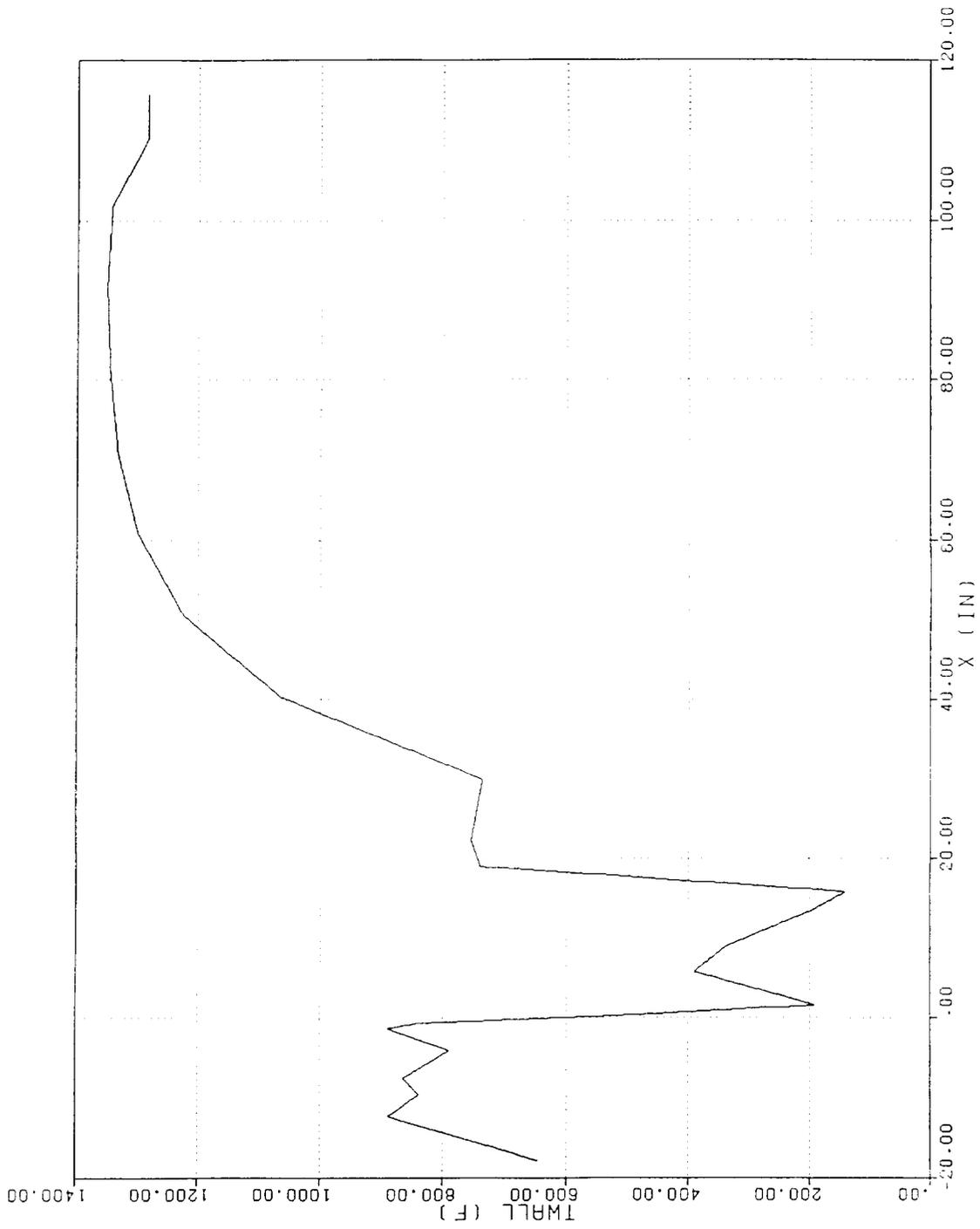
Figure 10. Input Wall Temperature vs X. 650K STME

T930345

23
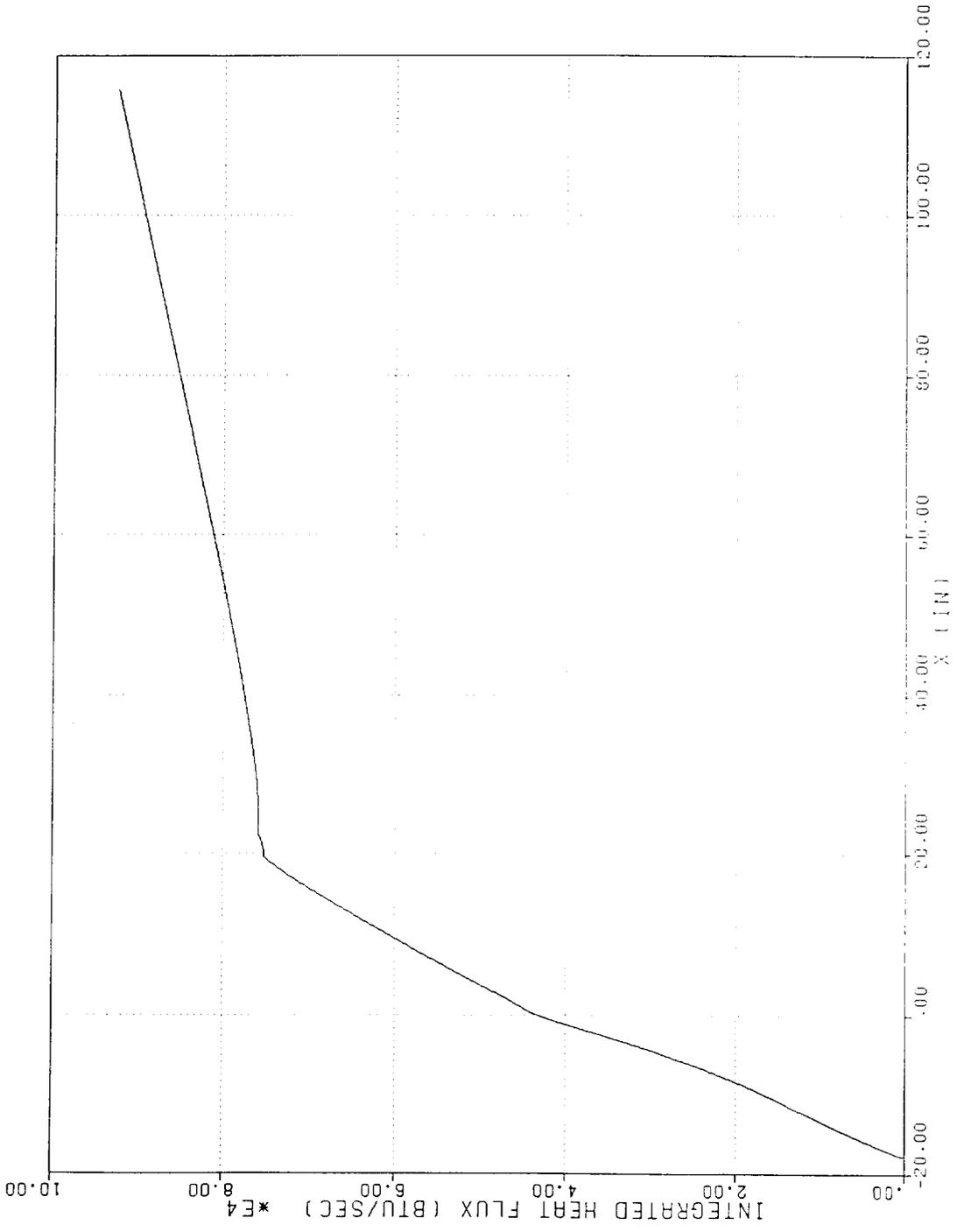
Figure 11. Heat Flux Integrated Over the Wall Surface Area vs X. 650K STME

T930345

24

Figure 12. Wall Shear Stress Integrated Over the Wall Surface Area vs X. 650K STME

T930345
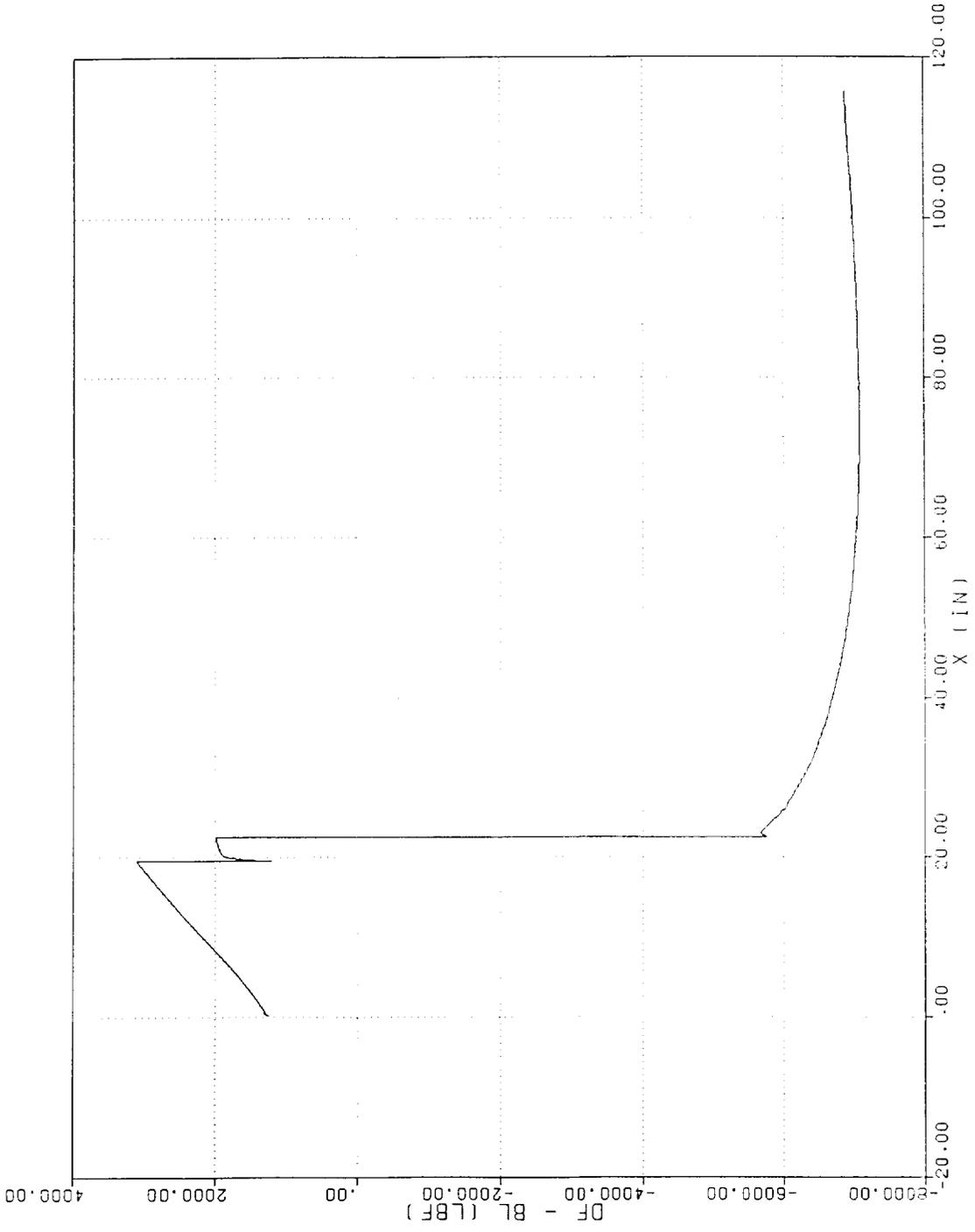
Figure 13. Boundary Layer Thrust Decrement vs X. 650 STME

T930345

26
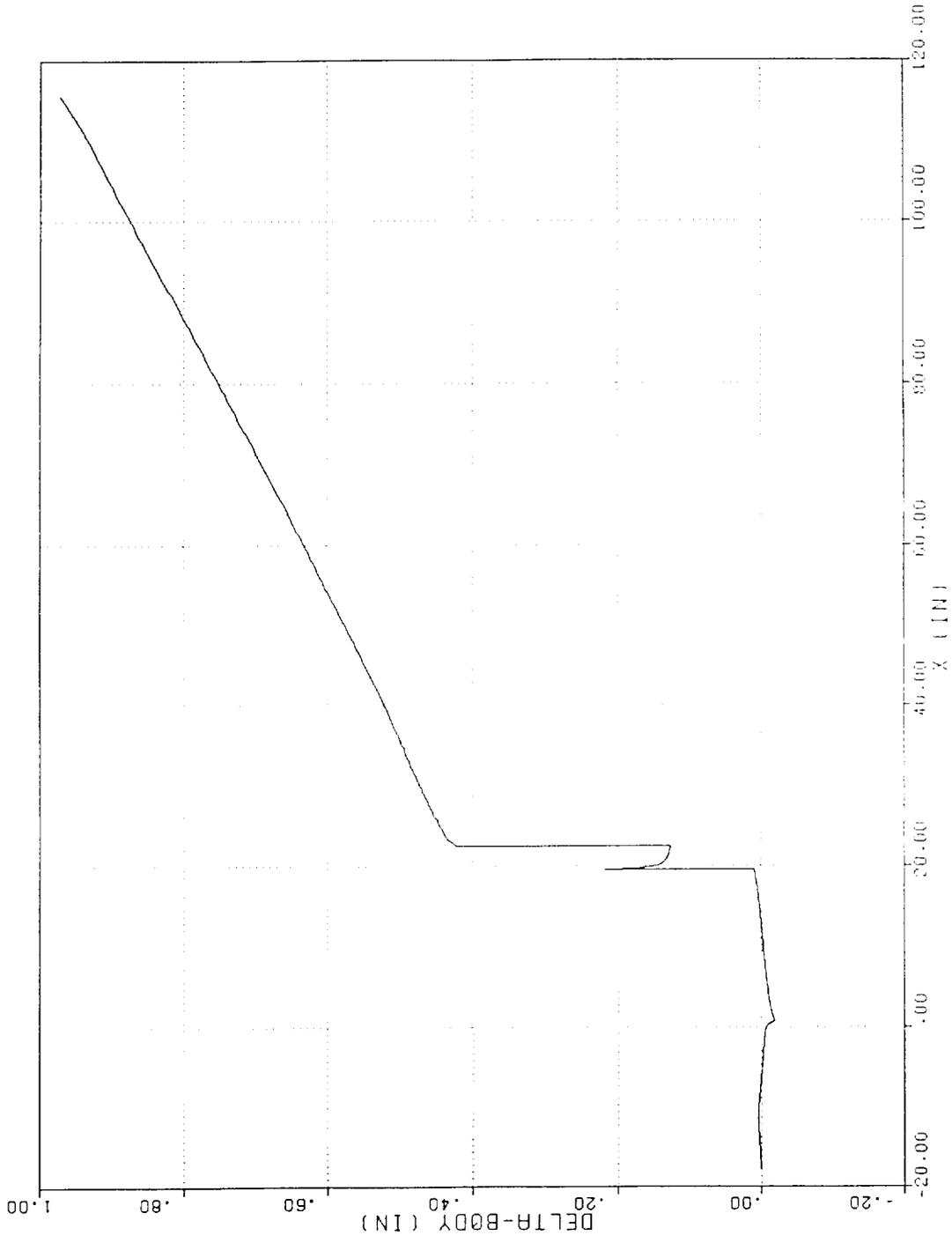
Figure 14. Body Displacement vs X. 650K STME

T930345

27

Figures 15 through 20 show TDK calculations of pressure and temperature along the wall (which is the edge condition for the boundary layer) and the flow centerline. In Figure 15 and 16 a slight compression can be seen at the end of the circular arc used to define the downstream side of the throat. This disturbance travels to the flow centerline where it is reflected. It can be seen at the X/r*=11 position in Figures 17 and 18. As would be expected in an axially symmetric flow, the disturbance is stronger when it reaches the flow center.

Figures 19 and 20 show pressure and temperature across the nozzle exit plane. The horizontal line at the top of Figure 20 represents the interface (or slipline) separating the core flow into inner and outer regions. The outer region contains 7.5% of the flow, and this flow is contained within the small annulus shown in Figure 20.

The results plotted in Figure 6 through 20 discussed above were obtained using the x-y arrays requested in Task 6 of the Phase II SOW.

Task 4 of the SOW specified that certain output values be printed for use in an engine power cycle code. Example output for the 650K STME calculation is shown in Table 5. Note that the primary flow has been separated into two zones 1) an outer region containing 7.5% of the flow at a mixture ratio of 7.2149:1, and 2) an inner region containing 92.5% of the flow at a mixture ratio of 5:1. The combined over-all mixture ratio for the core flow is 7:1. Table 5 gives results based on the assumption of one-dimensional isentropic flow.

Table 5. Performance Summary for the 650K STME
(one-dimensional, core flow)

			ODE ISP & CSTAR SUMMARY				
ZONE	ODE ISP	ODF ISP	ODE CSTAR	ODF CSTAR	ZONE MASS FLOW	M.R.	OX. FRAC
1	449.186	421.249	7353.3	7217.8	.92500	7.2149	.8783
2	460.286	449.064	7870.4	7776.1	.07500	4.9999	.8333

```
            ODE MASS AVERAGED ISP    =    450.019
            ODF MASS AVERAGED ISP    =    423.335
            ODE MASS AVERAGED CSTAR  =    7392.1
            ODF MASS AVERAGED CSTAR  =    7259.7


            MASS AVERAGED O/F    =    6.99357
```
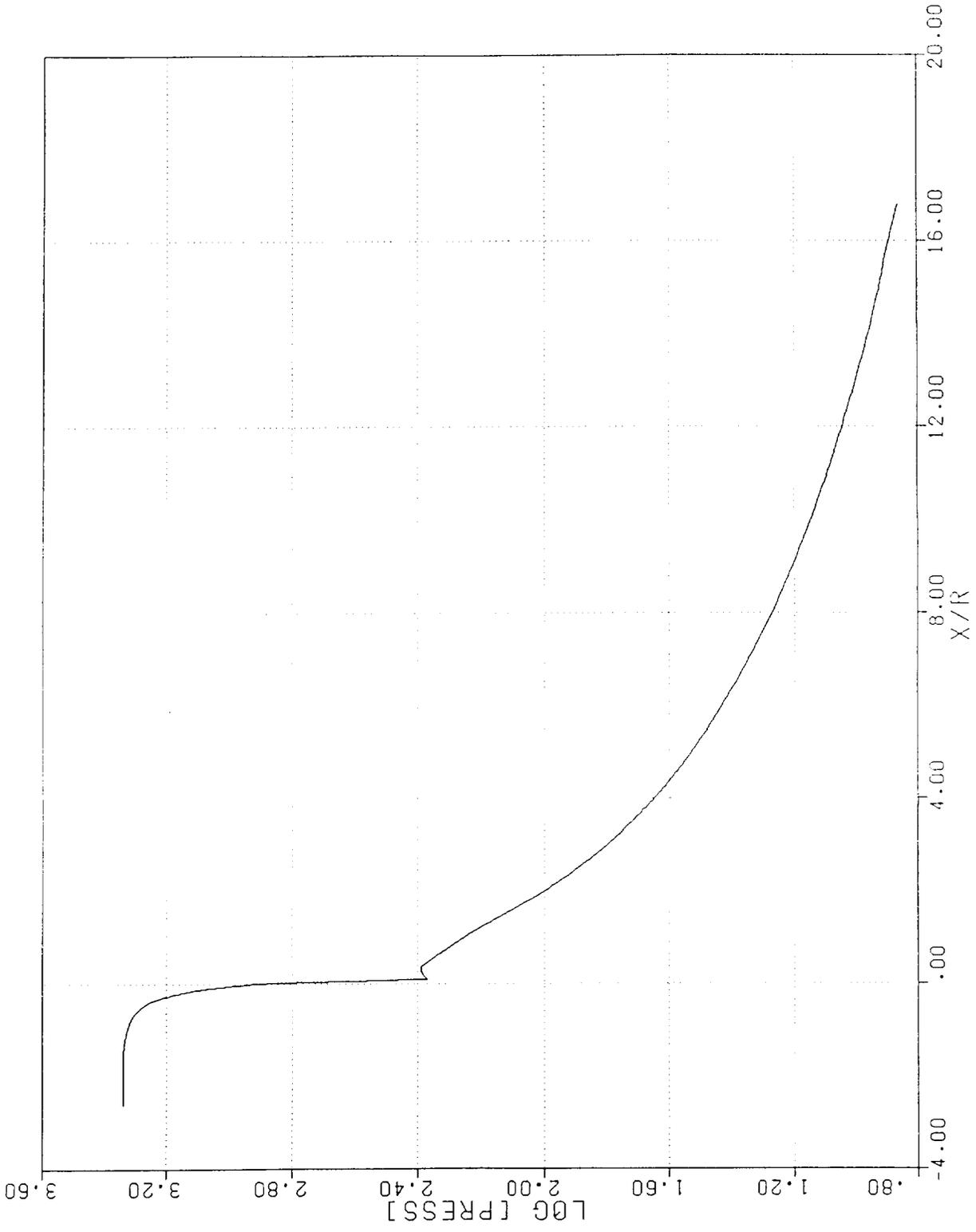
Figure 15. Log of Pressure (psi) vs X/r* Along the Boundary Layer Edge. 650K STME

T930345

29
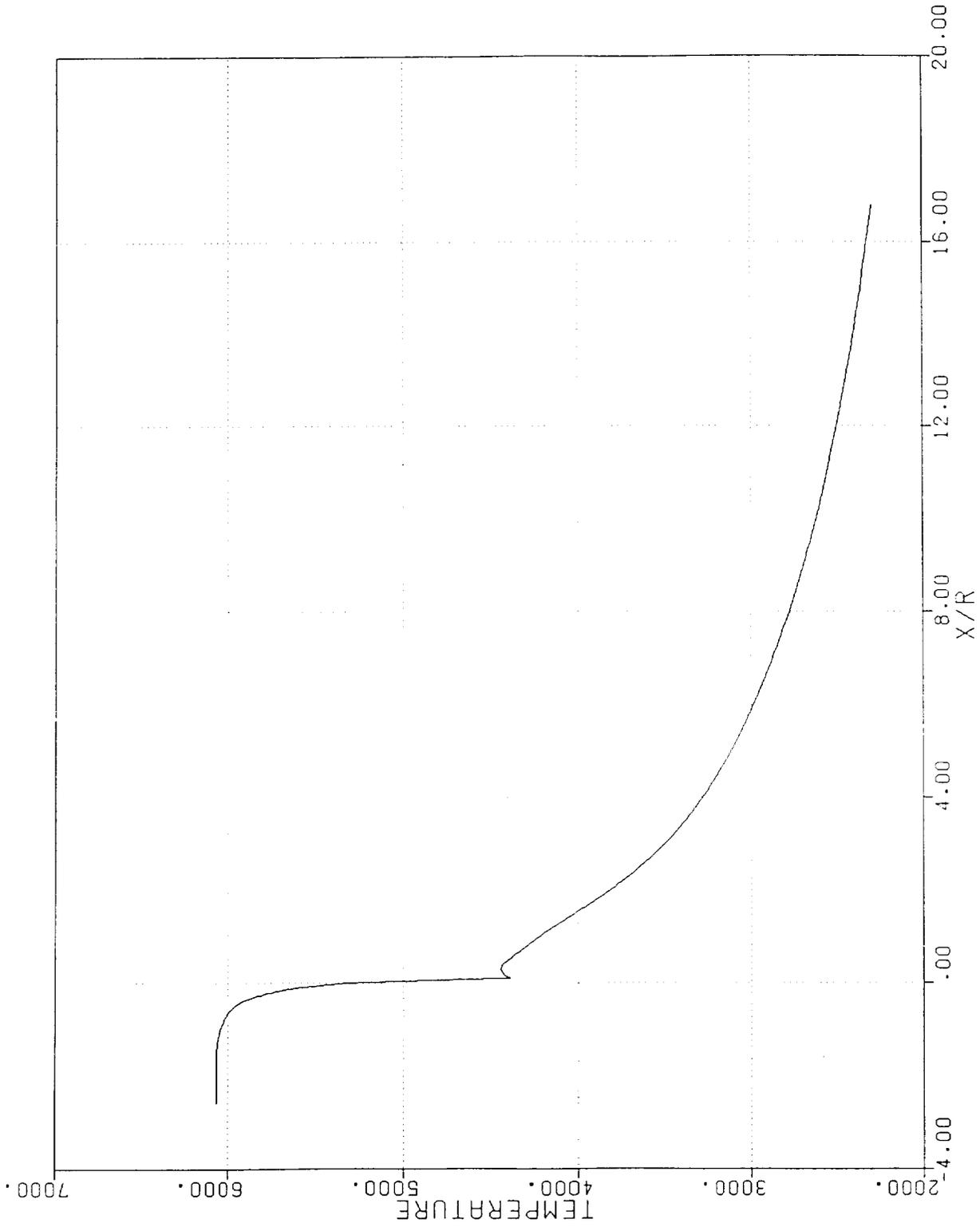
Figure 16. Temperature (°R) vs X/r* Along the Boundary Layer Edge. 650K STME

T930345

30
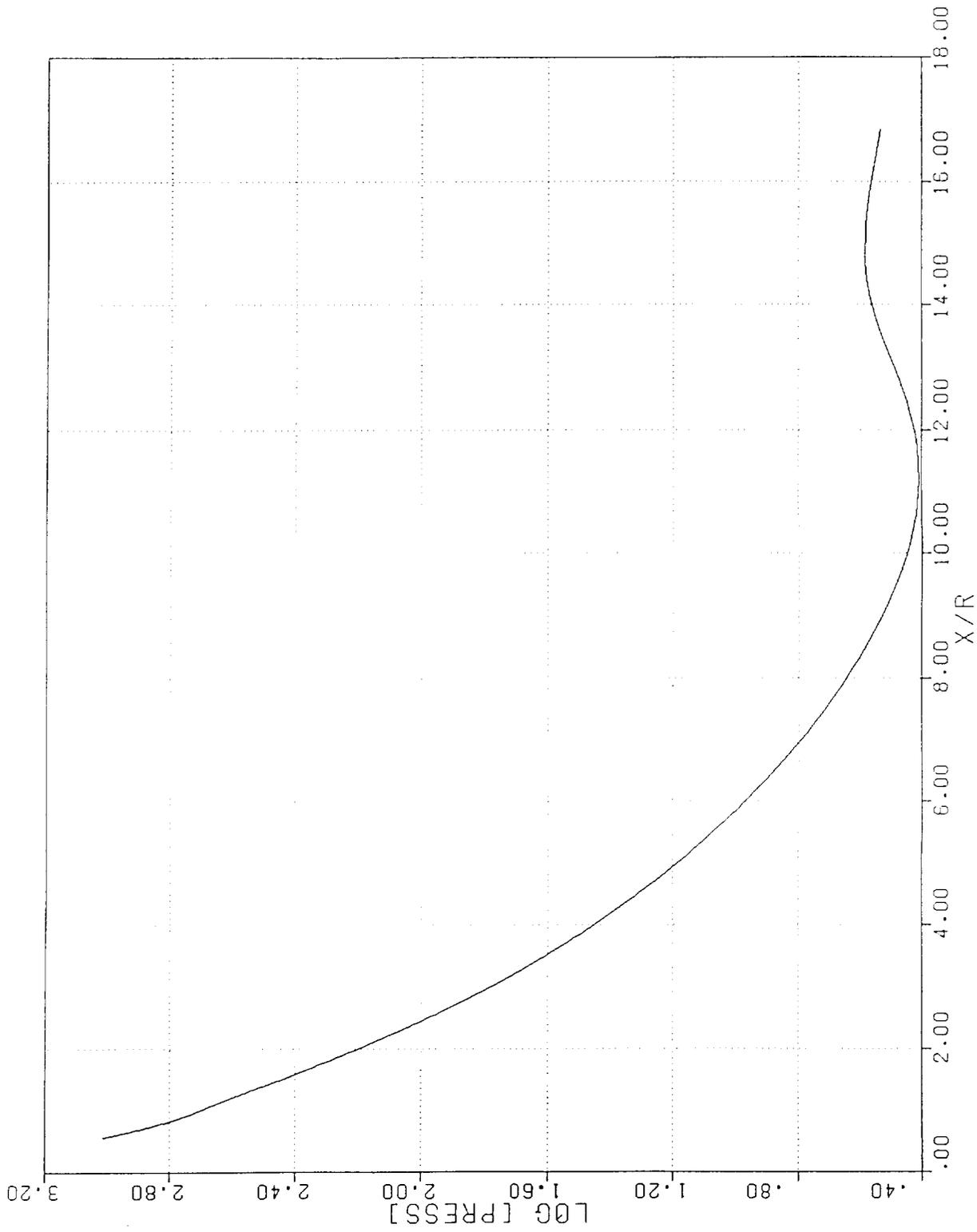
Figure 17. Log of Pressure (psi) vs X/r^* Along the Centerline. 650K STME

T930345

31
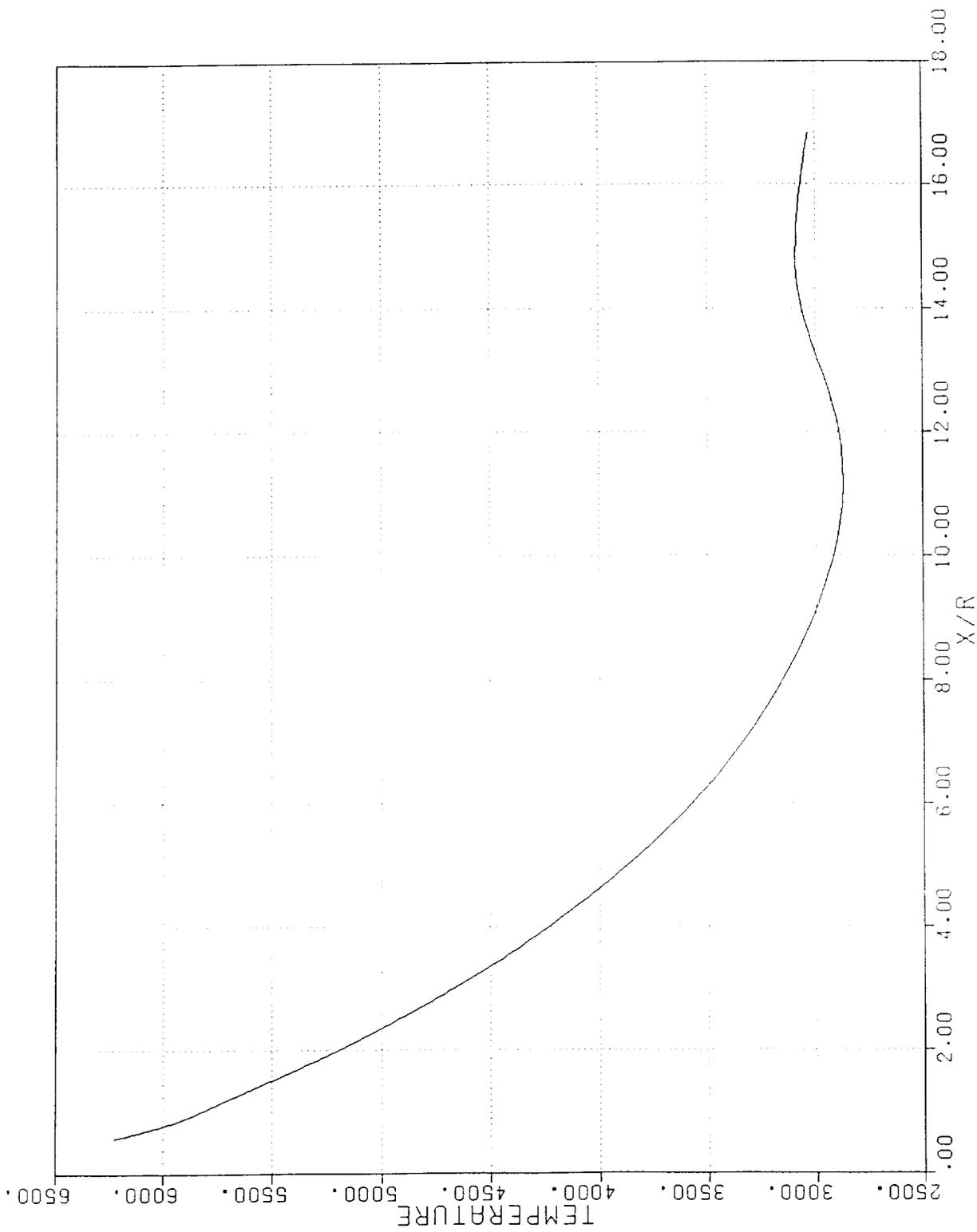
Figure 18. Temperature (°R) vs X/r* Along the Centerline. 650K STME

T930345

32
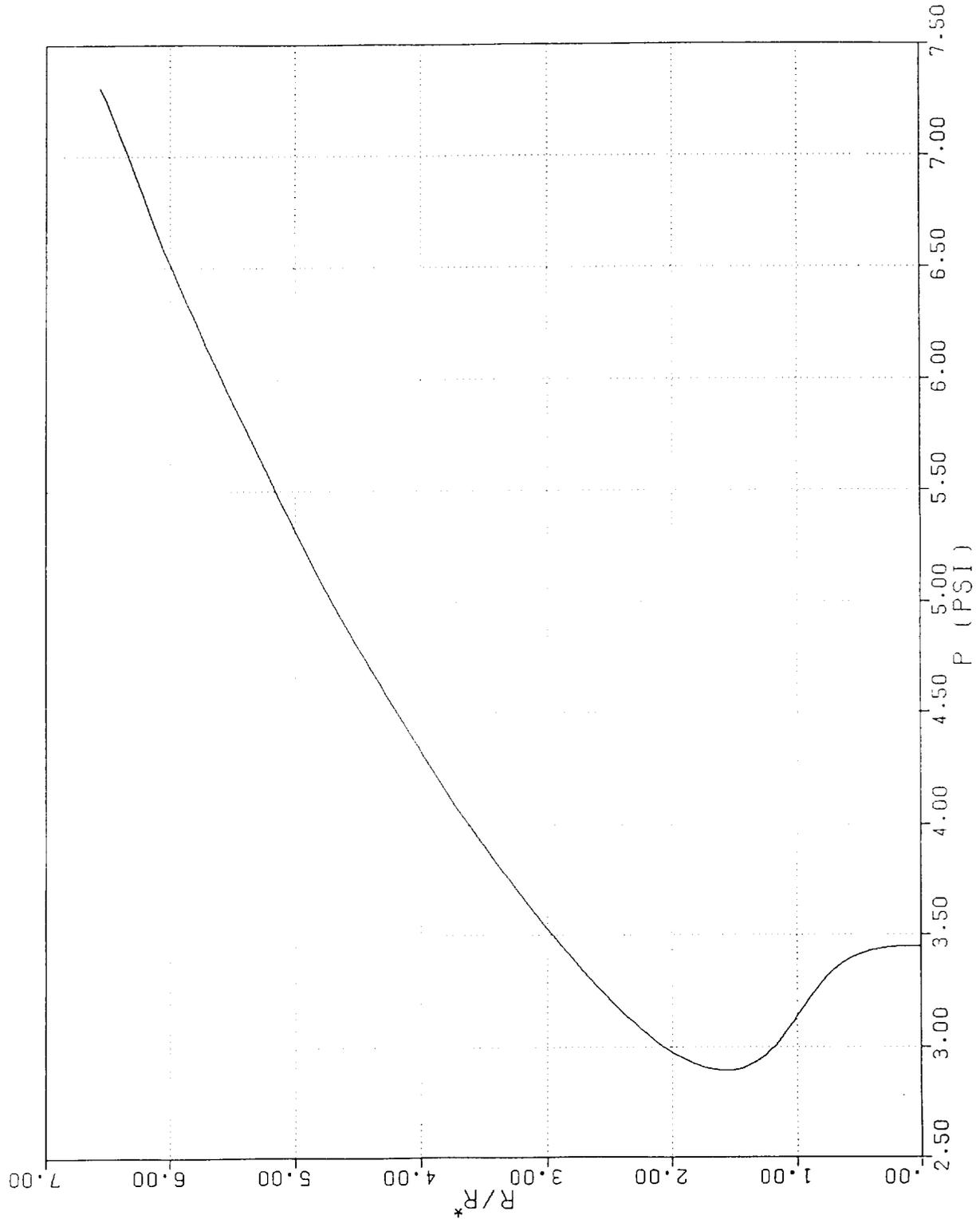
Figure 19. Pressure (psi) vs r/r* at Nozzle Exit. 650K STME

T930345

33
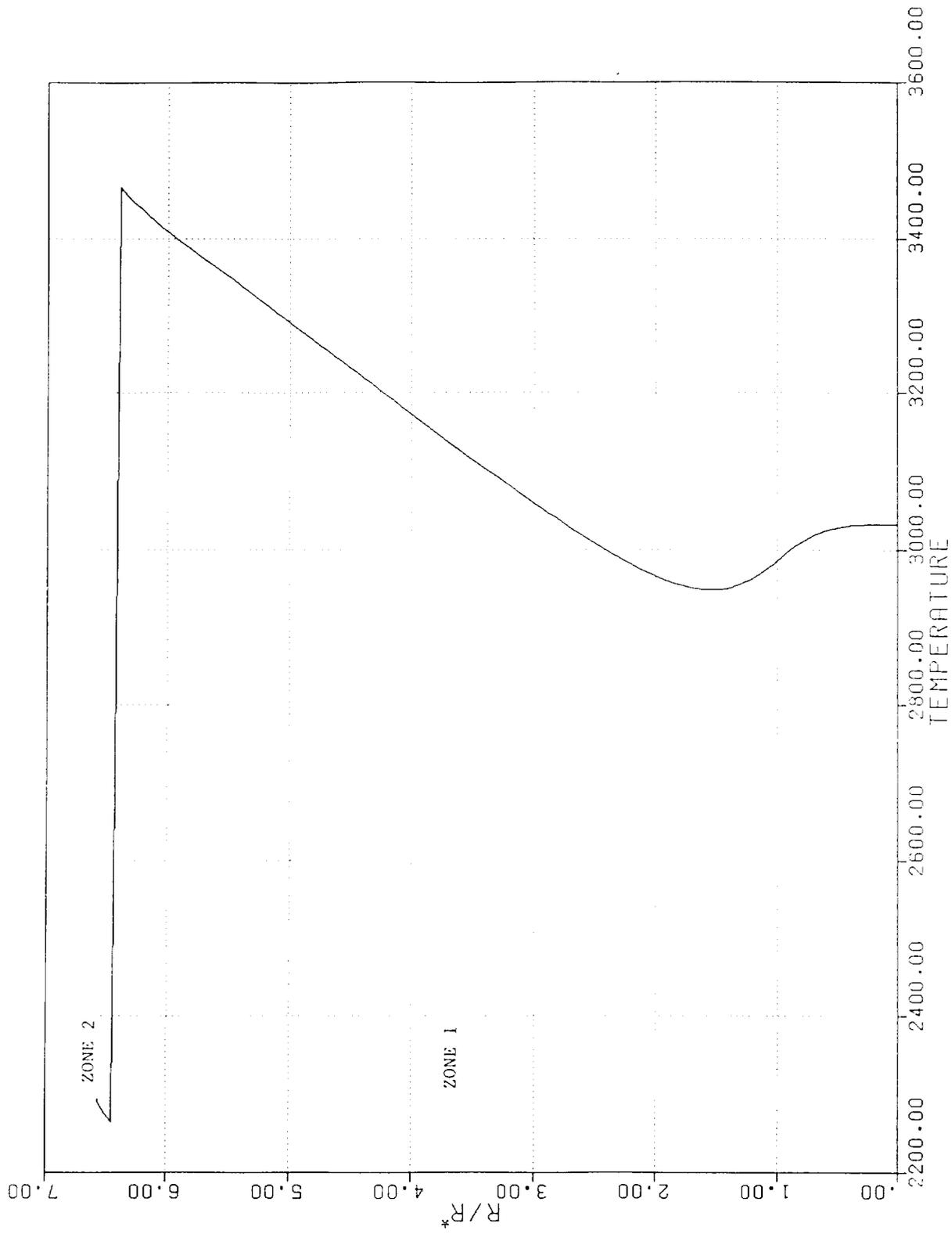
Figure 20. Temperature (°R) vs r/r* at Nozzle Exit. 650K STME

T930345

34

The overall performance summary for the 650K STME is given in Table 6. These results are intended only as an example. From this information the kinetic, two-dimensional, and boundary layer losses and their associated efficiencies with respect to ODE solutions can be identified. The energy release loss, consisting of the microscale mixing and evaporation processes, are not included in this analysis. A planned JANNAF workshop for the "Standardization of Injector Performance", which was approved by the Combustion Subcommittee, had to be canceled after considerable preparation by several parties involved, since the workshop coordinator did not receive the proper support from his organization. The requested review of the principles, used in the DROPMIX computer program[4], for discussion at the workshop is presented in Appendix A. One method, concerning the energy release, has been provided by means of the SCAP module coupling with the TDK program under an SBIR phase II activity[5] for hydrocarbon propellants. This information is available to the government only at this time.

---

4.   Nurick, W.H., *DROPMIX-A PC Based Program for Rocket Engine Injector Design*, 27th JANNAF Combustion Meeting, Vol. II, pp 435-468, Cheyenne, Wyoming, November 1990.

5.   Nickerson, G.R., and Johnson, C.W., *The Chemical Kinetics of LOX/Hydrocarbon Combustion*, SBIR 88-1, Phase II, Contract NAS8-38468, Software & Engineering Associates, Inc., Carson City, Nevada, 25 July 1992.

Table 6. Performance Summary, 650K STME

PRIMARY CHAMBER OPERATING CONDITIONS

CHAMBER PRESS	[PSIA]	2250.000
CHAMBER TEMP	[R]	6659.095
MIXTURE RATIO	[-]	6.993572
H (OXID)	[CAL/MOLE]	-2899.000
H (FUEL)	[CAL/MOLE]	-1963.000
HCHAM (ODE)	[BTU/LB]	-309.6788
DELH (AVERAGE)	[BTU/LB]	52.26500
DELH1 (AVE)	[BTU/LB]	.0000000E+00

PRIMARY CHAMBER GEOMETRY

ECRAT	[-]	2.682000
RI	[-]	1.598000
THETAI	[DEGREES]	25.42000
RWTU	[-]	.4940000
RSI	[INCHES]	6.900000
RWTD	[-]	.2000000
NIT	[-]	149.0000
THE	[DEGREES]	8.312000
THETA	[DEGREES]	29.22800
EP (NOZZLE)	[-]	43.09743

EXIT FLOW PROPERTIES

P (AXIS,EXIT)	[PSIA]	3.376344
P (WALL,EXIT)	[PSIA]	7.344903
T (WALL,EXIT)	[R]	2284.013
V (WALL,EXIT)	[FT/SEC]	13825.06
MA (WALL,EXIT)	[-]	4.012410

ONE-DIMENSIONAL FLOW PERFORMANCE

ISP (ODE)	[SECONDS]	450.0189
ISP (ODK)	[SECONDS]	.0000000E+00
ISP (ODF)	[SECONDS]	423.3352
CSTAR (ODE)	[FT/SEC]	7392.1
CSTAR (ODK)	[FT/SEC]	.00000E+00
CSTAR (ODF)	[FT/SEC]	7259.7

TWO-DIMENSIONAL FLOW PERFORMANCE

CD	[-]	.9830918
CF (TDE)	[-]	1.914218
CSTAR (TDE)	[FT/SEC]	7520.139
THRUST (TDE)	[POUNDS]	644201.9
WDOT (TDE)	[LB/SEC]	1439.825
ISP (TDE)	[SECONDS]	447.4168

BOUNDARY LAYER PARAMETERS

DFOPT (MABLE)	[POUNDS]	-4740.005
DF (MABLE)	[POUNDS]	-6740.552
DISP (MABLE)	[SECONDS]	-4.548628
THETA (EXIT)	[INCH]	.3118915
DEL* (EXIT)	[INCH]	.5427712
DEL* (THROAT)	[INCH]	-.6042980E-02
WDOT (GG)	[LB/SEC]	42.06187
EP (REGEN)	[-]	6.809522
SQDOT (REGEN)	[BTU/SEC]	75429.73
SQDOT (LOSS)	[BTU/SEC]	17633.74
SUM QDOT	[BTU/SEC]	93063.48
DH (SUM QDOT)	[BTU/LBM]	62.80066

B/L PARAMETERS WITH MASS ADDITION

DEL* BODY	[INCH]	.9672369
DF THETA	[POUNDS]	13132.39
DF DEL* BODY	[POUNDS]	-2000.547
DF MDOT	[POUNDS]	-17872.40

THRUST CHAMBER PERFORMANCE

THRUST (TC)	[POUNDS]	650942.4
CF (TC)	[-]	1.882642
MR (TC)	[-]	6.330408
WDOT (TC)	[LB/SEC]	1481.887
ISP (TC)	[SECONDS]	439.2659

4.0 RECOMMENDATIONS

The focus of this work effort has been to upgrade the TDK[3] code so that it is better suited for use in supporting STME design and evaluation studies. Several recommendations are made here that would further the usefulness of the program in this respect.

1) TDK presently requires that distributed energy release efficiency be calculated using input of results from another code. In practice these inputs are usually not available. It is recommended that a simplified method, such as that developed by Nurick[4] (see Appendices) be added to TDK so that a creditable procedure for estimating distributed energy release efficiency is available to the user. The method should be expanded to include all propellants and injector types of current and projected interest.

2) The next logical step in developing the TDK software system is to add the VIPER[2] code as a module for the purpose of calculating the expansion of nozzle exhaust downstream of the throat plane. The need for a nozzle boundary layer calculation downstream of the throat plane would then be eliminated since viscous wall effects are included in a fully coupled manner by the PNS method. This would eliminate the need for a second pass through TDK. Many users of the code find the JANNAF procedure for core flow-boundary layer iteration to be confusing. Use of a PNS code eliminates this part of the procedure. SEA's version of VIPER currently has the capability of treating tangential slot injection with finite rate chemical kinetics.

3) It is recommended that TDK be provided with a Graphics User Interface (GUI) for input and output. MOTIF with X-Windows should be used for this purpose since it is now becoming a standard for computer work stations. It appears that in the near future all important software application codes will be expected to operate in an X-Windows environment.

REFERENCES

1. Nickerson, G.R., Coats, D.E., Dang, A.L., Dunn, S.S., and Kehtarnavaz, H., *Two-Dimensional Kinetics (TDK) Nozzle Performance Computer Program, Volume I, II, and III*, Software and Engineering Associates, Inc., NAS8-36863, dated 31 March 1989, prepared for George C. Marshall Space Flight Center.

2. Kawasaki, A.H., Berker, D.R., Coats, D.E., Dunn, S.S., and Nickerson, G.R., *Viscous Interaction Performance Evaluation Routine for Two-Phase Nozzle Flows With Finite Rate Chemistry, VIPER 2.0, Computer User's Manual*, Software & Engineering Associates, Inc., PL-TR-92-3053, January 1993 prepared for Phillips Laboratory.

3. Nickerson, G.R., Berker, D.R., Coats, D.E., and Dunn, S.S., *Two-Dimensional Kinetics (TDK) Nozzle Performance Computer Program Volume III, Users Manual*, Software and Engineering Associates, Inc., NAS8-39048, dated 31 March 1993, prepared for George C. Marshall Space Flight Center.

4. Nurick, W.H., *DROPMIX-A PC Based Program for Rocket Engine Injector Design*, 27th JANNAF Combustion Meeting, Vol. II, pp 435-468, Cheyenne, Wyoming, November 1990.

5. Nickerson, G.R., and Johnson, C.W., *The Chemical Kinetics of LOX/Hydrocarbon Combustion*, SBIR 88-1, Phase II, Contract NAS8-38468, Software & Engineering Associates, Inc., Carson City, Nevada, 25 July 1992.

APPENDIX A

Review of the DROPMIX Computer Program

Introduction

At the request of the NASA/MSFC, a review of the DROPMIX methods and computer program was conducted. DROPMIX is documented in Reference A-1. The computer program was supplied to SEA, Inc. by NASA/MSFC. It is written in the BASIC language for a personal computer, and was installed at SEA on a 486 PC with DOS. The program was provided to SEA, Inc. for evaluation purposes only. A trip was taken to Irvine to discuss the DROPMIX analysis and its supporting data base with the author, Mr. William Nurick, who was most helpful and generous with his time.

Discussion

As discussed in Reference A-1, DROPMIX is one of a series of engineering analysis codes developed by W.J. Schafer Associates, Inc. for the Air Force for the purpose of assisting that organization in developing a booster engine for the Advanced Launch Vehicle. DROPMIX is the injector engineering analysis code in that series. It provides inputs to a thrust chamber vaporization model program, PC DER, which is based on an adaptation of the Standardized Distributed Energy Release program developed by Rocketdyne in 1978.

The methods used by DROPMIX are discussed in some detail in Reference A-1, a copy of which is provided with this report as Appendix B. A review of the paper by SEA, Inc. revealed errors in several of the equations. These were shown to the author who was found to be aware of most of them. The copy of the paper given in Appendix B has been annotated by SEA, Inc. with corrections, and also with notes that are intended to clarify certain items. It must be stated that the errors found are nearly all typographical in that a cross-check of the DROPMIX source code detected no errors of any importance.

The methods presented in the paper are empirical, and take advantage of the fact that measurements of spray distributions obtained using both single elements and multi-element injectors exhibit the same distribution whenever the measured mixing efficiency, E_m, is the same. Thus, if E_m can be predicted with reasonable accuracy, then a powerful tool is available for estimating combustion chamber distributed energy release efficiency. Nurick believes that his methods allow E_m to be estimated to within ~1%. However, these methods involve using the PC DER code for which documentation is not yet available.

A-1.   Nurick, W.H., *DROPMIX-A PC Based Program for Rocket Engine Injector Design*, 27th JANNAF Combustion Meeting, Vol. II, pp 435-468, Cheyenne, Wyoming, November 1990.

Measured mixing efficiency, E_m, was originally defined by Rupe[A-2], and in the limit of an arbitrarily large number of samples corresponds to equation (1) in Reference A-1. The distribution function used by Nurick is given by equation (3) in Reference A-1. These functional relationships are explored in some detail in Appendix C, which also contains charts illustrating their behavior.

The difficulty with an empirical approach of this type, of course, is that it cannot be extended beyond its existing data base with any confidence. To do so could lead to large errors. Furthermore, the data base is not of uniform quality. Large engines are emphasized over small engines, and for some injector types little or no data is presently included.

Nevertheless, the data base contained in DROPMIX does include the results of many years of engine testing and the code itself is thought to provide a reasonably good description of the over-all mixing and atomization processes that occur in real rocket engines. The approach offers the possibility of becoming a highly valuable tool in the near term. That is, it should be applicable to the development of the next generation of large rocket engines.

In contrast to Nurick's methods, this author is of the opinion that the CFD methods now being developed are not only years away from adequately modeling these processes, but also are very expensive to apply. The Nurick approach offers a practical way to bridge the gap that presently exists in this area, and will continue to exist until proven CFD analysis becomes available at some unknown time in the future.

A-2.   Rupe, J.H., "The Liquid Phase Mixing of a Pair of Impinging Streams", Progress Report No. 20-195, JPL, Pasadena, California, August 1953.

APPENDIX A REFERENCES

A-1. Nurick, W.H., *DROPMIX-A PC Based Program for Rocket Engine Injector Design*, 27th JANNAF Combustion Meeting, Vol. II, pp 435-468, Cheyenne, Wyoming, November 1990.

A-2. Rupe, J.H., "The Liquid Phase Mixing of a Pair of Impinging Streams", Progress Report No. 20-195, JPL, Pasadena, California, August 1953.

APPENDIX B

DROPMIX-A PC Based Program For Rocket Engine Injector Design

William H. Nurick
W.J. Schafer Associates, Inc.
Irvine, CA

INTRODUCTION

In 1987 the Astronautics Laboratory of Air Force Systems Command initiated development of a Personal Computer based engineering analysis codes for application to the Advanced Launch Vehicle engine development study. The codes included: (1) Engine Balance; (2) Turbopump; (3) Injector; (4) Stability; (5) Thrust Chamber Performance; (6) Regenerative Heat Transfer including Fins; and (7) Nozzle Performance design and analysis programs. The outputs from these programs have been compared against existing system component operation/ performance as well as proposed component designs for Step Transportation Main (STEP) Engines. These models have proven helpful in that independent analysis of Space Transportation Main (STEP) Engine components have identified several potential problem areas early in the design effort. This has allowed for design modifications to be made by the Contractor in a timely manner. In addition, specific deficiencies in process technology impacting predictive capability have also been identified. This paper describes the injector engineering analysis code (DROPMIX).

DROPMIX has been developed to define propellant spray dropsize and mixture ratio distributions produced by rocket engine injectors. This program utilizes the current state-of-art injector single element mixing and atomization correlations and includes two new relationships, one for defining spray mass/mixture ratio distribution and the other for defining the impact on overall injector mixing quality of intra-element mixing. Most injector element designs and propellant combinations of current interest are included in the program. The output from the DROPMIX program provides the definition of the spray characteristics for a specified injector design, which is input to the thrust chamber vaporization model program, PCDER. The PCDER program is an adaptation of the Standardized Distributed Energy Release program developed by Rocketdyne in 1978. This program is used to calculate overall C* performance for a given thrust chamber configuration with specified spray characteristics. (The PCDER program is not discussed in this paper.) The predictions from these models have been compared with a range of operating flight engines as well as Research/Development engines. The results have correlated typically within 1% with measured engine performance. The formulation of DROPMIX is described in this paper.

INJECTOR SPRAY CHARACTERISTICS

The propellant distribution and liquid dropsize(s) within the combustion chamber impacts engine performance, chamber material life, and combustion stability. Therefore, achievement of the required spray characteristics is key to meeting engine mission duty cycle specifications. The propellant distribution characteristics are defined by injector element selection, manifold/element design, and face pattern. In this section the mixing and atomization processes are described relative to specific element design parameters. However, it is important to note that although the manifold design specifications can impact element mixing and atomization characteristics, the current model formulation does not include manifold impacts on propellant distributions. Consequently, the results from the DROPMIX program assume that acceptable manifold design criteria have been applied to the design.

MIXING

The interaction of the oxidizer and fuel propellant streams as they exit the injector face plane define the element mixing characteristics. Any geometric design or flow parameter that impacts the condition (i.e. shape of the exit stream, velocity, etc.) or direction of the injected propellant stream therefore impacts mixing. The interaction of the resulting element-to-element spray then defines the overall mixing within the thrust chamber. The definition of spray mixing quality is discussed below, followed by presentation of both single and multi-element mixing design criteria and characteristics for several element types.

Spray Mixing Quality

Mixing quality is defined as the sum of the mass-weighted deviations in mixture ratio from the injected mixture ratio. This is graphically shown below (next page):

This plot is for an O_2/H_2 System

$MR = 6.15$

$E_m \approx .93$

Vol:
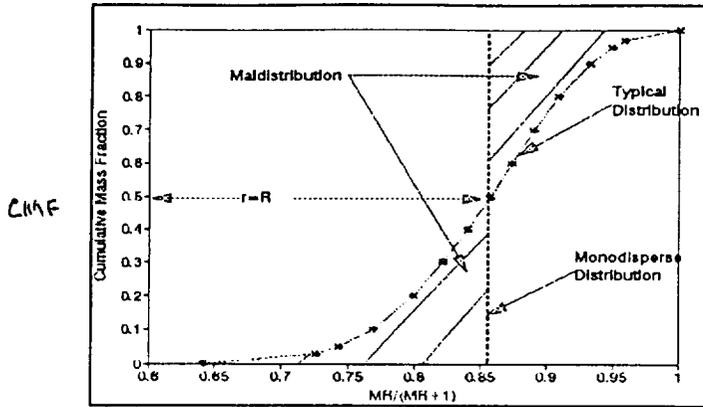
$R = ox\ fraction = \dfrac{o}{o+f}$

$MR = o/f$

Where: R= MR/(1+MR), Injected
r= MR/(1+MR), At any point within the spray $\quad and \quad MR = r/(1-r)$

Note that the shaded area between the injected MR and the actual distribution curve represents the non-uniformity of the mixture. It is easily shown that the expression describing this deviation is:

$$E_m = 1 - \frac{\int_0^{MF_{(r=R)}} (R-r)\, dMF}{\int_0^R dr} - \frac{\int_{MF_{(r=R)}}^1 (R-r)\, dMF}{\int_1^R dr} \qquad (1)$$

Since in practice the mixing distributions are obtained by capture of finite quantities of the propellant simulants occupying discrete flow areas, Equation 1 can be converted to a finite difference form identical to that of Rupe, Ref 1:

$$E_m = 1 - \sum_{i=1}^{n} \frac{MF_i\,(R-r_i)}{R}\bigg|_{r<R} - \sum_{i=1}^{n} \frac{MF_i\,(R-r_i)}{(R-1)}\bigg|_{r>R} \qquad (2)$$

Using this expression, complete mixing is represented by a value of Em of 1 and complete non-uniformity by 0.

Measurements of spray distributions obtained using single element and multi-element injectors have been plotted for a wide range in overall mixing quality (i.e. Em = 50 to 90%). Typical plots are shown in Figure 1. While all have a characteristic "s" shape the steepness of the curve, as expected, depends on the mixing quality, Em. Further analysis has shown that for a given Em the distribution is the same regardless of whether it was generated using a single or multi-element injector; and, in addition, it is also independent of the element type. The spray distribution data suggested that the relatively simple expression:

$$CMF = e^{(-b\ f(r/R)^n)} \qquad (3)$$

satisfactorily describes the distribution. The boundary conditions (i.e. necessary to define b & f[r/R]) were chosen consistent with the measured distribution data which clearly shows that the curve follows a well defined asymptote as r approaches 1 and tends to ~~go to zero at real~~ be small for values of r near 0. The resulting value for the constant in Equation 3 is:

$$b = 0.693$$

$$b = -\ln\tfrac{1}{2}$$

The functionality expression is:

$$f(r/R) = [(r-1)/(R-1)]$$

The value of n depends on the mixing quality (Em). Therefore, affixing a value to n in Equation (3) requires first defining the parameter Em, which relates the shape of the curve to the overall distribution. Typical curves for several values of Em compared with prediction using Equation 3 are shown in Figure 2. As indicated in Figure 2, the prediction for mixing distributions compared against cold flow data is excellent. It should be noted that comparisons with a wide range of element types and element configurations have been made with the same degree of fidelity as that shown in Figure 2.

436
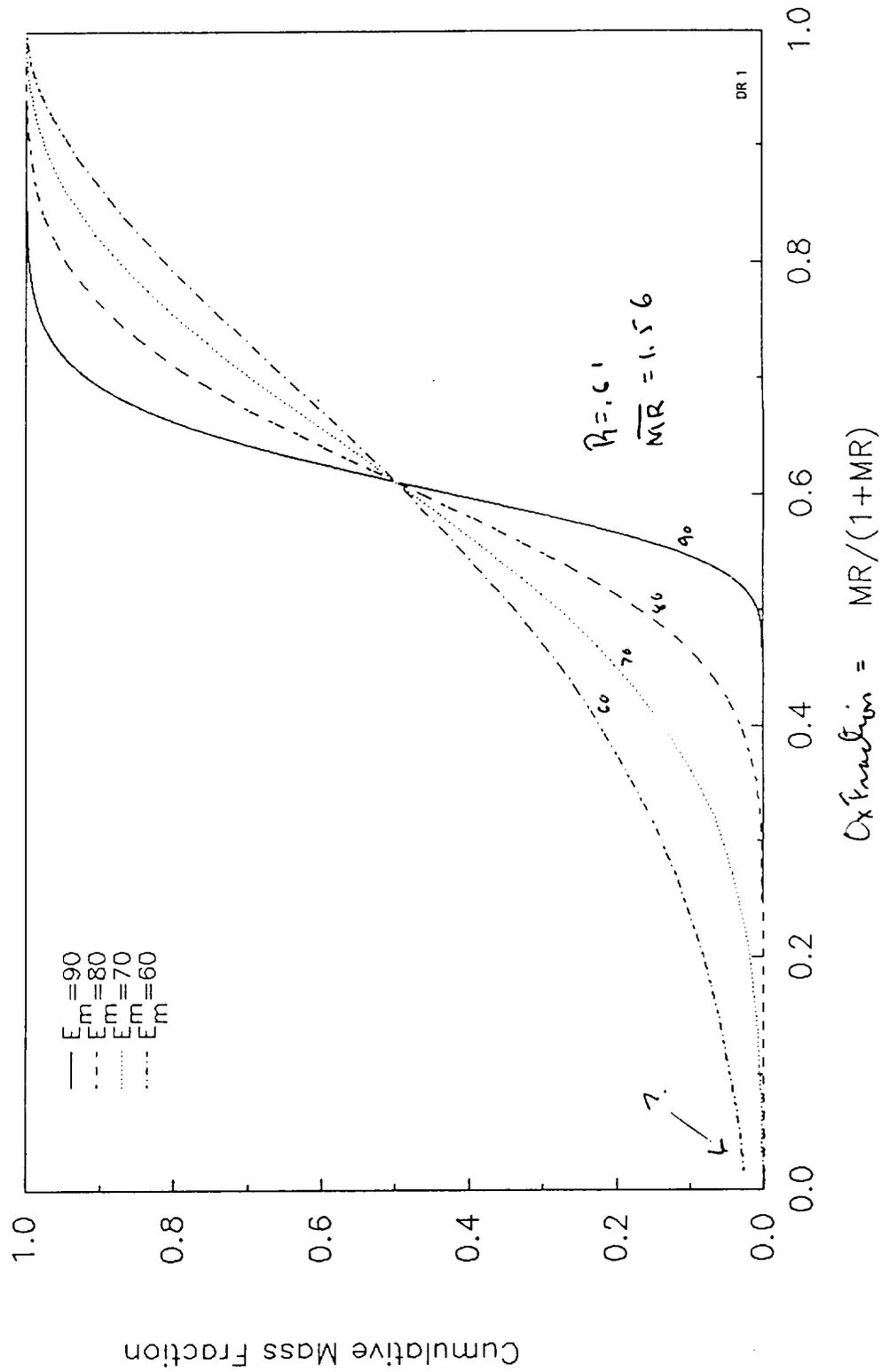
Fig. 1, Predicated Mixing Distribution Uniformity for several values of E_m using Equation 3.

* ROCKETDYNE DATA — MULTIELEMENT LIKE DOUBLET INJECTORS
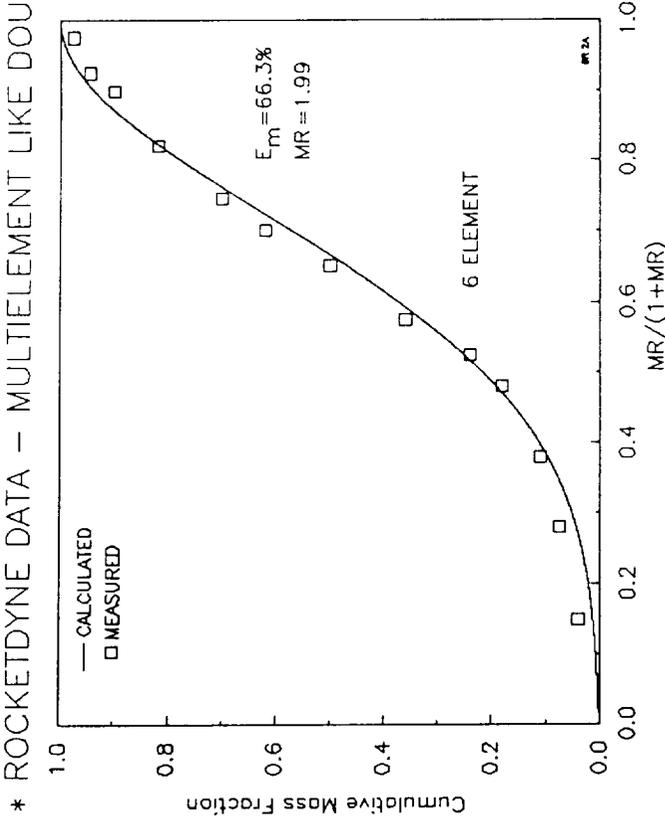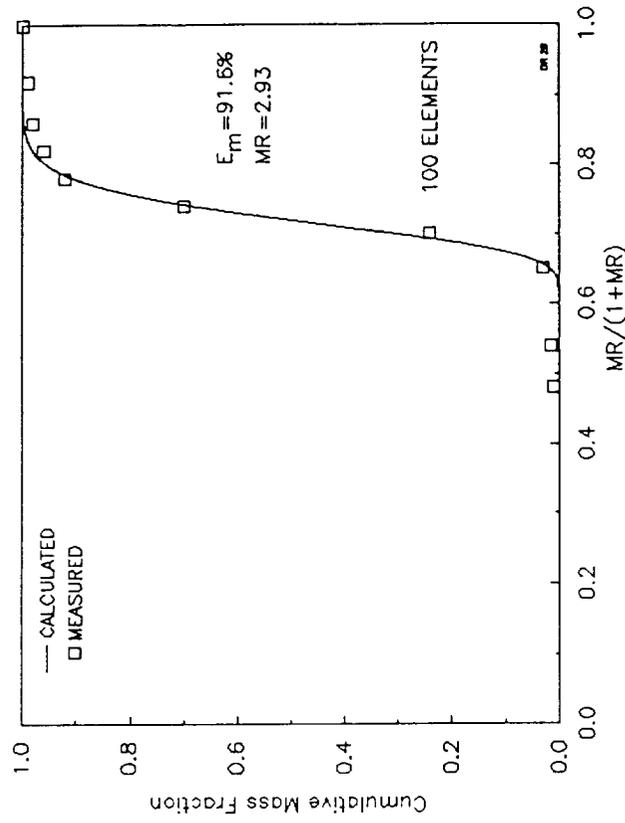
* AEROJET TECHSYSTEMS DATA — SINGLE ELEMENT LIKE DOUBLET
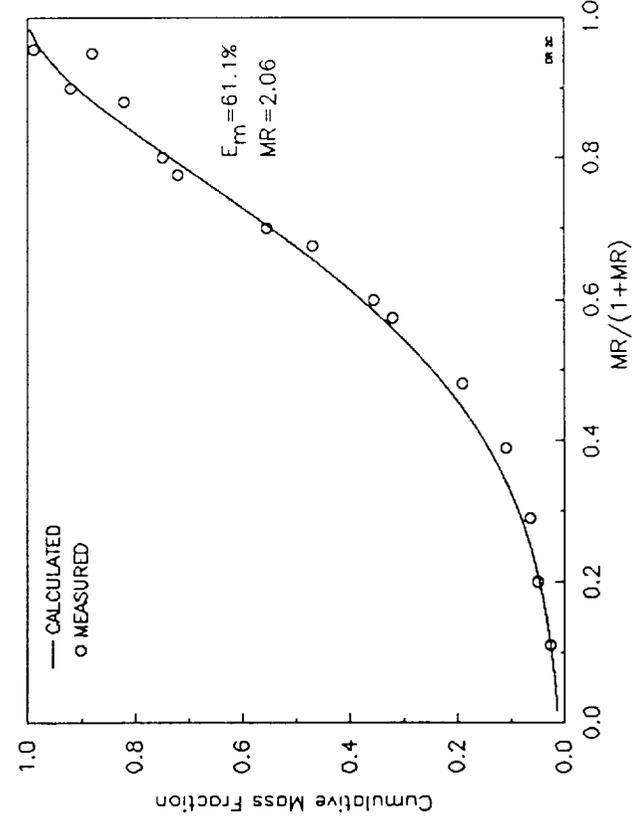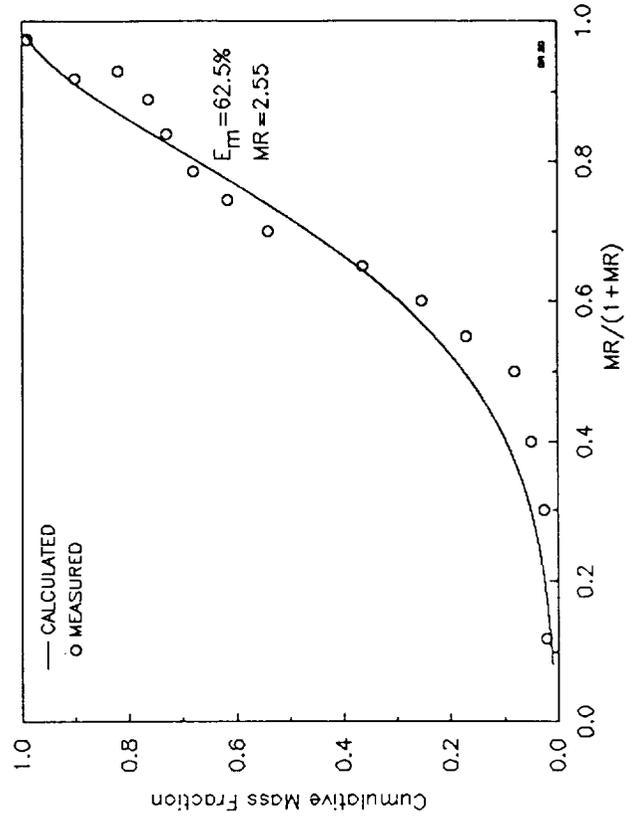
Fig. 2, Comparison of Measured Mixture Ratio vs. Calculated Distribution

438

B-4

Single Element Mixing

Within the combustion environment measurement systems do not currently exist that can determine the mass and mixture ratio distribution produced near the injector by an element. This limitation has led to the development of cold flow techniques using nonreactive propellant simulants. The initial development studies we conducted at JPL (Ref. 2, 3, and 4), and later by the engine development Contractors (Ref 5, 6, and 7). Over the years the simulation techniques have been refined as it was determined that other variables such as orifice cavitation and gas density were important to simulate, as they impacted the spray distributions. Currently, measurements are being made in pressurized chambers simulating both the cavitation and chamber gas density using spray collection measurement systems. Unfortunately, to date there are only limited mixing data available that were obtained under these simulated back pressure conditions. These data, although limited, have been utilized to screen much of the early cold flow mixing data and reject that which is clearly invalid. The equations presented in this paper are considered by the Author to be the best currently available. However, it is obvious that these relationships should be verified as new data obtained under more representative simulation conditions become available and, where appropriate, changed. Currently the Astronautics Laboratory is undertaking an experimental program to develop mixing and atomization data for several element types. It is planned to incorporate the results into DROPMIX.

Single element mixing data were used to establish several parameters: (1) the maximum attainable value of Em; (2) the dynamic and geometric conditions providing the maximum Em; and (3) an expression for defining the value of Em given the element design and operating conditions. The effort concentrated on element types and propellant combinations of current interest. The mixing quality characteristics for the element types and propellants contained in DROPMIX are given below:

TABLE 1 - MAXIMUM SINGLE ELEMENT MIXING QUALITY

Propellant State	Element Type	Mixing Quality
Gas/Gas	Coaxial	99%
Gas/Liquid	Coaxial	95%
	Like Doublet	65%
	UnLike Triplet	81.5%
	Unlike Pentad	81.5%
Liquid/Liquid	Like Doublet	80%
	Unlike Doublet	80%
	Unlike Triplet	93.2%
	Unlike Pentad	94.7%

It should be noted that these values of maximum Em represent those from specific single element configurations typically having orifice L/D's of 10 or greater and in some cases rounded inlets. They should therefore be considered only as generic values. When mixing quality data are available for a specific design it should be substituted for the generic value. The conditions providing maximum Em for the various elements are discussed below:

Gas/Gas Propellants

Design criteria for mixing of gas/gas elements are limited to the coaxial element.

Coaxial Element - A correlation for the gas/gas coaxial element describing the mixing characteristics as a function of geometric and flow parameters was developed by Dickerson (Ref 8) in the late 1970's. This correlation was successfully applied in the 1980's to advanced combustor systems using gaseous propellants. The correlation, however, while predicting the mixing characteristics of two concentric gaseous jets, does not provide for a single expression for maximum mixing. Obtaining the required mixing level, therefore, requires a series of iterative calculations. This correlation is not currently included in the DROPMIX program, although there are plans to include it in the future.

Gas/Liquid Propellants

Design criteria for gas/liquid elements are limited to the coaxial, like impinging doublet, and the unlike impinging triplet and pentad elements.

Coaxial Element - Gas/liquid coaxial elements have been divided into two types: (1) shear and (2) swirl. For the shear coaxial element both the gas and liquid flow axially with no tangential flow component. In the swirl coaxial element one or both of the propellants are swirled. Sufficient cold flow mixing characteristics for the swirl coaxial element are not currently available, although some limited data of Aerojet suggest that the mixing characteristics for their hollow cone swirl coaxial element are insensitive to flow dynamics. Currently, Aerojet assumes that the mixing levels are constant at Em=80%. Other data of Rocketdyne using a different liquid swirler design that distributes the liquid throughout the cone, suggests that the mixing is similar to that of the shear coaxial element. Until more detailed correlations are developed and made available DROPMIX assumes that both shear and swirl elements produce the same mixing levels, regardless of the extent of

swirl. It should also be noted that cold flow data show that the size of the element does not significantly impact the element mixing quality levels.

For the shear coaxial element the mixing characteristics from Ref 9 are shown in Figure 3. Note that the mixing quality was found to be a function of the gas mass flux, the ratio of liquid to gas mass flow rate, and the liquid velocity. The mixing level is also shown to depend on the liquid post recess. Based on these data the maximum mixing quality occurs at:

$$(E_m)_{max} \frac{(\rho_g V_g)^2}{MR \ V_l} - 2000; \ For \ Recess-1 \qquad (4)$$

DROPMIX contains both the above equation as well as a curve fit relationship for the recess of zero curve, shown in Figure 3. In addition, an expression relating recess to mixing at a given operating condition is also included in DROPMIX.

Like Doublet Element - Like doublet gas/liquid mixing design criteria developed by Falk (Ref 10) were used in DROPMIX to define the impact of design parameters on mixing quality. Falk varied the fan spacing and fan cant angle, Figure 4. The results provided the design criteria resulting in maximum mixing quality as:

Fan Spacing = 0
Fan Cant Angle = 15 degrees

DROPMIX contains relationships describing the mixing characteristics shown in Figure 4 so that single element mixing quality can be determined for any design condition.

Unlike Triplet and Pentad Elements - Limited mixing data for these elements exists so the correlation should be considered as only interim at this time. Maximum mixing occurs when the liquid jet penetrates to the center of the gas jet, or:

$$(E_m)_{max} @ \ 1.25 \ SIN \ (\alpha) \ (\frac{W_{out}}{W_{in}}) \ (\frac{\rho_{in}}{\rho_{out}})^{0.5} \ (\frac{d_{in}}{d_{out}}) - 0.5 \qquad (5)$$

Only limited data are available showing the impact of off-design conditions on mixing quality for the triplet and none exists for the pentad. Consequently, the ability to define mixing quality for these elements in DROPMIX is limited. DROPMIX does, however, include off-design conditions for the triplet element. The results using these correlations should be used with some caution until more mixing data are available.

Liquid/Liquid Propellants

Design criteria for liquid/liquid elements are well documented and DROPMIX includes analysis for the like impinging doublet element as well as the unlike impinging doublet, triplet, and pentad elements.

Like Doublet Element - Single element mixing for the like doublet is defined as that occurring between an adjacent fuel and oxidizer fan, each formed by impingement of two jets of the same propellant. Extensive mixing studies have evaluated the impact of relative fan location, fan cant angle, and whether the fans mix on edges or flat sides of the fan. Studies, Ref 7 and 11, have shown that edge fan mixing provides the highest level of mixing quality. The correlations provided below are for edge-on-edge fan mixing only, although flat side fan mixing can be included at a latter date.

Curves showing the impact of fan cant angle and fan spacing are shown in Figure 5. Note that the highest mixing quality occurs when the fans are in-line (i.e. 0 spacing) with an included cant angle of 45 degrees. Further, mixing studies have also determined the minimum flow momentum required to achieve maximum mixing, Ref 12. These criteria are currently included in determining the maximum attainable mixing quality for an optimum design like doublet element. Lastly, a curve fit of the mixing characteristics shown in Figure 5 is included in DROPMIX for off-optimum design mixing level determination.

Unlike Impinging Doublet, Triplet, and Pentad Elements - Numerous studies have been conducted to define mixing characteristics for unlike impinging elements. In all cases mixing quality tends to maximize according to a balance between the relative fuel/oxidizer momenta. Typical curves showing mixing quality characteristics are shown in Figure 6. The general equation that describes mixing characteristics is:

$$(E_m)_{max} @ \ (W_{out}/W_{in})^2 \ (\rho_{in}/\rho_{out}) \ (A_{in}N_{in}/A_{out}N_{out})^C \ (D_{out}/D_{in})^D_H - E \qquad (6)$$

440

B-6

Mixing Uniformity (E$_m$), %

$(\rho_g V_g)^2/(MR \cdot V_L)$, LBM^2/FT^5–SEC

100

80

60

40

50   100   1000   1E4

ν 3500?

○ Recess = 0
● Recess = 1

DR3
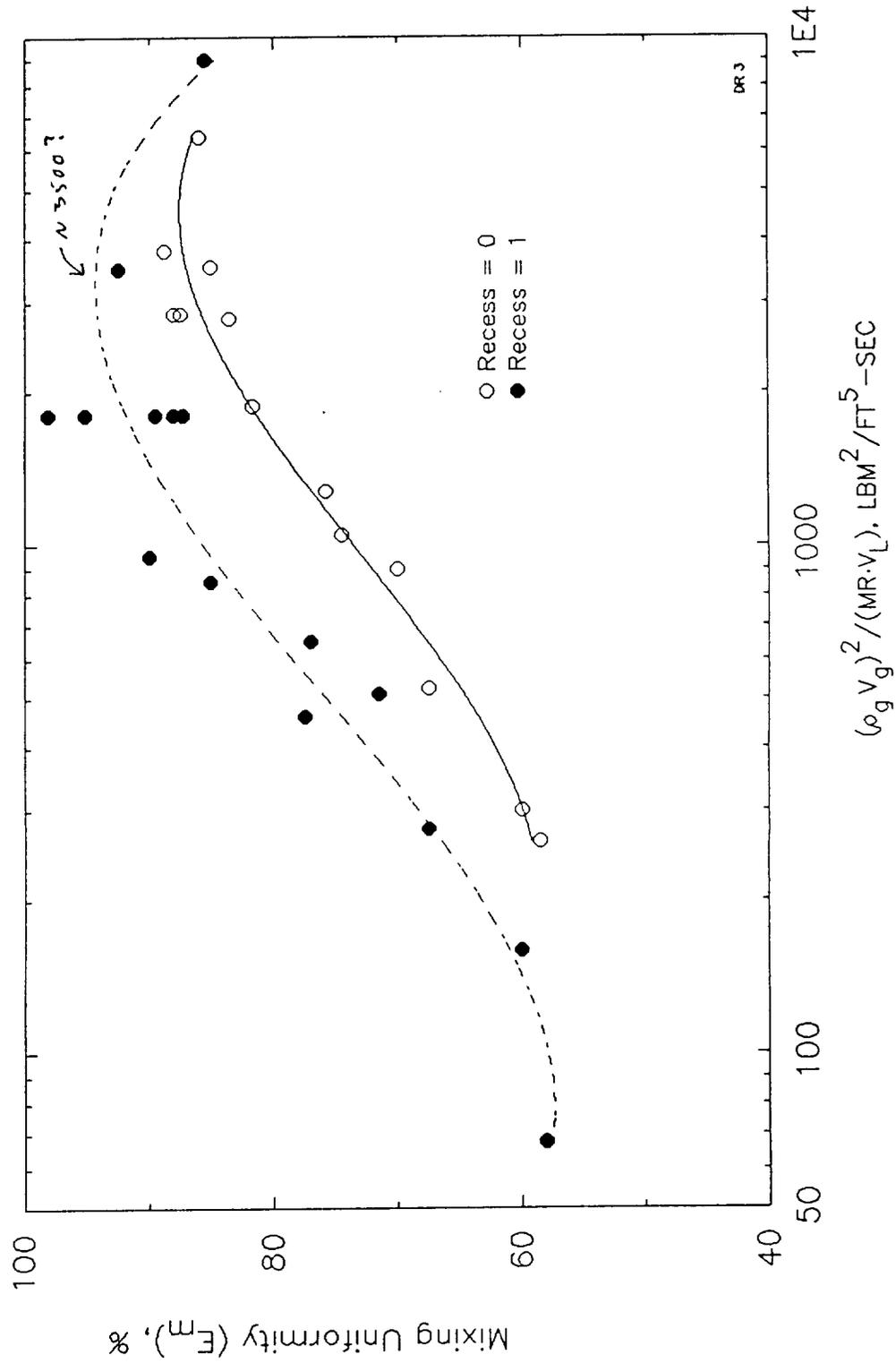
Fig. 3, Mixing Quality Characteristics for a Shear Coaxial Element
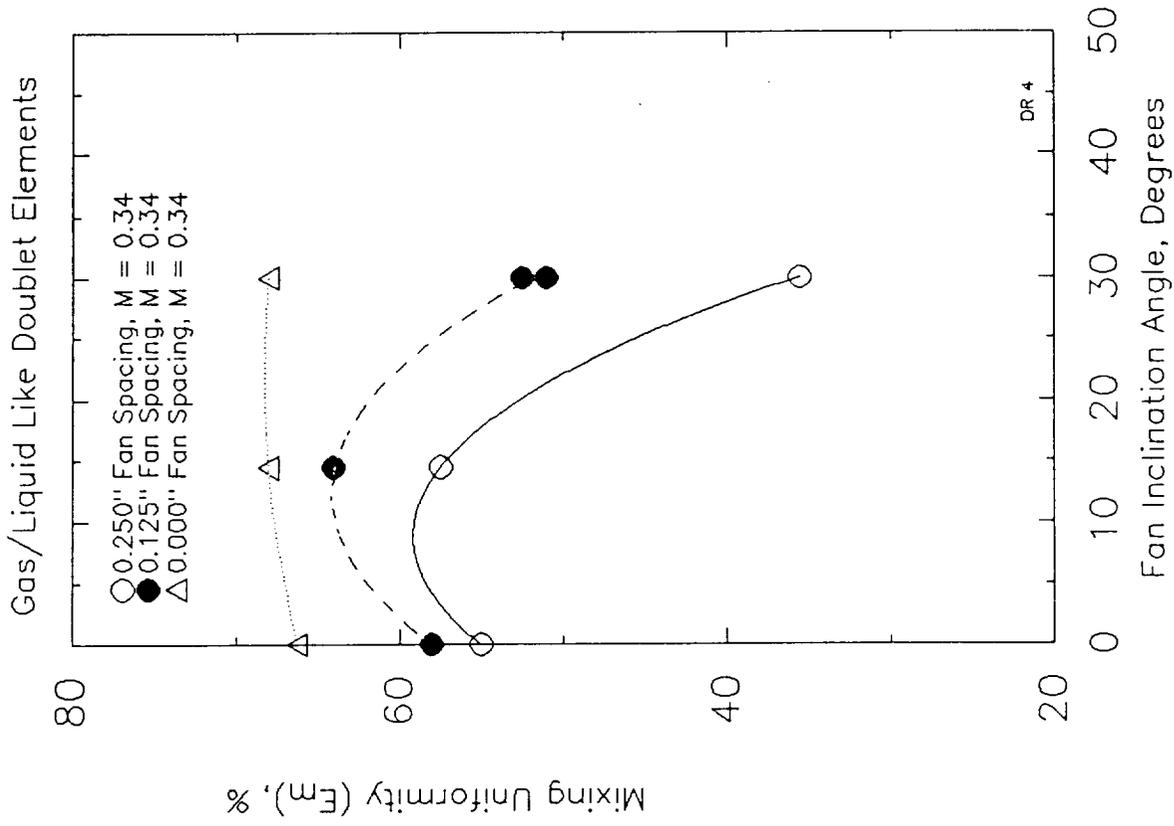
Fig. 4, Effect of Fan Spacing and Inclination Angle on the Mixing Index.
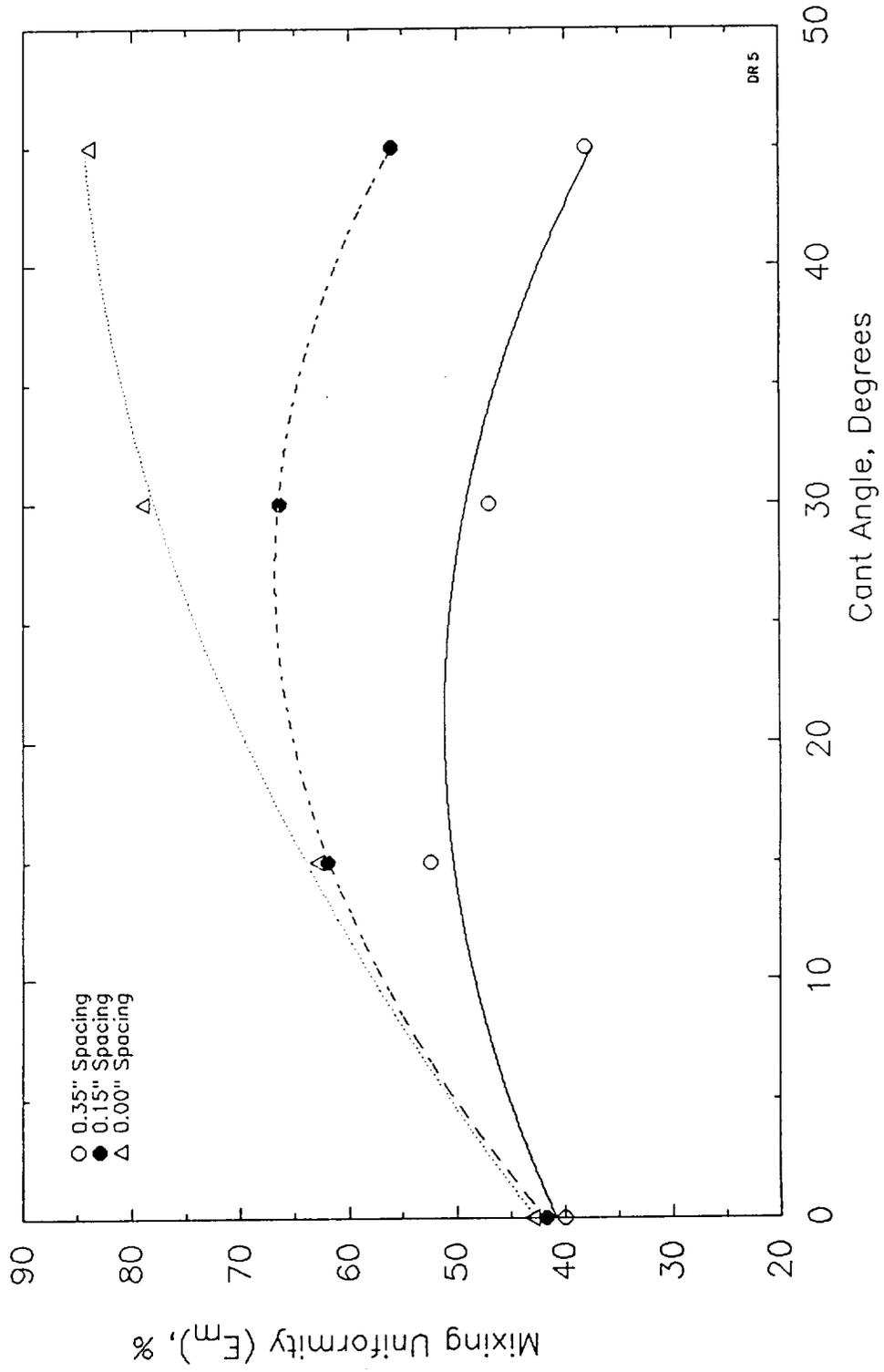
Fig. 5, Like Impinging Doublet Mixing Uniformity Characteristics for Several edge-on-edge Spacing vs. Cant Angle.
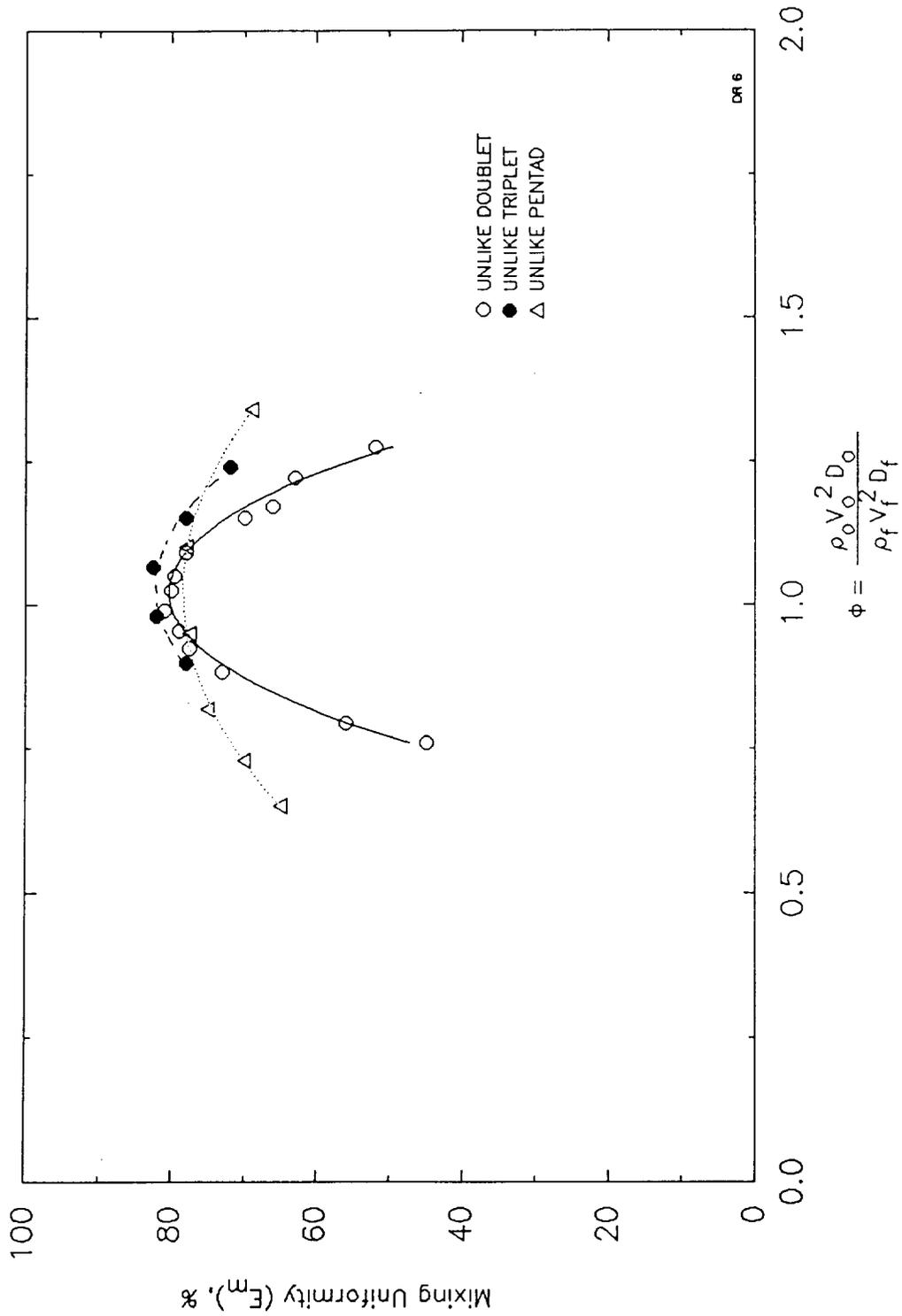
Fig. 6, Mixing Uniformity Characteristics for Several Unlike Impinging Elements.

The plot axes read:

Mixing Uniformity (E_m), %

$$\phi = \frac{\rho_o V_o^2 D_o}{\rho_f V_f^2 D_f}$$

Legend:
○ UNLIKE DOUBLET
● UNLIKE TRIPLET
△ UNLIKE PENTAD

DR 6

Early work by Rupe (Ref 1), Elverum (Ref 4), and others suggested that optimum mixing occurred when:

C=2, D=1 and E=1; Unlike Doublet, Ref 1
C=2.75, D=1 and E=0.66, Unlike Triplet, Ref 4
C=2.25, D=1 and E=2.75; Pented Element, Ref 4

The work of Elverum Ref 4 did not generate a broad data base to justify their relationships, and they noted the limited data upon which their correlations were based. Since that time considerably more mixing data have been generated (Ref 13) that has revealed that for all of the above element types mixing maximizes when:

C=2, D=1 and E=1

regardless of element type. This result is physically more realistic in that the same physical process governs mixing regardless of the number of impinging orifices. It should be further noted that regardless of orifice ratios, optimum mixing always occurred at E=1, although the maximum level of mixing at this condition is somewhat dependent on the hydraulic diameter ratio. In fact, testing over wide ranges in diameter ratio suggest, for circular orifices, this effect is generally small. An exception of this is for non-circular orifices where the hydraulic diameter ratio has a significant impact on mixing quality. In the current formulation, the independent impact of hydraulic diameter ratio on optimum mixing is only considered for non-circular orifices. Should the result of work planned by the Astronautics Laboratory (In-house) provide more extensive data on this variable the results will be integrated into DROPMIX.

Equation 6 is utilized in DROPMIX to define optimum mixing for the unlike impinging elements. The mixing characteristic curves for the various elements are included in DROPMIX for off-optimum design mixing quality prediction.

Multi-Element Mixing

The overall mixing efficiency for multi-element burner systems is not only dependent on the single element mixing level but on the inter-element mixing. The degree of inter-element mixing depends on the element density (i.e. the spacing between the elements). A plot of overall mixing quality for several injector element designs ranging from single to 120 elements, as a function of the element area density is shown in Figure 7. The element density is plotted in terms of injector face area per element (in^2/element). Note that in addition to optimum element designs, non-optimum elements are also shown. The straight line relationships suggest an Arrhenius type of equation. The general expression describing the type of relationship shown in Figure 7 is:

$$E_m = A \ \ln(x) + \ln(B) \qquad (7)$$

where: x = injector face area/element; in^2/element

The values of A and B vary as a function of the single element mixing level (assumed to be that corresponding to x=100) with the resulting relationships:

$$E_{mo} = 6.67 A + 100 \qquad (8)$$

$$E_{mo} = 2.60 B - 160 \qquad (9)$$

resulting in the final expression for the overall mixing quality of:

$$E_m = (0.15 \ E_{mo} - 14.99) \ \ln(x) + 0.385 \ E_{mo} + 61.5 \qquad (10)$$

Equation 10 can be used to define overall mixing uniformity given the single element mixing level and injector face pattern.

It should be noted that the above correlation may not be totally descriptive and a better physical relationship currently being investigated is:

$$E_m = A \ \ln[(1-No \ elements)(W_{tot}/A_o)] + \ln(B) \qquad (11)$$

Boundary Layer Cooling

Boundary layer cooling can be achieved in two ways: (1) the use of fuel injected near and parallel to the wall (i.e. film cooling) and (2) biasing the outer row of elements so that the mixture ratio differs from that of the other elements (i.e. core). For film cooling DROPMIX first calculates the injector distribution on the basis of removing the boundary layer flow from the core. Then Equation 12, adapted from Ref 14, is used to define the interaction of the coolant with the outer row of elements, which defines the outer zone mixture ratio and mass fraction. Currently the distribution of the mass/mixture ratio in the outer zone is assumed uniform, however the program is being modified to distribute the coolant evenly across the interaction portion of the

445

B-11
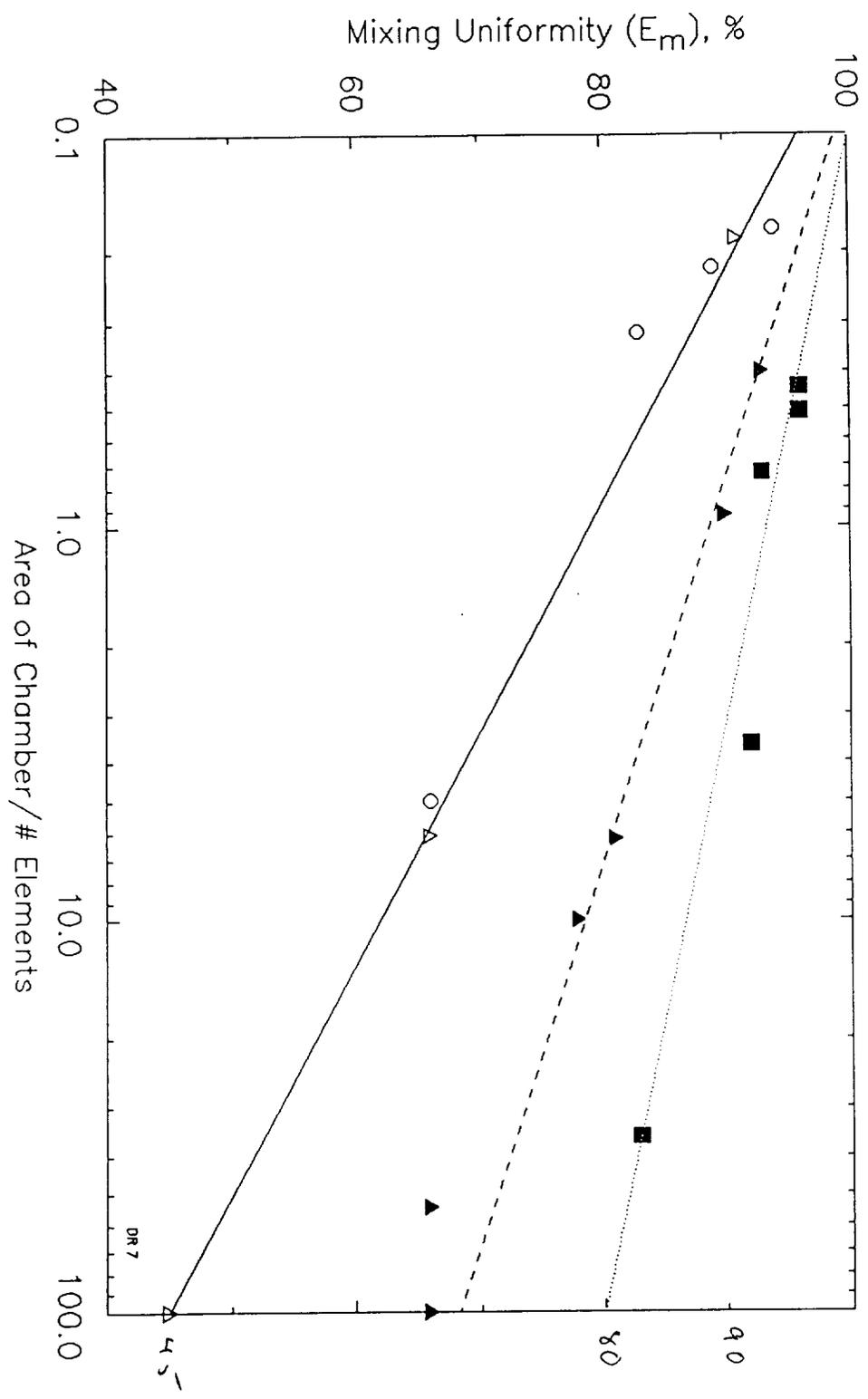
Fig. 7, Overall Injection Mixing Uniformity Characteristics

$$P_{INTERACTION} - 0.1[L'/D_c] W_{TC} \qquad (12)$$

outer element mass which is distributed as defined for the core.

Mixing Limited C* Performance

The mixing limited C* performance is defined by Equation 13.

$$\eta_{mix} - (1/C_t^*) \int_0^1 C_{(MR_t)}^* \, dMF \qquad (13)$$

Equation 13, in finite difference form, is included in DROPMIX for calculation of mixing limited performance.

ATOMIZATION

Atomization is known to occur in two processes: (1) primary atomization produced from interaction of the fuel and oxidizer propellant streams near the injector face; and (2) secondary atomization which occurs downstream due to drag forces applied to the primary droplet surface as the thrust chamber gas velocity relative to the droplet velocity increases. Both primary and secondary dropsize prediction correlations are discussed below.

Primary Atomization

The equations currently in DROPMIX defining primary dropsize for the different elements are for the most part based on wax studies conducted in the 60's and 70's. The validity of the wax technique has recently been supported by injector element spray measurements conducted at Aerojet Techsystems and UTRC, with various simulants using noninterference laser diagnostic systems ,Figures 8 and 9. Note the excellent correlation in not only the quantitative value of dropsize for the different fluids, but also the slopes; i.e. velocity and orifice size functionality.

Primary dropsize equations for the various elements are given below:

Gas/Liquid

Coaxial Element - The coaxial element is divided into two distinct types; the shear and swirl element. For the purposes of this report the shear element is defined by having both the fuel and oxidizer injected axially (i.e. without any tangential velocity component), and the swirl element is limited to only the liquid oxidizer having swirl.

Shear Coaxial. The dropsize correlation for the shear gas/liquid coaxial element was taken from the work of Falk and Burick (Ref 15) obtained using wax/nitrogen simulants at atmospheric pressure. The data suggest that for low values of the correlating parameter $[(V_g-V_l)/(MR \, V_l)]$ the dropsize was constant as indicated in Equation 14, while for larger values the dropsize decreased according to Equation 15.

$$D_m - 7112 \, (D_l \, FP) \qquad (14)$$

$$\text{when } (V_g-V_l)/(MR \, V_l) < 0.55$$

and:

$$\text{for: } (V_g-V_l)/(MR \, V_l) \geq 0.55$$

$$D_m - 5842 \, (D_l) \, [(V_g-V_l)/(MR \, V_l)]^{0.317} \, FP \qquad (15)$$

$$FP - (\mu_l/3)^{0.167} \, (\rho_g/.067)^{-0.14} \, (\sigma_l/17)^{0.33} \, (\rho_l/47.7)^{-0.58} \quad (16)$$

447
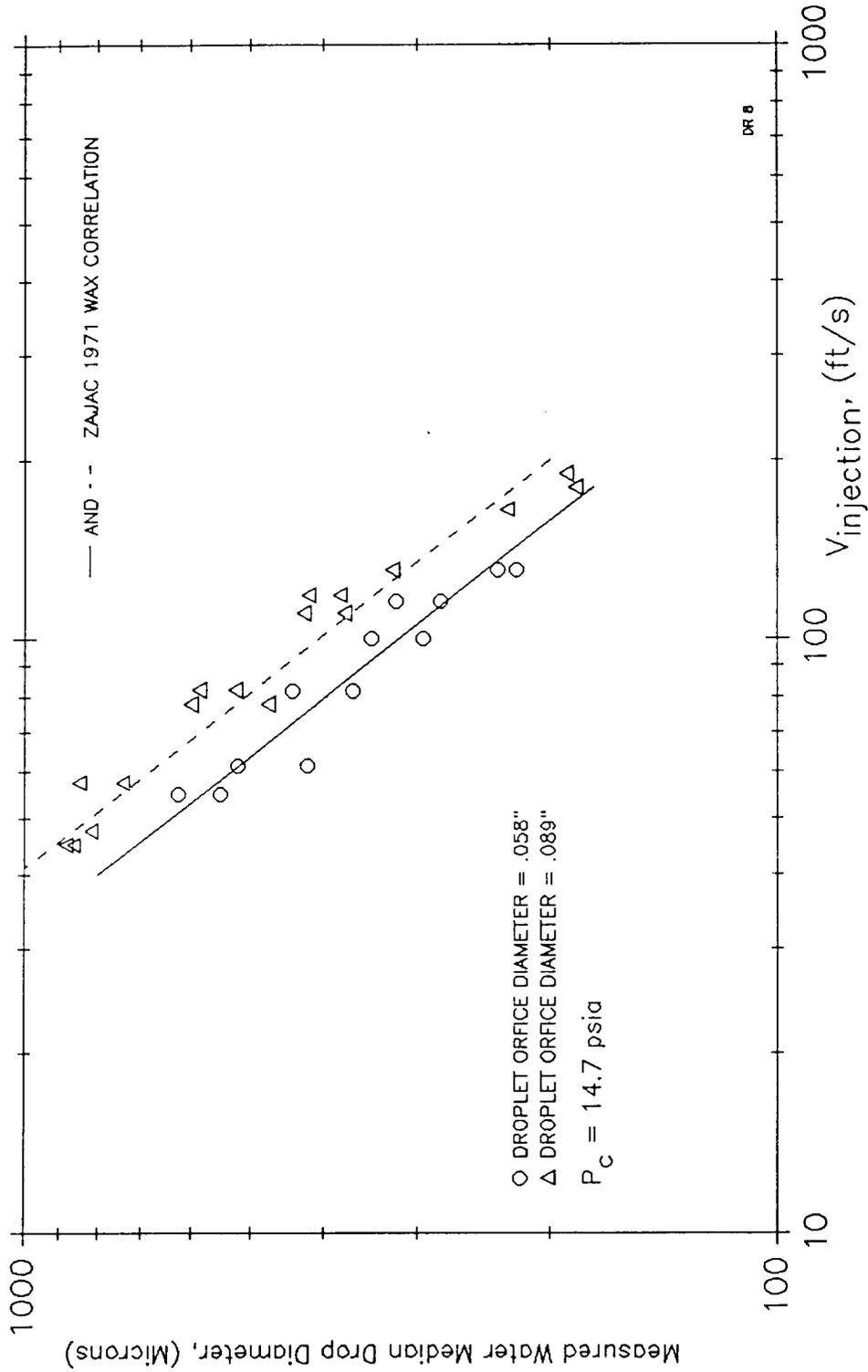
Fig. 8, Comparison of Dropsize Measurement Made Utilizing a Malvern Instrument and the Correlation obtained using Wax (Aerojet Ref 21)
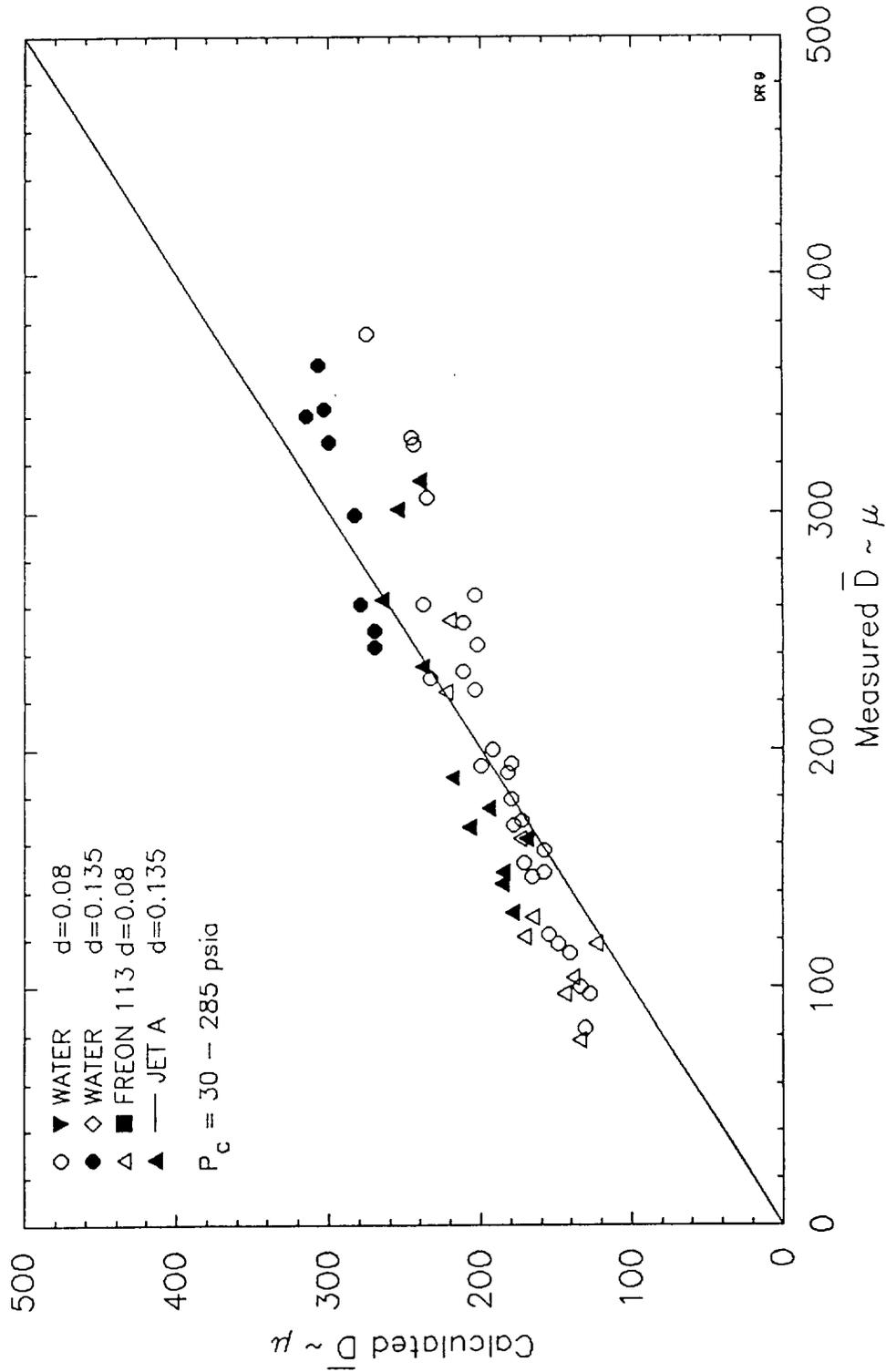
Fig. 9, Comparison of Dropsize Measurement made utilizing Malvern Instrument and the Correlation obtained using Wax. (p&W Ref 22)

449

Swirl Coaxial. Two types of liquid swirl designs are currently employed. The first uses tangential slots to swirl the fluid near the entrance of the central tube producing a hollow cone atomized spray. The other design utilizes a mechanical swirler (i.e. helix wound metal insert) to swirl the fluid producing a full flowing spray cone. For the hollow cone spray the best correlation currently available is that of Aerojet (Ref 16). The Aerojet correlation is not currently included in DROPMIX, but will be incorporated in the near future. DROPMIX currently utilizes the air blast atomization correlation by Lorebzetto and Lefebvre (Ref 17):

$$D_m - 1.41 \, [(\sigma_l \, W_l)^{0.33} / (V_r \, \rho_l^{0.37} \, \rho_g^{0.3} \,] \, [1 + W_l / W_g \,]^{1.7}$$

$$+ 0.13 \mu_l \, [D_o / (\sigma_l \, \rho_l)]^{0.5} \, [1 + W_l / W_g \,]^{1.7} \qquad (17)$$

It should be noted that there are no experimental data using swirl injection that has been used to check the accuracy of using Equation 17 with hollow cone swirl injector elements. Limited data do, however, suggest that it is a reasonable correlation for the full flow swirl injector element.

Like Doublet Element - The like doublet element correlation included in DROPMIX is that developed by Zajac (Ref 18) and Nurick (Ref 19) for liquid/liquid propellants in combination with that of Zajac (Ref 20) which accounts for the gas velocity effects at the point of injection. The correlation is:

$$D_m - \tau \, D_{oo} \qquad (18)$$

$$\boxed{A = LW} \qquad A = n\left(\frac{D}{2}\right)^2$$

$$\therefore D_j = \sqrt{\frac{4LW}{\pi}}$$

$$R_e = \rho \, V_j \, D_j / \mu$$

and for Re > 10,000

all should be lower case d

$$D_{oo} - 1.03 \times 10^5 \, V_l^{-1} \, (D_j^{0.59} \, P_l^{-0.1} \, FP \qquad (19)$$

$$.57$$

$$P_j = 1 + 13.6 \left(\frac{40}{Re}\right)^{1/2}$$

for Re < 10,000

$$D_{co} - 8700 \, V_l^{-.43} \, D_j^{0.57} \, P_l^{-0.52} \, FP \qquad (20)$$

and finally:

$$\tau - [1 + 7 \times 10^5 \, D_m \, V_l / L \, \sqrt{(V_l / V_{gas})}]^{0.41} \qquad (21)$$

$$Co \quad L \text{-} 2 \quad \text{for all cases} \qquad \text{i.e. fuel, gas}$$

It should be noted that application of the above equations to define dropsize from a like doublet injector assumes that the gas is applied uniformly over the jet rather than an impinging fan as in current like doublet gas/liquid injectors. This equation should therefore be used with some caution.

Triplet Element - Insufficient dropsize data are available for gas/liquid triplet elements. However, the process is not dissimilar to that of injecting a single liquid jet into a gas stream, as long as the gas jet diameter is infinite relative to the jet penetration length. For triplet elements where the penetration of the liquid jet is equal to or less than the gas jet radius the correlation of Nukiyama and Tanasawa (Ref 29) is utilized in DROPMIX. The Nukiyama-Tanasawa[4] equation is:

$$D_m - [585/(V_g - V_l)] \, A + 597 \, B \, (1000 \, \rho_l / (\rho_g \, V_g))^{1.5} \qquad (22)$$

$$\text{where} \quad A - (\sigma_l / \rho_l)^{0.5}$$

$$B - [\mu_l / (\sigma \rho_l)^{0.5}]^{0.45}$$

For other conditions it is assumed that the element operates similar to a like impinging element with a surrounding gas stream so that Equation 18 applies. The accuracy of application of these equations to the triplet element is highly questionable and should therefore be considered interim equations at this time.

Pentad Element - Insufficient dropsize data exists for the gas/liquid pentad element. Since the processes are similar to that of the triplet element, the pentad element is treated identically to that of the triplet gas/liquid element. The accuracy of this approach is the same as that of the triplet and therefore should again be used with caution.

450

Liquid/Liquid

Like Doublet - The like doublet element has been studied extensively by Zajac (Ref 19), Nurick (Ref 19), VanKleeck (Ref 21) and Hauptman (Ref 22). The resulting best fit equation, considering all of these studies, is that presented above as Equations 19 and 20. $\gamma = 1$

Unlike Doublet - The unlike doublet element atomization characteristics have been documented by Dickerson (Ref 23) and Nurick et al (Ref 13). These data are not as extensive as for the like impinging doublet and therefore some judgment was required in defining both the laminar/turbulent expressions as well as the jet development impact. The resulting equations which best fit all of these data are:

Fuel Side

for Re < 10000

$$-.766$$

$$D_m - 29000 \ V_f^{0.766} \ P_f^{-0.65} \ D_f^{0.293} \ P_D^{0.165} \ (d_o/d_f)^{0.023} \ FP \qquad (23)$$

fuel orifice hydrolic diameter

for Re >= 10000

$$D_m - 34400 \ V_f^{-0.16} \ V_o^{-0.82} \ d_f^{0.27} \ d_o^{0.023} \ (\rho_f/\rho_o)^{0.41} \ FP \qquad (24)$$

Oxidizer Side

for Re < 10000

$$D_m - 27200 \ V_o^{-0.57} \ P_o^{-0.3} \ d_o \ P_D^{-0.25} \ (d_o/d_f)^{-0.17} \ FP \qquad (25)$$

for Re >= 10000

$$D_m - 36600 \ V_o^{-0.41} \ V_f^{-0.64} \ d_o^{0.4} \ d_f^{-0.2} \ (\rho_o/\rho_f)^{0.32} \ FP \qquad (26)$$

It should be noted that these equations require further verification before they can be used with complete certainty. It is recommended that the user include other unlike doublet equations for comparison of prediction with the above expressions. Since the laser diagnostics systems can not currently discriminate between two fluids, it is possible that additional wax measurements can be made to better define unlike doublet atomization characteristics.

Unlike Triplet - The triplet element is the least studied of the liquid/liquid elements. The atomization equations available are very limited in the range of parameters tested and should, at this time, be used with extreme caution. The equations included in DROPMIX are:

Fuel Side

$$D_m - 10400 \ d_f^{0.68} \ d_o^{-0.35} \ V_f^{-0.575} \ FP \qquad (27)$$

Oxidizer Side

$$D_m - 10400 \ d_o^{0.68} \ d_f^{-0.35} \ V_o^{-0.575} \ FP \qquad (28)$$

The user should utilize any other equation available or hot fire data to verify the predictions before general use of the above equations.

Unlike Pentad - The pentad element has been studied more extensively than the other unlike impinging elements although additional data would be welcomed for verification of prediction. The equations utilized for this element are:

Fuel Side

$$D_m - 160000 \ d_f^{0.68} \ d_o^{-0.35} \ V_o^{-0.57} \ V_f^{-0.56} \ FP \qquad (29)$$

Oxidizer Side

$$D_m - 36000 \ d_f^{0.1} \ d_o^{0.12} \ V_o \ \widehat{(-0.08)} V_f^{-0.89} \ FP \quad (30)$$

Secondary Atomization

The secondary atomization correlations are also based on wax measurements; however, these correlations are lacking in several key physical process descriptions. For example, the correlations are only in terms of input/output parameters correlated against the maximum gas velocity achieved in the test chamber. Application of the secondary breakup equation requires selection of a "maximum" gas velocity for breakup and, further, that all of the breakup occurs in less that 2 inches from the injection plane. The latter assumption appears to be experimentally verified. For small space engines having chamber lengths of 1 to 4 inches, the exact location/or conditions producing secondary breakup are required. The selection of the maximum gas velocity is also critical to the degree of secondary breakup achieved. However, insufficient data are available to discern whether this velocity should be that consistent with the maximum delta-V between the droplet and gas, that occurring in the chamber at the start of convergence, or that at the nozzle throat. Another complication is that in cold flow tests vaporization of the droplet does not occur. Consequently, the only parameter impacting breakup is the dynamic interaction. However, in the combustion chamber the dropsize is changing due to both dynamics and vaporization.

Inspection of the secondary breakup characteristics shown in Ref. 25, suggests that the secondary dropsize decreases rapidly as the gas velocity is increased and then reaches a minimum dropsize. The gas velocity corresponding to this minimum dropsize is reasonably small (i.e. about 300 ft/sec) suggesting that for normal large engines with contraction ratios in the range of 2 to 3, secondary breakup will occur quickly and reach the minimum secondary dropsize consistent with the initial primary dropsize. DROPMIX currently utilizes the gas velocity at the start of convergence (i.e assuming complete vaporization) which assures that the minimum secondary dropsize is always attained. An option is also included that allows for "short" chamber lengths (i.e.less than about 6 inches), for secondary atomization to occur in two steps, first in the chamber and secondly in the nozzle where the maximum gas velocity at the throat is used for the second breakup calculation. To be physically realistic in cases where breakup can occur in two steps, PCDER should be run to the start of convergence then the breakup expression applied to the remaining spray before proceeding into the convergence section of the nozzle. For small space engines where the total length to the throat is about 2 inches or less secondary breakup is applied in one step using the nozzle throat velocity as the maximum gas velocity in the secondary breakup expressions.

Two different breakup equations are included in DROPMIX. The first correlation is for the coaxial element and the other for all other elements. The shear coaxial element secondary droplet breakup characteristics, developed by Falk (Ref 24) are shown in Figure 10. The resulting best fit equation of the correlation line is given below:

$$D_s / D_p - 0.2314 + 0.3185 \ S - 0.0461 \ S^2 + 0.0016 \ S^3 \quad (31)$$

$$where \quad S - \ln[(D_p / 110)^3 \ ABS \ (V_g - V_f)] \quad (32)$$

The secondary breakup equation for the other elements is that of Zajac (Ref 25):

$$for \ -1 \leq \Delta V / V_f \leq 1.25$$

$$'_s - D_m [1 - 1.77 \times 10^{-3} \ D_m \ \Delta V / V_f \ e^{(-0.24 \ \Delta V / V_f, | \Delta V / V_f |)}] \quad (33)$$

$$for \ \Delta V / V_f > 1.25$$

$$+ 2.678 \text{ to be continuous at } \Delta V / V_f = 1.25$$

$$D_s - \tau \ D_m [1 - 1.52 \times 10^{-3} \ D_m] - 12 \ \ln(\Delta V / V_f) \quad (34)$$

MANIFOLD/ORIFICE DISCHARGE COEFFICIENT

The manifold/orifice discharge coefficient can vary significantly from one design to another. For most impinging element injectors the propellant enters the manifold either: (1) directly at the rear of the injector, is diffused into a dome like manifold then distributed to the individual element orifices via axial step drilled passages, or (2) into a ring manifold surrounding the injector diameter, then fed directly into radial step drilled passages to the individual element orifices. In general these element orifice inlets are sharp edged, with relatively short L/D's (i.e. 2 to 5). It should be noted that the passages intersect the element orifices at some angle (i.e. 30 to 120 degrees are typical). For these types of designs the discharge coefficient at typical engine chamber pressures will vary from about 0.5 to 0.85 depending on the specific design conditions. Coaxial element designs are more complicated with control orifices or tangential slots at

452
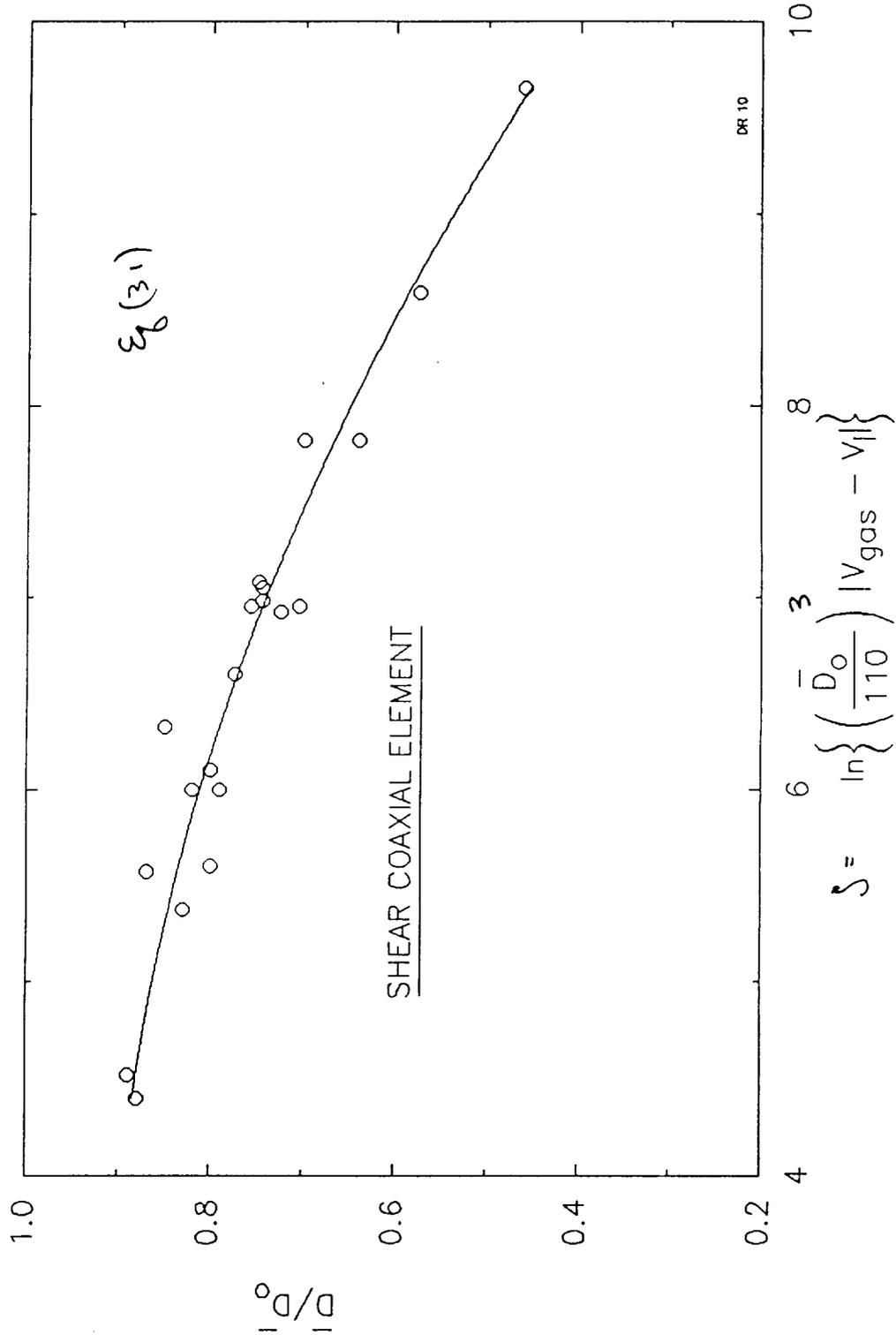
Fig. 10, Correlation of Droplet Breakup (Atomization) Data

$$\zeta = \ln\left\{\left(\left(\frac{\overline{D}_o}{110}\right)^3 |V_{gas} - V|\right)\right\}$$

SHEAR COAXIAL ELEMENT

$\overline{D}/\overline{D}_o$

DR 10

B-19

453

the liquid entrance to the central post as well as slots on the annulus of the gaseous outer sleeve. For these designs the overall discharge coefficient can range from 0.2 to 0.9. The myriad of possible designs makes incorporating a generalized manifold C_d routine impractical.

DROPMIX includes equations for calculating discharge coefficients for sharp edged orifices as a function of L/D and Reynolds Number, in addition to the liquid post and gaseous annulus discharge coefficient for coaxial elements. The manifold pressure drop is input by the user. The user also has the option to input any value of orifice discharge coefficient for his particular design.

The orifice discharge coefficient is defined from Figure 11, after Lichtarawitz (Ref 25) with the resulting equation:

$$Re_h = \frac{\rho \Delta V}{\mu} d$$

$$1/C_d = 1/C_{d_u} + 20/Re_h (1+2.25\ L_o/d) - 0.005\ L_o/d/A \quad (35)$$

$$\text{where } A = [1+7.5\ (\log(00015\ Re_h)^2\ ]$$

Note: (from B.E.

$$g\ d\,P = -\rho\ d\,V^2/2$$

$$\Delta V = [2\ g\,\delta ?/\rho]^{1/2}$$

$$\rho\,\Delta V = [2\,g/\,\Delta ?]^{1/2}$$

$$Re_h = [2\ g\ \rho\ \Delta P\ ]^{0.5}\ d/\mu \quad (36)$$

$$\text{for } 2 \le L_o/d \le 10\ ;\ 10 \le Re_h \le 20{,}000 \quad \Big\}\ \text{see Figure 11}$$

$$C_{d_u} = 0.827 - 0.0085\ L_o/d \quad (37)$$

For Re > 2x104, C_d is equal to C_{du}. This equation is limited to L_o/d of 2 or greater. Calculations of C_d from Equation 31 have been verified against data taken with typical injector designs.

The procedure for determination of discharge coefficient for coaxial elements is also included in DROPMIX.

ANALYSIS PROCEDURE

The above equations are programed into an analysis procedure which can be used to define the "optimum" design, off-optimum design, or simply predict the mixing quality and dropsize for an existing or proposed injector design. An overall flow diagram for DROPMIX is provided in Figure 12.

The initial calculation defines the "optimum" injector design for the given input requirements (i.e. element type, propellant, engine operating conditions, and overall mixing quality). In this initial calculation the minimum delta-p is set at 20% of chamber pressure based on chug stability criteria. The other propellant delta-p is defined from optimum mixing requirements. The number of elements per square inch of injector face area is determined from the mixing quality limit selected. The injector can include film cooling or outer zone mixture ratio bias. Currently the interaction of the outer boundary flow with the core flow, to determine the overall mixing quality as well as the mean gas temperature near the wall, is defined by the % interaction. Once the mixing quality, distribution, and element sizes are determined, the resulting primary and secondary dropsizes are specified for an optimum element design.

After the initial calculational procedure is completed then the user can change a number of variables sequentially to either investigate the impact of the changes on mixing and atomization or to represent an actual injector design. The variables that can be changed are:

- o C_d
- o Element Type
- o Mixing Level
- o Delta-p
- o Thrust/Element
- o Chamber Gas Velocity
- o BLC Parameters

When the user is satisfied with the specifications, an output is requested. A Typical output is given in Table 1. Note that in addition to the input specifications, all injector design parameters, dimensions, and dropsizes are also given. Of particular interest for input into PCDER are the values of secondary dropsize and the mixing parameter "n" defined in Equation 3. In the event that boundary layer cooling or mixture ratio bias is included in the design, then the various mixture ratios and mass fraction in the boundary layer are also required inputs to PCDER.

MODEL FIDELITY

A verification of the ability of the DROPMIX Engineering Analysis program to adequately predict the injector mixing quality and atomization was accomplished by utilizing the DROPMIX output as input into PCDER, calculating the energy release efficiency then comparing the predictions against actual engine data. To be thorough, flight as well as research engines were analyzed. The results are described below. Currently, small space engines have not been analyzed in sufficient detail to verify the fidelity of the formulation for this

454
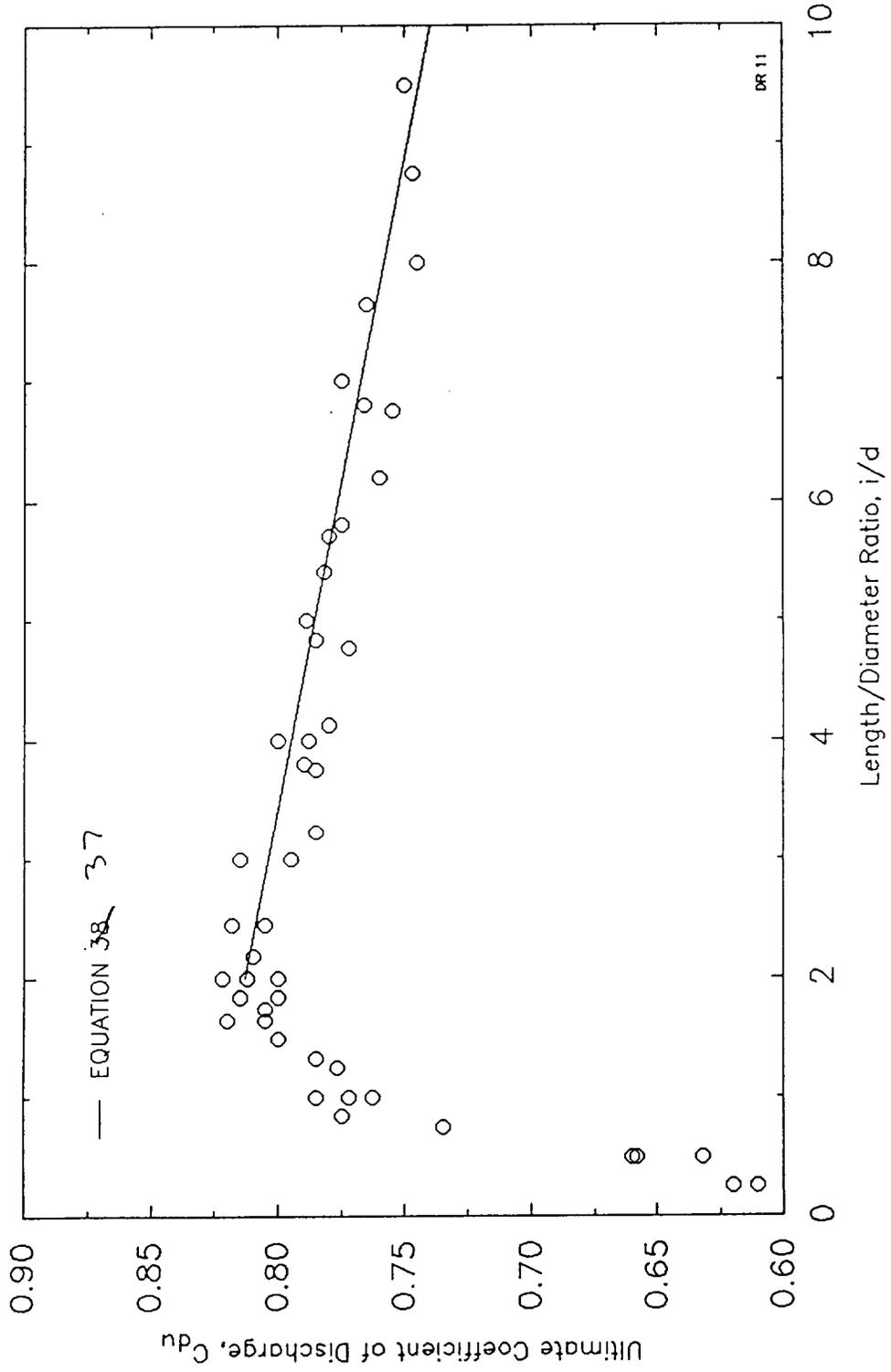
Fig. 11, Variation of the Ultimate Value of Discharge Coefficient with Length/Diameter Ratio.

455

B—21

INPUT
· ELEMENT TYPE
· ENGINE DESIGN/OPERATING CONDITIONS
· PROPELLANTS
· OVERALL MIXING REQUIREMENTS

BOUNDRY LAYER LAYER COOLING

SPECIFICATION
STABILITY
DELTA – P LIMITS

MIXING ANALYSIS

ATOMOZATION ANALYSIS
· PRIMARY
· SECONDARY

INJECTOR DESIGN BASED ON OPTIMUM CRITERIA

NON-OPTIMUM INJECTOR DESIGN
SPECIFY:
· ELEMENT TYPE
· MIXING LEVEL
· DELTA – P
· THRUST/ELEMENT
· CHAMBER GAS VELOCITY
· BLC PARAMETERS

INJECTOR SPECIFICATIONS
ELEMENT TYPE:
NUMBER OF ELEMENTS:
BOUNDRY LEYER COOLANT ELEMENT:
OVERALL ERA:
ORIFICE DIAMETER:
DELTA – P's:
MASS/MIXTURE RATIO DISTRIBUTION:
INJECTION VELOCITY:
PRIMARY DROPSIZE:
SECONDARY DROPSIZE:

FIG. 12 DROPMIX FLOW SCHEMATIC

class of engines. It is planned that this will be accomplished in the next year.

FLIGHT ENGINES

Several large launch flight vehicle main engines were analyzed to compare measured performance with that predicted by entering DROPMIX specifications into PCDER. The engines analyzed are:

o J-2 (LOX/H$_2$)
o J-2S (LOX/H$_2$)
o SSME (LOX/H$_2$)
o F-1 (LOX/RP-1)

In each case the injector and thrust chamber design as well as operating conditions were obtained and input into DROPMIX to define both the mixing uniformity and liquid propellant dropsize. The output from dropmix was then input into PCDER and overall mixing efficiency determined. For the LOX/H$_2$ engines all injector designs were shear concentric tube elements. The LOX/RP-1 engine utilized like-impinging doublet elements. The analysis for all of these injectors revealed that vaporization was virtually complete within the combustion chamber requiring that the resulting performance is that defined by mixing. The results of the analysis are presented in Table 2. Note that in all cases the predicted C* performance is within 1% of that measured. These comparisons provide only a partial verification of DROPMIX since vaporization was complete or nearly complete in all cases. These comparisons, however do provide some confidence in the ability of the DROPMIX model to adequately predict mixing limited efficiency.

RESEARCH ENGINES

Several research injector/thrust chamber assemblies were evaluated wherein both mixing and vaporization, limited the C* performance. Those evaluated include:

o MSFC (LOX/ CH$_4$)
o Aerojet (LOX/RP-1)
o Rocketdyne (NTO/50-50)
o Rocketdyne (LOX/RP-1)
o Rocketdyne (LOX/RP-1/CH$_4$)

MSFC LOX/CH$_4$ Study

The NASA-MSFC LOX/CH$_4$ TCA design evaluated utilized several shear concentric tube injectors, described in detail in Ref 27. Tests were conducted over a range of about 2 to 4 in mixture ratio and 1200 to 2400 psia in chamber pressure. For these injector/ thrust chamber designs DROPMIX/PCDER predicted 100% vaporization efficiency, as in the flight engines discussed above. It should be noted, however that these test engines utilized a different fuel propellant. Consequently, as for the flight engines these predictions are based only on the mixing limit as impacted by element design, mixture ratio, and chamber pressure. The results are shown in Figure 13. Note that the comparison between measured and predicted C* are in general excellent. Also note that the two points that do not compare within 1/2 % are clearly inconsistent with the other measured C* efficiencies and are therefore suspect.

Aerojet LOX/RP-1 Study

A detailed cold flow/hot fire test program was conducted at Aerojet, Ref 28, as part of the Advanced Launch System Advanced Development Program studies. In these studies both unlike impinging triplet and like impinging doublet injectors were tested. Tests were conducted over a wide range in chamber length (8 to 20 inches). Mixture ratio, and chamber pressure variations were relatively small. In the analysis the actual cold flow measured mixing uniformities (i.e. Em) were input to DROPMIX. A comparison of the predicted and measured performance are provided in Figure 14. Note that the predictions are within 1% of the measured values. Also note that the C* predictions with chamber length virtually match the hot fire measured values suggesting that the vaporization formulation in PCDER is technically acceptable.

Rocketdyne NTO/50-50 Study

This study (Ref. 30) conducted in 1967 tested a number of like doublet, unlike doublet and pentad elements firing NTO/50-50 propellants at 5000 LBf. Tests were conducted at 300 psia chamber pressure and chamber lengths (L') of between about 4 and 16 inches. For the unlike impinging elements, blowapart was experienced which makes that data unacceptable for analysis. The analysis was therefore limited to the like impinging elements. It should be noted that blowapart criteria has been developed and can be included in Dropmix.

Both six element and 100 element configurations were tested. Three configurations of the six element injector were studied which were identical except that the element fan-to-fan spacing was varied from zero (i.e. in-line) to 0.35 inch fan spacing between adjacent fuel and oxidizer fans. The 100 element configuration was designed with zero fan spacing.

The six element injectors were tested with chamber to throat lengths (L') of 4.57, 9.57, 13.97, and 19.97 inches. A comparison between the predicted and measured C* performance is given in Figure 15. Note the excellent agreement for all the data except for the two lowest performance values (i.e. about 65% C*). Based

TABLE 1, TYPICAL DROPMIX OUTPUT.

ENGINE SPECIFICATIONS

CHAMBER PRESSURE, psia	1974
SEA LEVEL THRUST, lb	26313
MIXTURE RATIO	3.52
OXIDIZER FLOWRATE, lb/sec	68.78
FUEL FLOWRATE, lb/sec	19.54
THROAT DIAMETER, in	3.31
CHAMBER DIAMETER, in	5.66
CHAMBER GAS VELOCITY, ft/sec	881
CHAMBER GAS DENSITY, lb/ft3	0.57
SPECIFIC HEAT	1.24

SPRAY SPECIFICATION

LOX:

VELOCITY, ft/sec	133
PRIM. DROPSIZE, micron	94
SEC. DROPSIZE, micron	77

FUEL:

VELOCITY, ft/sec	614
PRIM. DROPSIZE, micron	0
SEC. DROPSIZE, micron	0

MIXING EFFICIENCY, %	98.73
DISTRIBUTION FACTOR	6.5008

M/MR DISTRIBUTION

MMR	MMF
2.156	0.0058
2.341	0.0248
2.549	0.0656
2.786	0.1187
3.059	0.1598
3.374	0.1706
3.745	0.1519
4.186	0.1173
4.720	0.0806
5.380	0.0502
6.216	0.0285
7.309	0.0147
8.799	0.0068
10.951	0.0027

INJECTOR SPECIFICATIONS

ELEMENT TYPE: COAXIAL LIQUID/GAS	
NUMBER OF ELEMENTS	82
THRUST PER ELEMENT, lb	321
OVERALL MIXING, %	90
SINGLE ELEMENT MIXING, %	51.9

LOX:

POST WALL THICKNESS, in	0.035
POST ID, in	0.134
POST OD, in	0.204
POST RECESS/DL	1.00
Cd	0.47
DELTA-P, lb/in2	560

FUEL:

GAP, in	0.010
Cd	0.7
DELTA-P, lb/in2	684

PROPELLANT SPECIFICATIONS

PROPELLANT COMBINATION: LOX/CH4

OXIDIZER:

TEMPERATURE. F	-249
DENSITY, lb/ft3	64.78
VISCOSITY, cp	0.12

FUEL:

TEMPERATURE, F	24
DENSITY, lb/ft3	8.24
VISCOSITY, cp	GAS

458

TABLE 2, COMPARISON OF DROPMIX C* PREDICTION VS. FULL SCALE ENGINE MEASURED C*.

	J-2	J2S	SSME
DROPMIX PREDICTIONS			
Dropsize ~ μ	174	167	115
$\eta \ c^*_{mixing} \sim \%$	97.8	99.4	99.7
$\eta \ c^*_{vaporization} \sim \%$	100	100	100
$\eta \ c^*_{delivered} \sim \%$	97.8	99.4	99.7
ENGINE MEASURED			
$\eta \ c^*_{delivered} \sim \%$	98	99	99.6

459
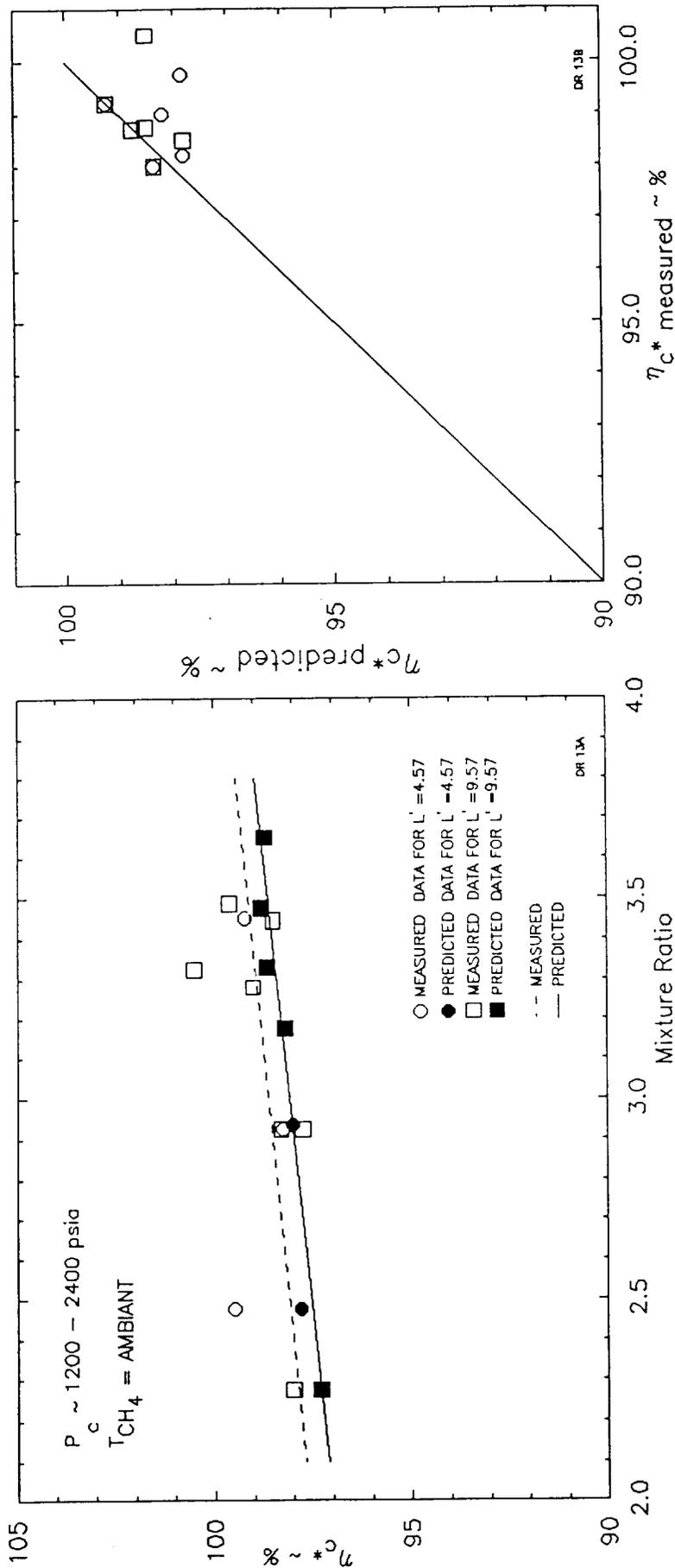
Fig. 13, Comparison of Measured and Predicted c^* Efficiency for Two Configuration of Concentr Tube Injectors Firing Lox/CH_4 Propellants (NASA-MSFC)

on the DROPMIX predictions, except for these two tests, all of the measured input values compare. For the two low performance tests a comparison between delta-p and flowrate was not obtained, suggesting that there is some inconsistency between the measured input data. This overall comparison is extremely encouraging since performance varied from 90% down to 65% resulting in an excellent check on the ability of DROPMIX to handle both mixing and vaporization limited combustion, as well as the validity of the mixing and atomization correlations (i.e. for like impinging doublets).

The 100 element injector was tested at only two chamber to throat lengths, 9.57 and 4.57 inches. Only the results of the 9.57 inch testing is presented since the data at 4.57 did not provide a reasonable check on the validity of the input data. Note that for the 9.57 inch chamber, the predicted and measured C* performance also check within 1%.

Rocketdyne LOX/RP-1 Study

During this study (Ref. 31) a total of five different injector designs were tested. Of these only the 16 element O-F-O triplet and 60 element circumferential fan like doublet injectors could be evaluated using built-in DROPMIX mixing correlations. The other designs utilized element designs and configurations not currently included in the program. It should be noted that, since dropsize correlations for most of the configurations are included, predictions could have been made if single element mixing experiments had been accomplished. The nominal test conditions are 2000 psia and L' of 19 inches.

The results for the triplet and like doublet are shown in Figure 16. Note that there are two data points for each injector. The open symbol are test results from earlier nominal 2 second steady state run testing and the solid symbol from a half second steady state. The like impinging doublet injector test results were nearly the same for both test series while there was a substantial difference between the two runs for the triplet injector. A reasonable explanation for this difference is not known at this time. Additional tests using the same hardware obtained in another study will be analyzed to determine consistence of the test results.

Rocketdyne LOX/RP-1/CH$_4$ Study

This study (Ref. 32) utilized two propellant combinations (LOX/RP-1,CH$_4$) at chamber pressures of 2000 psia, chamber diameter of 3.5 inches and L' of 19 inches. Only the LOX/CH$_4$ results will be discussed in this paper, however, it is planned that the LOX/RP-1 tests results will be analyzed at a later date. The LOX/CH$_4$ injector was a 58 element concentric tube injector. Three configurations of this basic injector were utilized: (1) uniform elements; (2) mixture ratio bias of the outer ring of elements and; (3) uniform injector elements with film cooling injected at the beginning of convergence. The mixture ratio bias configuration can not be analyzed at this time since DROPMIX can not currently handle two separate distributions.

A comparison of the predicted and measured test results are shown in Figure 17. Note that both the baseline and film cooling results compare reasonably well with the predictions.

<div align="center">CONCLUSIONS</div>

The results are encouraging in that the basic engineering formulation appears to be a reasonably good description of the mixing and atomization processes. While comparisons have been made using a wide range in engine designs, injector thrust/elements, and propellant combinations, not all of the element type correlations have been verified. As noted in the body of this paper, many of the correlations are lacking in an extensive data base and processes such as secondary breakup need further development. A need also exists to demonstrate the ability of the model to adequately predict mixing/atomization characteristics for small engine applications.

The Air Force Astronautics Laboratory is currently planning to conduct an extensive cold flow study in their new cold flow facility at the Astronautics Laboratory. The facility is capable of pressurized atmospheres of up to 2000 psia, and is equipped to measure both mixing uniformity and atomization. An additional study of secondary breakup is also planned. The correlations developed from these studies will be incorporated into DROPMIX and should provide most of the needed data. A large part of the study will also concentrate on developing manifold design criteria to ensure that these impacts can be accounted for in DROPMIX.

Lastly, the program has been loaned to several users in an effort to obtain independent checkout of the predictions. Feedback has been favorable, but application has been limited to large engines.

461
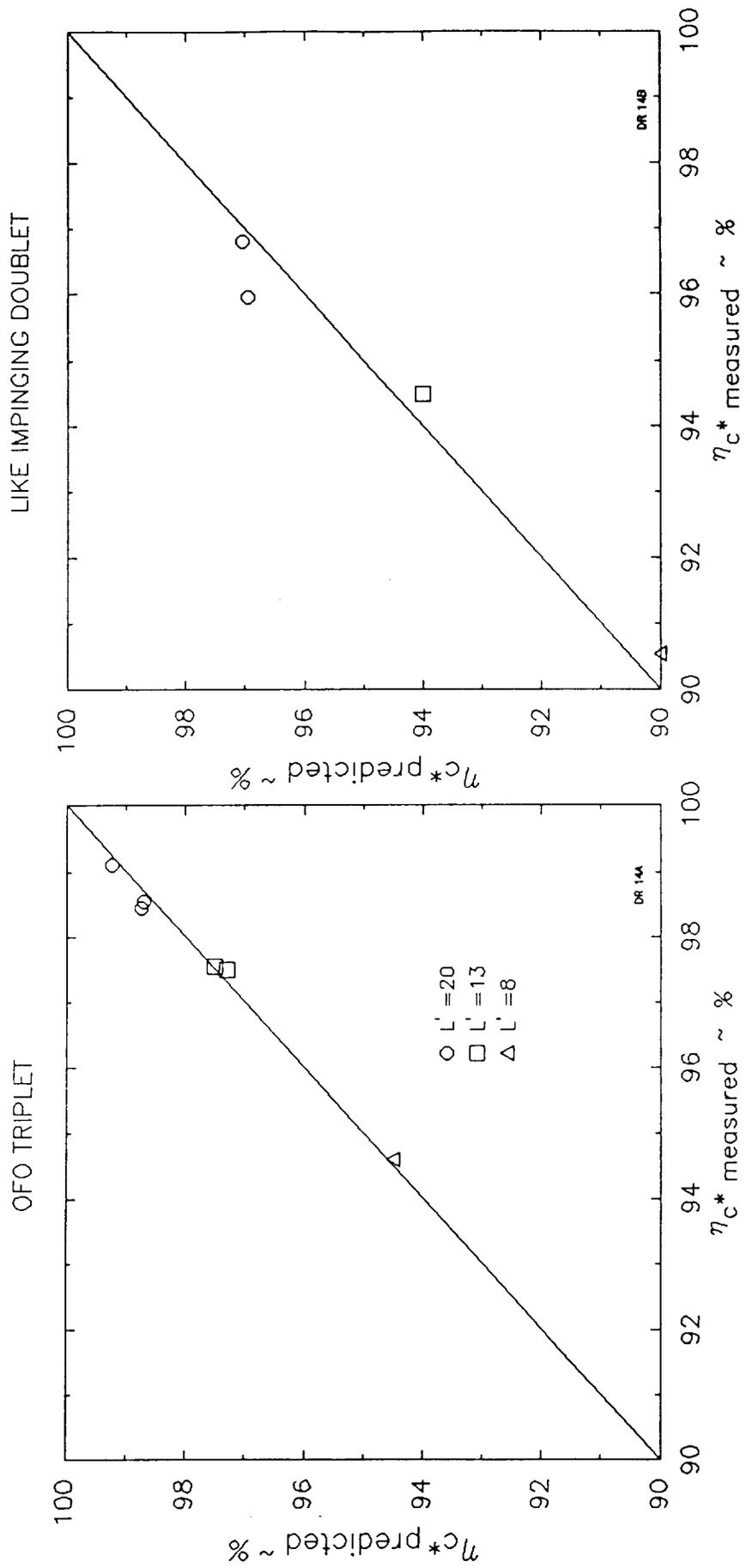
Fig. 14, Comparison of Aerojet Data vs. Dropmix/PCDER Prediction.
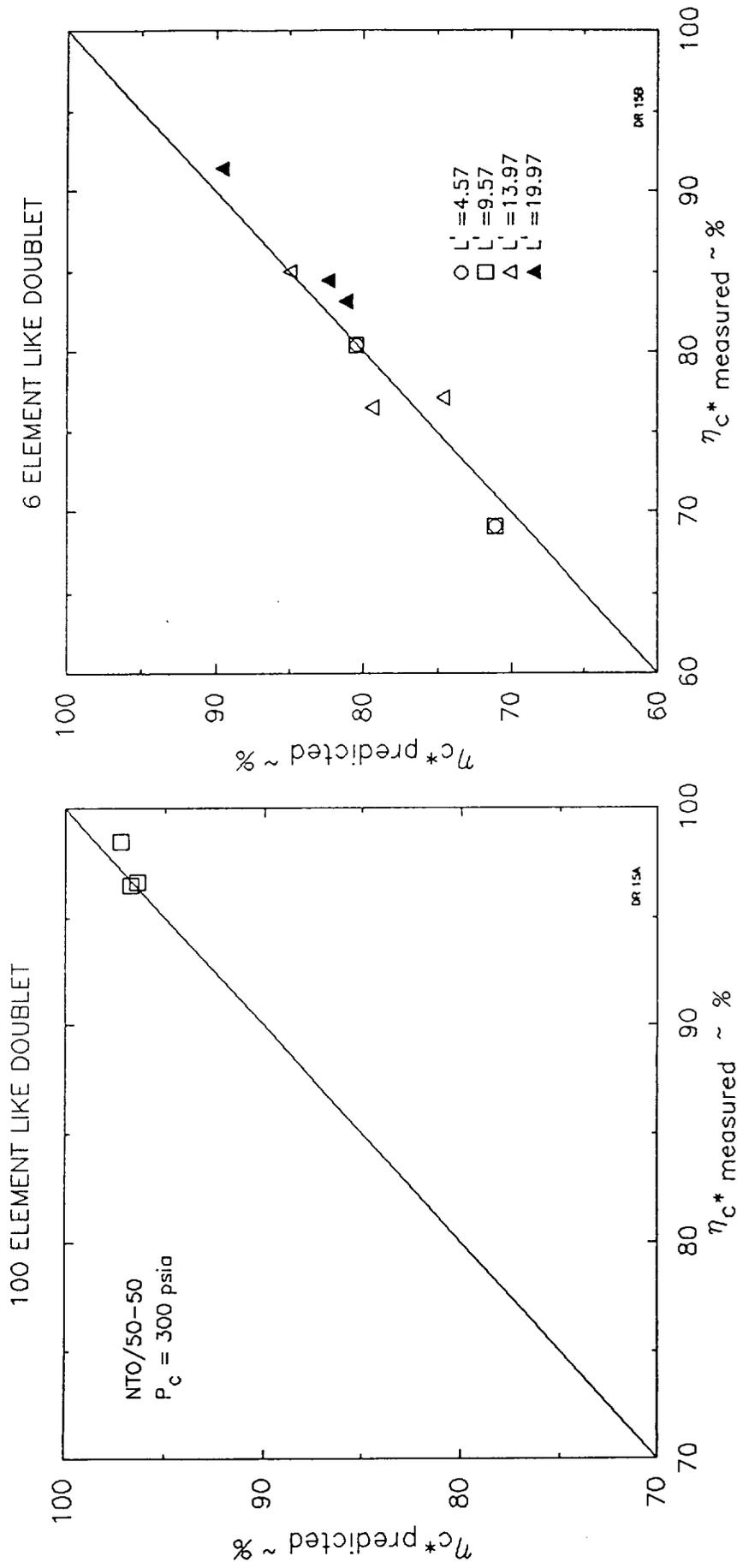
Fig. 15, Comparison of Rocketdyne Research Engine Data vs. Dropmix/PCDER Prediction.
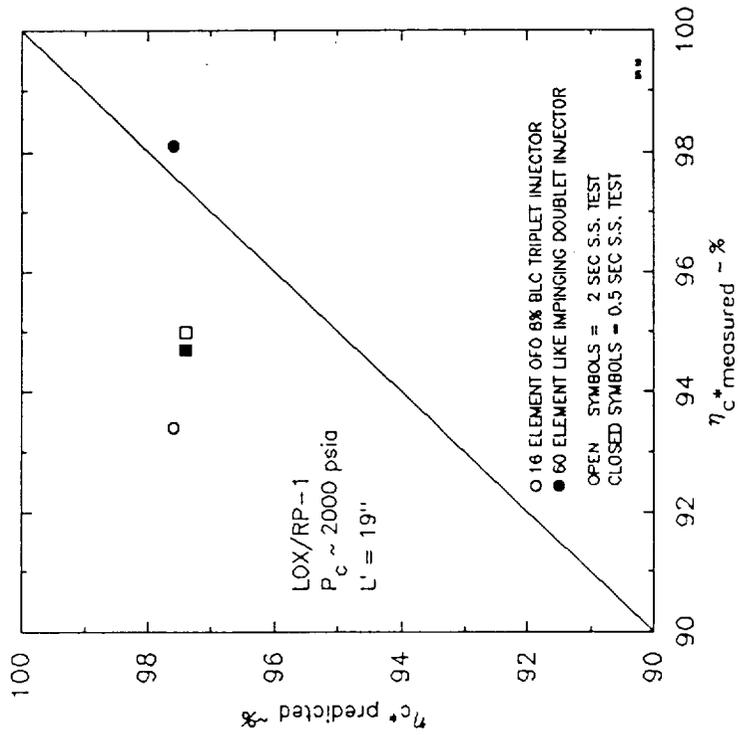
Fig. 16, Comparison of Predicted and Measured c* Efficiency for two Different Element Types. (Rocketdyne)
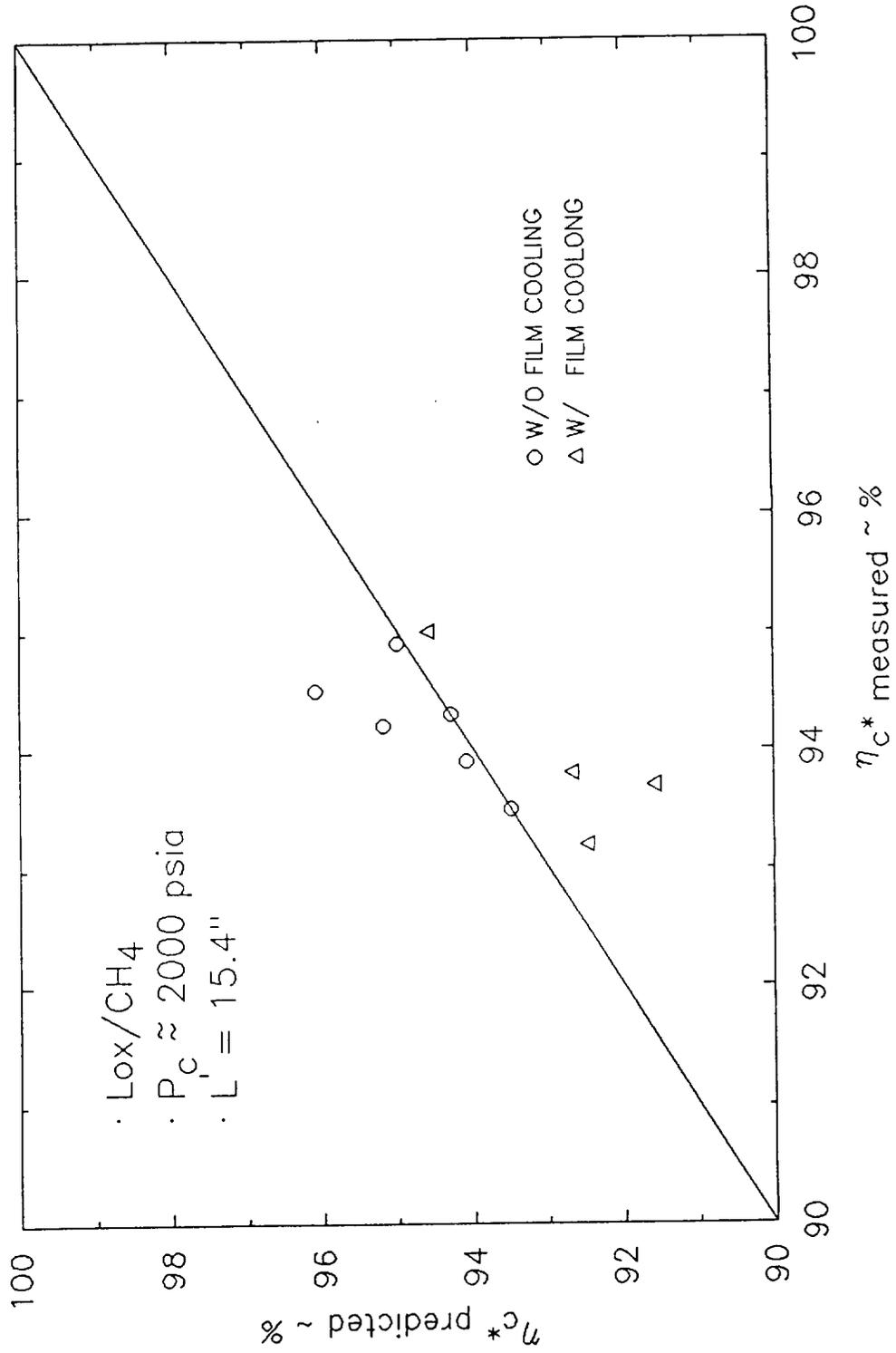
Fig. 17, Comparison of Measured and Predicted c* Efficiency for a 58 Element Concentric Tube Injector. (Rocketdyne)

B-31

465

NOMENCLATURE

A	= Orifice Area
b	= constant (0.693)
c^*	= C-Star
C_d	= Discharge Coefficient
CMF	= Cumulative Mass Fraction
d	= Orifice Diameter
D	= Dropsize
E_m	= Overall Mixing Uniformity Defined in EQ. 1
E_{mo}	= Single Element Mixing Uniformity
FP	= Physical Property Correction defined in EQ. 16
L	= Length
L'	= Distance from Injector Face to the Throat
MF	= Mass Fraction
MR	= Mixture Ratio (W_o/W_f)
N	= Number of Fuel or Oxidizer Orifices in Element
P_D	= Dynamic Pressure Ratio
P_j	= Velocity Profile Correction Factor - Ratio of Centerline to Mean Dynamic Pressure
ΔP	= Orifice Pressure Drop
r	= MR/(1+MR), Local Value
R	= MR/(1+MR), Injected Value
Recess	= Oxidizer Post Setback from Fuel S
Re	= Reynolds Number
V	= Velocity
W	= Flow Rate

Fan Spacing → Spacing Between Adjacent Fuel and Oxidizer Edges

Fan Cant Angle → Total Induced Angle Between Adjacent Fans relative to the Injector Face

Greek

α	= Orifice Element Impingement Half Angle
η_{mix}	= Mixing Limited c^* Efficiency
μ	= Viscosity
ρ	= Density
σ	= Surface Tension

Subscripts

c	= Chamber
co	= Primary with Zero Gas Velocity
f	= Fuel
g	= Gas
H	= Hydraulic
inn	= Inner
j	= Jet
l	= Liquid
m	= Mass Mean
max	= Maximum Value
o	= Oxidizer
out	= Outer

466

p   = Primary
r   = Relative
s   = Secondary
t   = Theoretical
TC   = Total Core

REFERENCES

1. Rupe, J. H., The Liquid Phase Mixing of a Pair of Impinging Streams, Progress Report No. 20-195, JPL, Pasadena CA, Aug, 1953

2. Rupe, J. H., A correlation Between the Dynamic Properties of a Pair of Impinging Streams and the Uniformity of Mixture-ratio Distribution in the Resulting Spray, Progress Report No. 20-209, JPL, Pasadena, CA, Mar, 1956

3. Clayton, R. M., et al, An Experimental Correlation of the Nonreactive Properties of Injection Schemes and Combustion Effects in a Liquid-Propellant Rocket Engine: Part II, Technical Report No. 32-255, JPL, Pasadena, CA., 1965

4. Elverum, G. W. Jr., and Morey, T. F., Criteria for Optimum Mixture-Ratio Distribution Using Several Types of Impinging-Stream Injector Elements, Memo No 30-5, JPL, Pasadena, CA, Feb, 1959

5. Dickerson, R., Tate, K. and Nurick, W., Correlation of Spray Injector Parameters with Rocket Engine Performance, Rocketdyne, a Div of Rockwell Inter., AFRPL-TR-68-11, Jan, 1968

6. Valentine, R., Dean, L, and Pieper, J., An Improved Method for Rocket Performance Prediction, (Aerojet-General Corp., Sacramento, CA), J. Spacecraft, V3, No9, Sept 1966

7. Nurick, W., and Clapp, S., An Experimental Technique for Measurement of Injector Spray Mixing, J. spacecraft, V6, No11, Nov 1969

8. Dickerson, R., Turbulent Jets, Simplified Correlation of Velocity and Composition Profiles, Rocketdyne Internal Letter CT 73-32, October 1973

9. Burick, R., Space Storable Propellant Performance-Coaxial Injector Characterization, Final Report NASA CR120936, Rocketdyne, Canoga Park, CA, June 1968

10. Falk, A., Space Storable Propellant Performance-Gas/Liquid Like-Doublet Injector Characterization, Final report, NASA CR-120935, Rocketdyne, Canoga Park, CA, Oct., 1972

11. Dodson, H., Cold-Flow Predicted Mixing Efficiency of the Flat Fan (Broadside) Impinging Like Doublets, Internal Memo., IL 8121-5082, Rocketdyne, Oct. 1968

12. Arbit, H., Cold Flow Tests of Single-element Self-Impinging Doublet Injector, Internal Memo., PS 68-340-13, Rocketdyne, April 1968

13. Nurick, W., and McHale, M., Phase I: Analytical and Experimental Study of Non-circular Injector Orifices, and Elements for Liquid/Liquid Injectors, Rocketdyne, NASA CR-108570, Sept 1970

14. Ewen, R., Hydrogen Film/Conductive Cooling, Aerojet, Sacramento, CA, NASA CR-120926, Jan 1970

15. Falk, A., and Burick, R., Injector Design guidelines for Gas/Liquid Propellant Systems, Rocketdyne, NASA CR-120968, May 1973

16. Muss, J., LOX/HC Injector Characterization Program Subscale LOX/RP-1 Injector Performance and Stability Anchoring and Anchored Full Scale LOX/RP-1 Predictions, Engineering Analysis Report 9984:0101g, to be released, Contract F04611-85-C-0100

17. Lorenzetto, G., and Lefebvre, A., Measurements of Drop Size on a Plain Jet Airblast Atomizer, AIAAJ., V15, No7, 1977

18. Zajac., L., Correlation of Spray Dropsize Distribution and Injector Variables, Rocketdyne, R-8455, NASA Contract NAS7-726, Undated (1969-1970)

19. Nurick, W., Physical Property Effect on Spray Atomization, Rocketdyne IR&D, ITR-73-014-C, Sept 1973

20. Zajac, L., Droplet Breakup in Accelerating Gas Flows Part I: Primary Atomization, Rocketdyne, NASA CR-134478, Oct 1973

21. VanKleeck, J., Oxygen/Hydrocarbon Injector Characterization, Cold Flow Test Report, Prepared by Aerojet Techsystems Company for AFAL, Contract Fo4611-85-C-0100, Nov 1988

22. Hauptman, J., Spray Characteristics of Like-On-Like Doublet Impinging Rocket Injectors, Presented at 29th

Aerospace Sciences Meeting, Reno, Nevada, Paper No. 91-0687, Jan 7-10, 1991.

23. Nurick, W., Dickerson, R. and Clapp, S., Correlation of Injector Spray Parameters With Rocket Engine Performance, Presented at 10th Liquid Propulsion Symposium, Las Vegas, Nev., Nov 1968

24. Falk, A., Coaxial Spray Atomization in Accelerating Gas Stream, Rocketdyne, NASA CR-134825, June 1975

25. Zajac, L., Droplet Breakup in Accelerating Gas Flows Part II: Secondary Atomization, Rocketdyne, NASA CR-134479, Oct 1973

26. Lichtarowicz, A., Duggins, R., and Markland, E., Discharge Coefficients for Incompressible Non-Cavitating Flow Through Long Orifices, Jour Mech Engr Sc, V7, No2, 1965

27. Bailey, R., Test Evaluation of Oxygen-Methane Main Injectors, JANNAF Propulsion Meeting, 1987

28. Oxygen/Hydrocarbon Injector Characterization, Monthly Report, Prepared by Aerojet Techsystems Company, for AFAL, Contract F04611-85-C-0100, February 1990

29. Nukiyama, S. and Tanasawa, Y., Experiments on the Atomization of Liquids in an Air Stream, Trans. Soc. of Mech. Engrs., Japan, V5, 1939

30. Dickerson, R., Tate, K., and Nurick, W., Correlation of Injector Parameters with Rocket Engine Performance, Special Technical Report, AFRPL-TR-68-11, Jan. 1968

31. LOX/Hydrocarbon Thrust Chamber Technology, Subtask 3-D Gas Side Heat Flux Study, LOX/RP-1, Subtask 3-E Supporting Technologies, LOX/RP-1, Task Report Prepared by Rocketdyne, Sept. 1990, to be Submitted to Air Force Astronautics Laboratory, Edwards Air Force Base, CA, Contract F04611-86-C-0088

32. LOX/Hydrocarbon Thrust Chamber Technology, Subtask 3-D (CH_4)/3-E (CH_4), Task Report Submitted to Air Force Astronautics Laboratory, Edwards Air Base, CA, July 1990, Contract F04611-86-C-00882

Software and Engineering Associates, Inc.

Title: Rocket Engine Injector Spray Mixing Quality

To: File

From: G. R. Nickerson and C. W. Johnson

Date: 5 February 1992

ABSTRACT

A method for predicting propellant spray drop size and mixture ratio distributions produced by rocket engine injectors is presented by Nurick in Reference 1. The method is empirical, and takes advantage of the fact that measurements of spray distributions obtained using both single element and multi-element injectors exhibit the same distribution whenever the measured mixing efficiency, E_m, is the same. The purpose of this memo is to discuss the properties of the distribution function used by Nurick to characterize the sprays. The relationship between the distribution function and the Rupe mixing efficiency, E_m, is also discussed. Charts of E_m as a function of the oxidizer fraction for the total propellant are presented for a series of shape factors.

Liquid Oxygen (LOX)/Hydrogen propulsion systems are normally operated at a mixture ratio of approximately one for fuel rich gas generators and pre-burners, and at a mixture ratio of approximately six for the main combustion chamber. For these operating conditions, charts are given that show both the mass density function, and the mass distribution function for a series of shape factors.

Ref. 1.   Nurick, W. H., "DROPMIX - A PC Based Program for Rocket Engine Injector Design," 27th JANNAF Combustion Meeting, Vol. II, pp 435-468, Cheyenne, WY, November 1990.

NOMENCLATURE

CMF	Cumulative Mass Fraction for the distribution. $\int_0^{cmf} dm = f(r)$
dm/dr	Mass Density function. $dm/dr = df(r)/dr$
E_m	Rupe mixing efficiency, see eqs (1) and (5)
f(r)	Mass Distribution function. $f(r) = \exp\left\{ \ln\frac{1}{2} \left[\frac{1-r}{1-R} \right]^n \right\}$
m	Cumulative Mass Fraction. $m = CMF$
m_1	Equivalent area displacement height, $r < R$. See Fig. 4
m_2	Equivalent area displacement height, $r > R$. See Fig. 4
MF_i	Fraction of mass measured in compartment i relative to the total mass measured. See eq. (1)
MR	Engine mixture ratio. $MR = R/(1 - R)$, $\qquad 0 \leq MR \leq \infty$
n	Shape factor exponent for f(r)
r	oxidizer fraction, $\qquad 0 \leq r \leq 1$
R	Engine over-all oxidizer fraction. $R = MR/(1 + MR)$, $\qquad 0 \leq R \leq 1$
r_{max} density	r value within the distribution where dm/dr is maximum, and where f(r) has inflection. See eq. (4)

Cold flow data is often available for rocket engine injectors so that data on injector/thrust chamber mixing efficiency is available. Typically, the simulants for the propellant oxidizer and fuel are flowed through the injector and collected downstream in a compartmentalized container. The oxidizer and fuel content of each compartment is determined, and a mixing efficiency, E_m, is calculated by the following formula:

$$E_m = 1 - \frac{1}{R} \sum_{\substack{i=1 \\ r_i < R}}^{N_1} MF_i(R - r_i) - \frac{1}{1-R} \sum_{\substack{j=1 \\ r_j > R}}^{N_2} MF_j(r_j - R) \tag{1}$$

where

R is the oxidizer fraction for the total flow

r_i is the oxidizer fraction for the ith compartment, and $r_i < R$

r_j is the oxidizer fraction for the jth compartment, and $r_j > R$

MF_i is the mass fraction found in compartment i

MF_j is the mass fraction found in compartment j

The total number of compartments is

$$N_T = N_1 + N_2$$

The mixing efficiency, E_m, given above is due to Rupe[2], and is known as "the Rupe mixing efficiency."

Ref. 2.   Rupe, J. H., "The Liquid Phase Mixing of a Pair of Impinging Streams," Progress Report No. 20-195, JPL, Pasadena, CA, August 1953.

The engine mixture ratio, MR, and engine oxidizer fraction, R, are related as

$$R = MR/(1 + MR) \qquad 0 \leq R \leq 1$$
$$MR = R/(1 - R) \qquad 0 \leq MR \leq \infty$$

The distribution function for the spray is an expression that gives cumulative mass fraction, m, as a function of oxidizer fraction, r. The distribution function, f(r), given by Nurick[1] contains two parameters, R and n, and is

$$\int_0^{CMF} dm = e^{[\ln \frac{1}{2}]} \left[\frac{1-r}{1-R} \right]^n = f(r) \tag{2}$$

The mass density function, (dm/dr), for this function is found as follows:

$$\int_0^r \left[\frac{dm}{dr} \right] dr = f(r)$$

$$d \int_0^r \left[\frac{dm}{dr} \right] dr = \left[\frac{dm}{dr} \right] dr = df(r)$$

$$\left[\frac{dm}{dr} \right] = \frac{df(r)}{dr}$$

and

$$\left[\frac{dm}{dr} \right] = \frac{-n \ln \frac{1}{2}}{1 - R} \left[\frac{1-r}{1-R} \right]^{n-1} f(r) \tag{3}$$

Example plots for equations (3) and (2) are shown in Figures 1 and 2, respectively. Note that for r=R, equation (2) gives a cumulative mass fraction (CMF) value of 1/2, i.e., in Figure 1 the area under the curve to the left of R=r is equal to the area under the curve to the right of R=r. Note also that Figure 2 has a total area of one. The distribution function is always greater than zero at r=0, equal to 1/2 at R=r, and equal to one at r=1 (all mass accounted for).

$$\left[\dfrac{dm}{dr}\right]$$
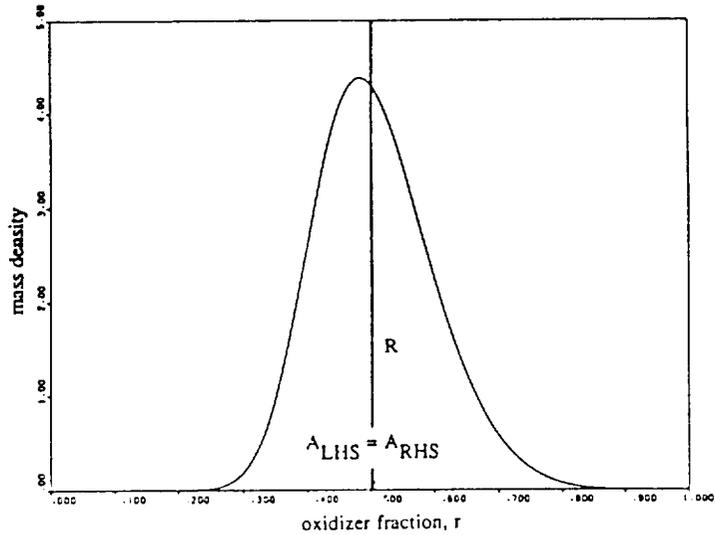
$$\dfrac{d\ CMF}{dr}$$

Figure 1. Mass Density Function, $(dm/dr) = - n \ln \tfrac{1}{2} (1-R)^{-n}(1-r)^{n-1}\ f(r)$
(In this example R =.5, and n = 6.22485)

$$m = \int_{0}^{r} \dfrac{dm}{dr}\ dr$$
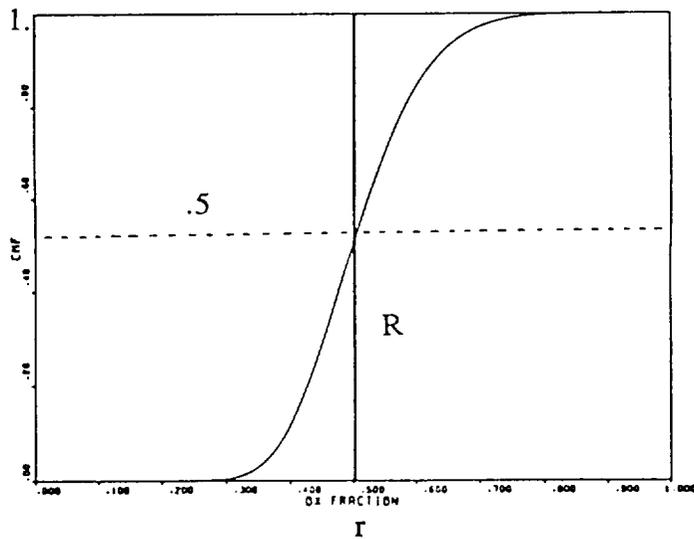
CMF

$$(r=R) \Rightarrow m=.5$$

Figure 2. Distribution Function, $m = f(r) = \int_{0}^{CMF} dm = \exp\left\{\ \ln \tfrac{1}{2}\left[\dfrac{1-r}{1-R}\right]^{n}\right\}$
(In this example R =.5, and n = 6.22485)

For the distribution function to have the characteristic "S" shape that is observed in spray distribution measurements, it is necessary that the mass density function have a maximum value on the interval $0 \leq r \leq 1$. The maximum are at

$$\frac{d^2 m}{d r^2} = 0$$

and it is found that

$$\left[\frac{dm}{dr} \right]_{max} \text{ is at}$$

$$r_{\substack{max \\ density}} = 1 - (1-R) \left[\frac{-1}{\ln \frac{1}{2}} \frac{n-1}{n} \right]^{1/n} \tag{4}$$

For this value to be real, it is required that n be greater than one. Equation (4) gives the inflection point seen in Figure 2. The inflection point occurs at $r = R$ only when $n \to \infty$ or at

$$n = 1/(1 + \ln \tfrac{1}{2}) = 3.25889$$

The minimum value for the inflection point is less than R, and only occurs when

$$(n - 1) \ln \left[\frac{-1}{\ln \frac{1}{2}} \frac{n-1}{n} \right] = 1$$

which is at

$$n = 6.22485$$

The corresponding maximum density value for r, is

$$\left[\begin{array}{c} r_{max} \\ density \end{array} \right]_{min} = \left[\begin{array}{c} r_{f(x)} \\ inflection \end{array} \right]_{min} = 1.03122R - .03122$$

As the mixing efficiency approaches unity, the areas A_1 and A_2 shown in Figure 3, below, approach zero.
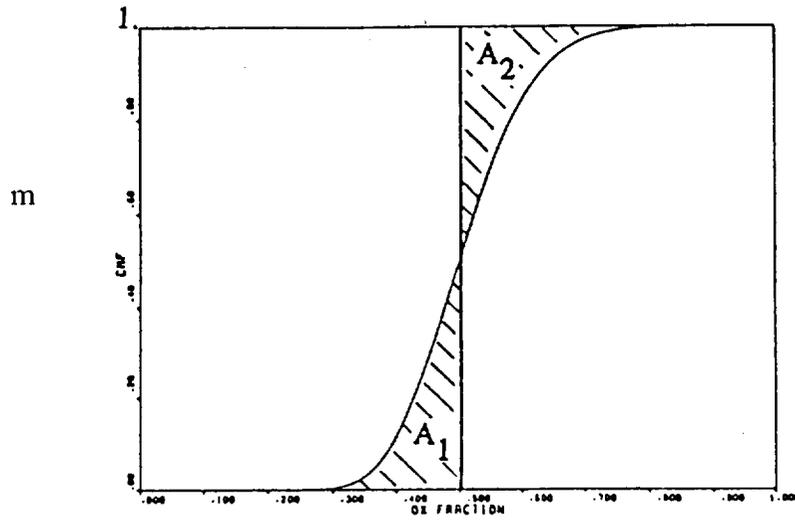

Figure 3. The Areas A_1 and A_2 that are Used to Indicate Mixing Efficiency

The hatched area shown in Figure 3 is

$$A = A_1 + A_2 = \int_0^R f(r)\, dr + \left[(1\text{-}R) - \int_R^1 f(r)\, dr \right]$$

The Rupe mixing efficiency, E_m, is defined in terms of the displacement heights, m_1 and m_2, as shown in Figure 4.
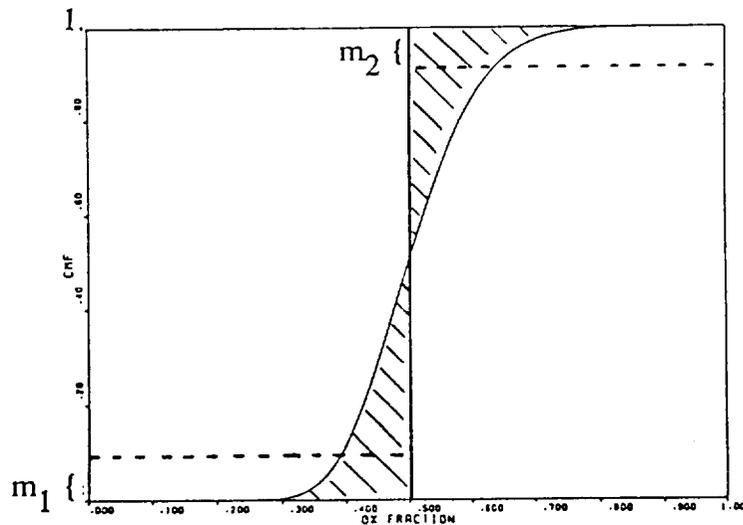

Figure 4. Displacement Heights, m_1 and m_2, Used to Define the Rupe Mixing Efficiency, i.e., $E_m = 1\text{-}m_1\text{-}m_2$

where

$$m_1 R = A_1 \quad \text{and} \quad m_2 (1-R) = A_2.$$

The geometric definition for E_m is

$$E_m \equiv 1 - m_1 - m_2$$

so that

$$E_m = 1 - \frac{A_1}{R} - \frac{A_2}{1-R}$$

$$A_1 \quad = \quad \int_0^R f(r)\, dr$$

$$A_2 \quad = \quad (1-R) - \int_R^1 f(r)\, dr$$

$$E_m \quad = \quad 1 - \frac{1}{R} \int_0^R f(r)\, dr - \frac{1}{1-R} \left[1 - R - \int_R^1 f(r)\, dr \right]$$

$$E_m \quad = \quad \frac{1}{1-R} \int_R^1 f(r)\, dr - \frac{1}{R} \int_0^R f(r)\, dr \tag{5}$$

The above expression is equivalent to equation (1) in the limit when an arbitrarily large number of samples are taken. It is also equivalent to equation (1) of Reference 1.

If the Rupe mixing efficiency, E_m, for a spray is known, then the spray distribution can be obtained using equation (5). This is done by setting $R = MR/(1+MR)$ and finding a value of n that satisfies equation (5). Once n is known, the spray distribution, f(r), given by equation (2) is known. Equation (5) is solved by numerically integrating f(r), and iterating values of n until the Right Hand Side equals E_m. Plots of E_m vs R for various values of n are presented in Figures 5 and 6. These charts can be used to conveniently estimate a value for n from given values of E_m and R.

The mass density function, eq. (3), is plotted in Figures 7 and 8 for a mixture ratio of one, i.e., R = 1/2 (typical of fuel rich O_2/H_2 gas generators). Figure 7 shows the function for values of n ≤ 8, and Figure 8 shows the function for values of n ≥ 8. The maximum curve for the function is also shown, as calculated by equation (4). Oxygen/Hydrogen systems are of primary interest, and for these systems the combustion chamber is usually operated at a mixture ratio of approximately six, i.e., R = .857. The mass density function for MR=6 is given in Figure 9 for values of n ≥ 8.

Figures 10, 11, and 12 show the distribution function, f(r), corresponding to Figures 7, 8, and 9, respectively.

As mentioned earlier, the mass distribution function, f(r), is always greater than zero at r=0, i.e.,

$$f(0) = CMF(0) = \exp \left\{ \ [\ln \tfrac{1}{2}] \ (1/(1-R))^n \ \right\}$$

In Figure 13, CMF(0) is plotted vs R for several values of n. Note that

$$\lim_{R \to 0} CMF(0) = 1/2.$$
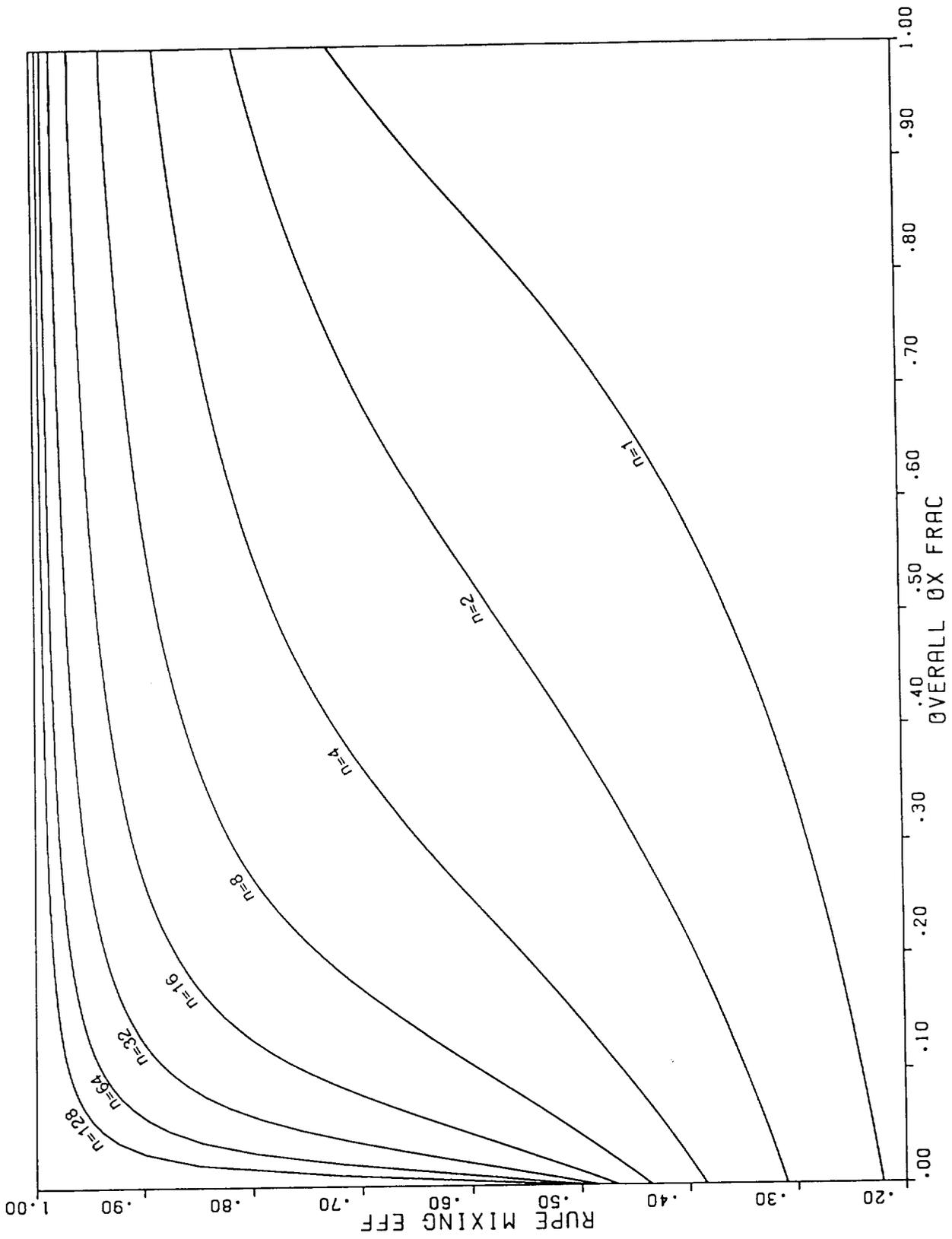
Figure 5. Rupe Mixing Efficiencies for Different Shape Factor Exponents (n).
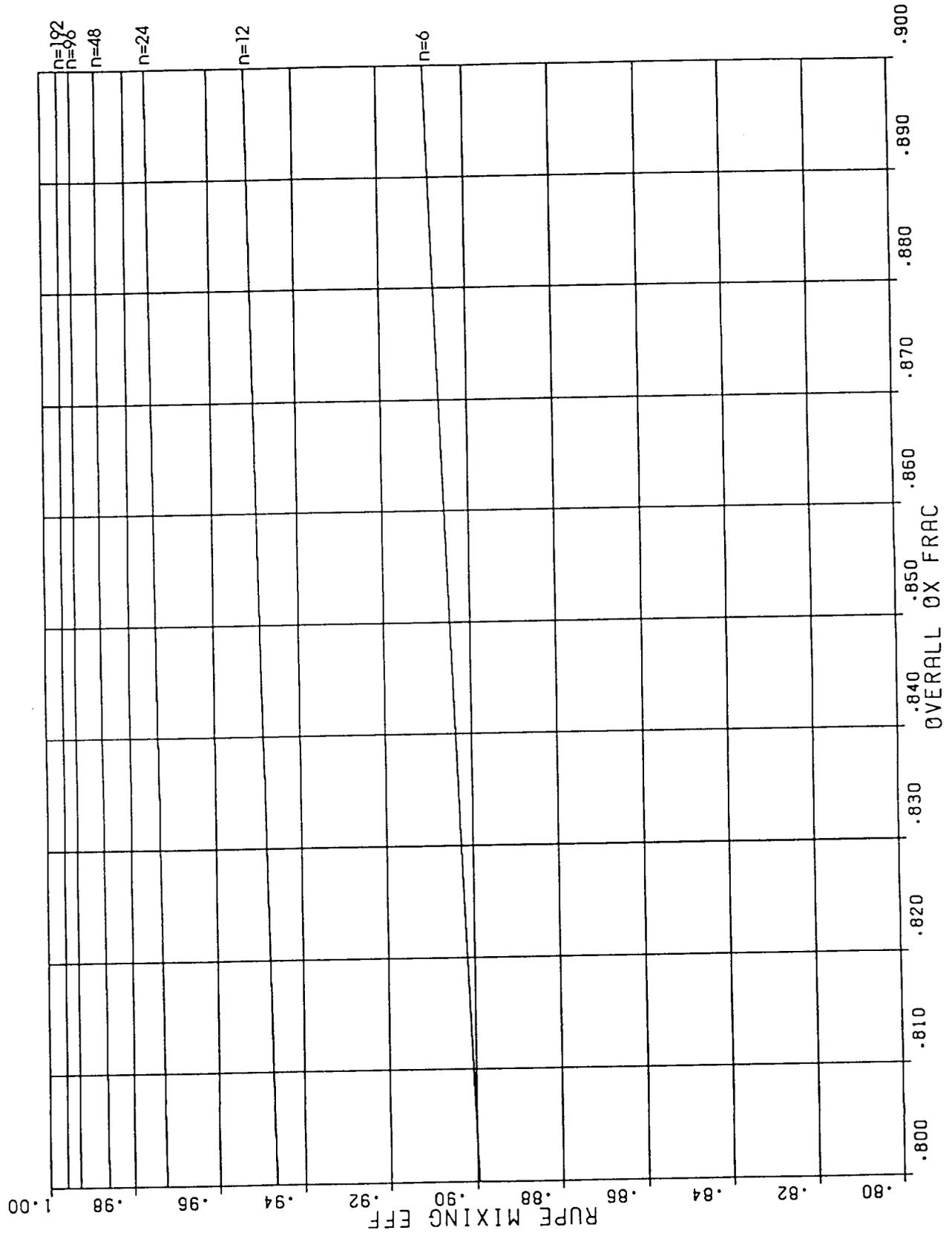
Figure 6. Rupe Mixing Efficiency for LOX/H2 Systems
.8<R<.9 and n=6,12, 24, 48, 96, 192
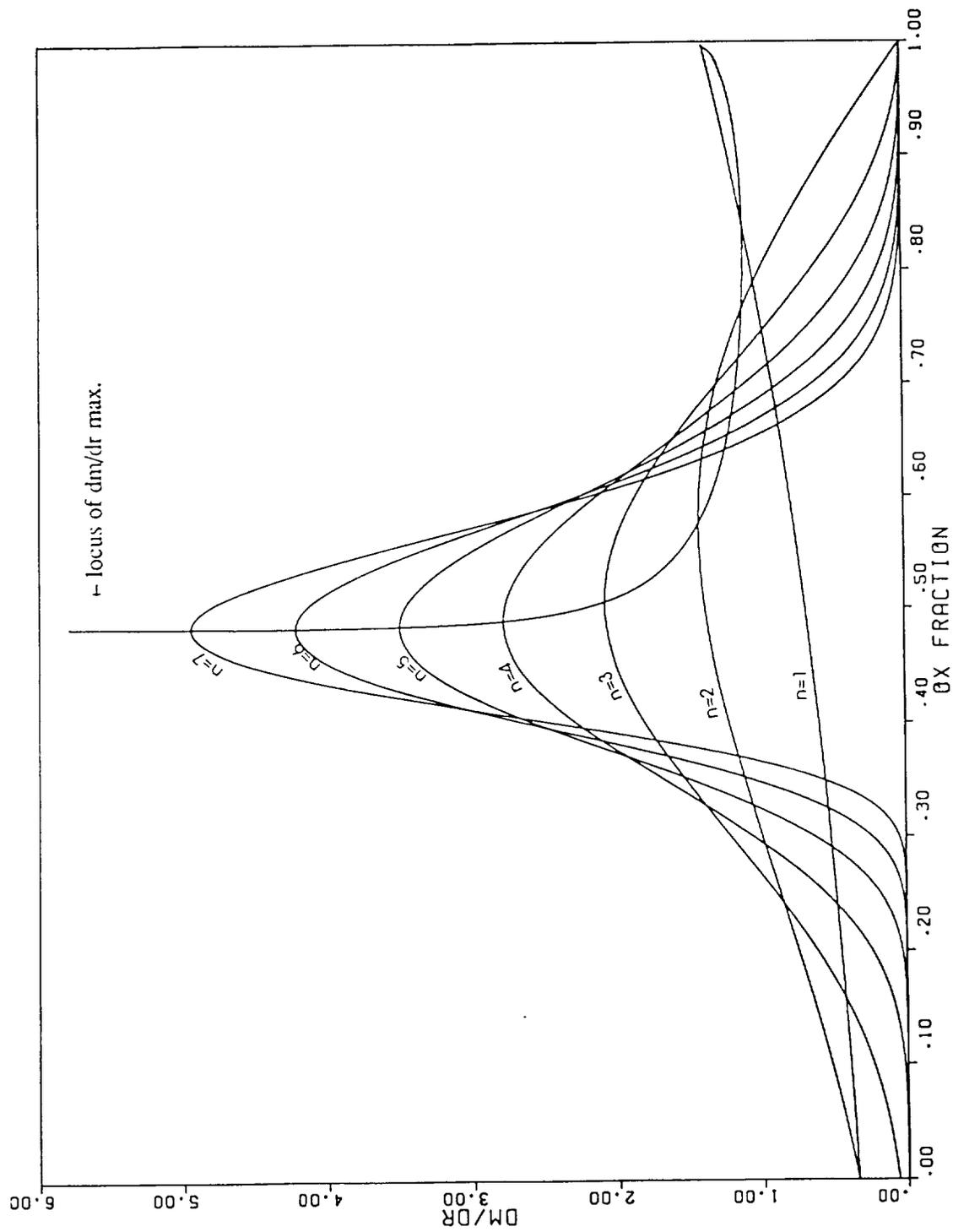
Figure 7. Mass Density Function vs r for n ≤ 7, R=0.5
(i.e. MR=1, typical of Fuel Rich LOX/H2
Gas Generators and Preburners)
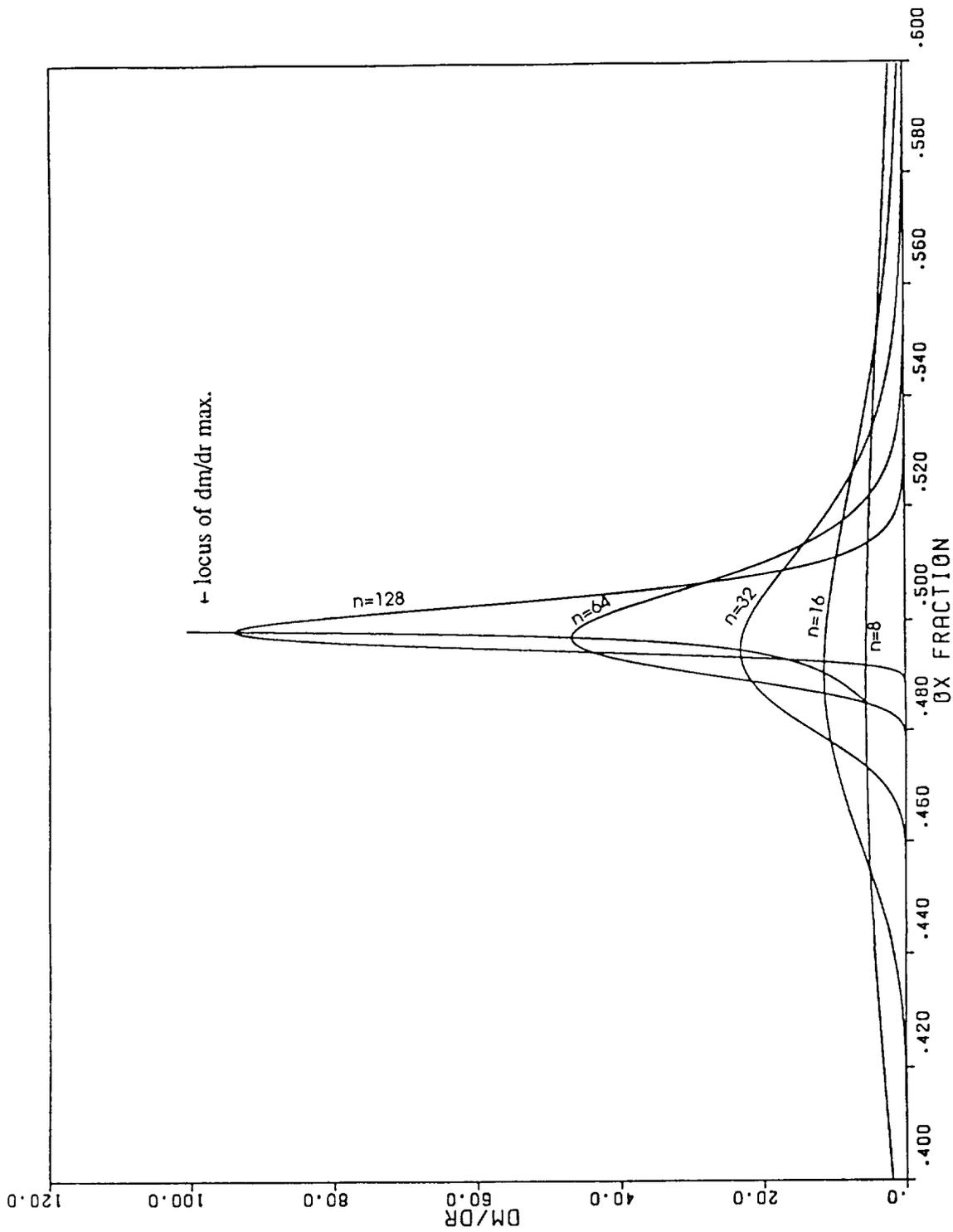
Figure 8. Mass Density Function vs r for n ≥ 8, R=0.5 (i.e. MR = 1, typical fo Fuel Rich LOX/H2 Gas Generators and Preburners)
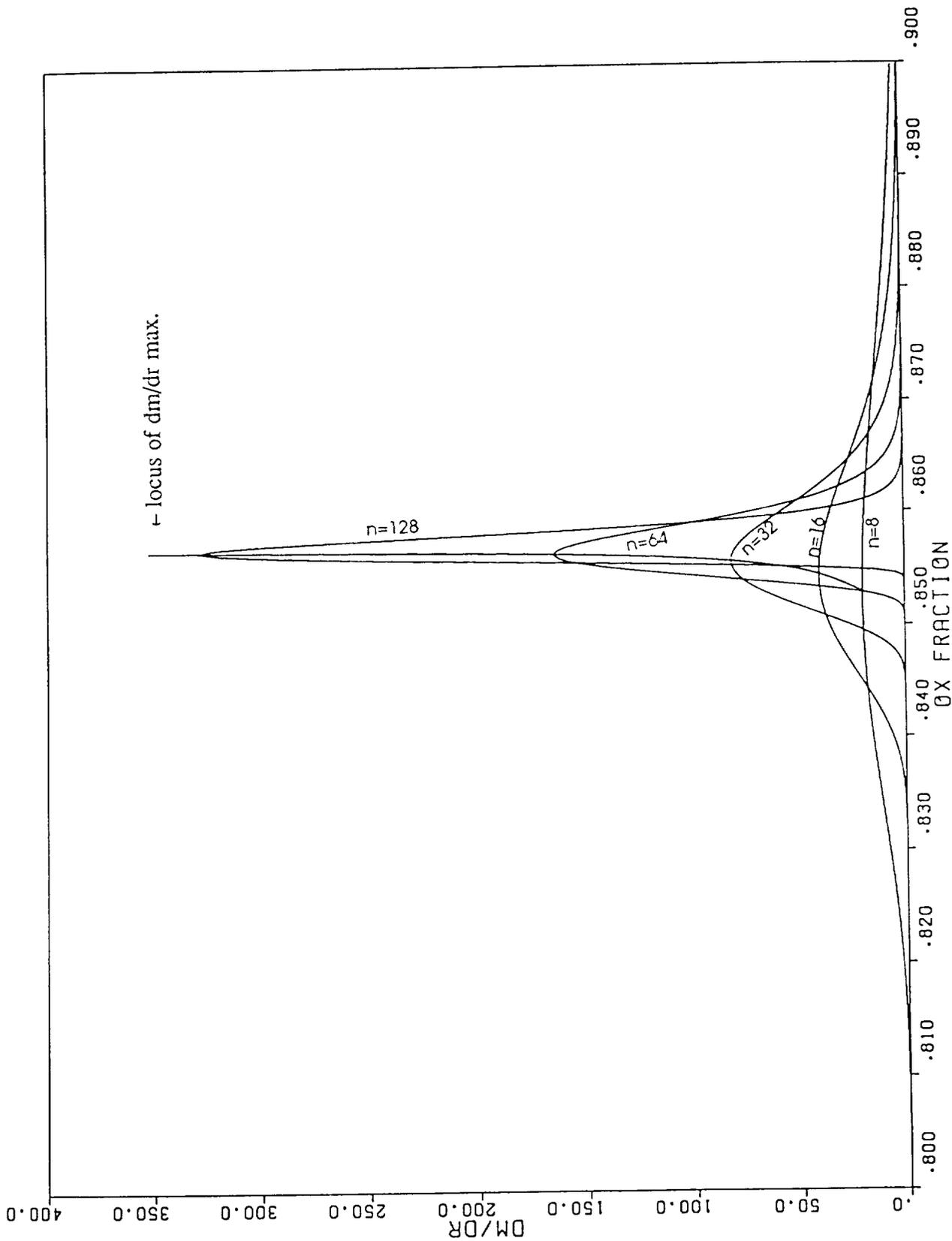
Figure 9. Mass Density Function vs r for n ≥ 8, R=0.857
(i.e. MR = 6, typical fo LOX/H2
Primary Combustion Chambers)
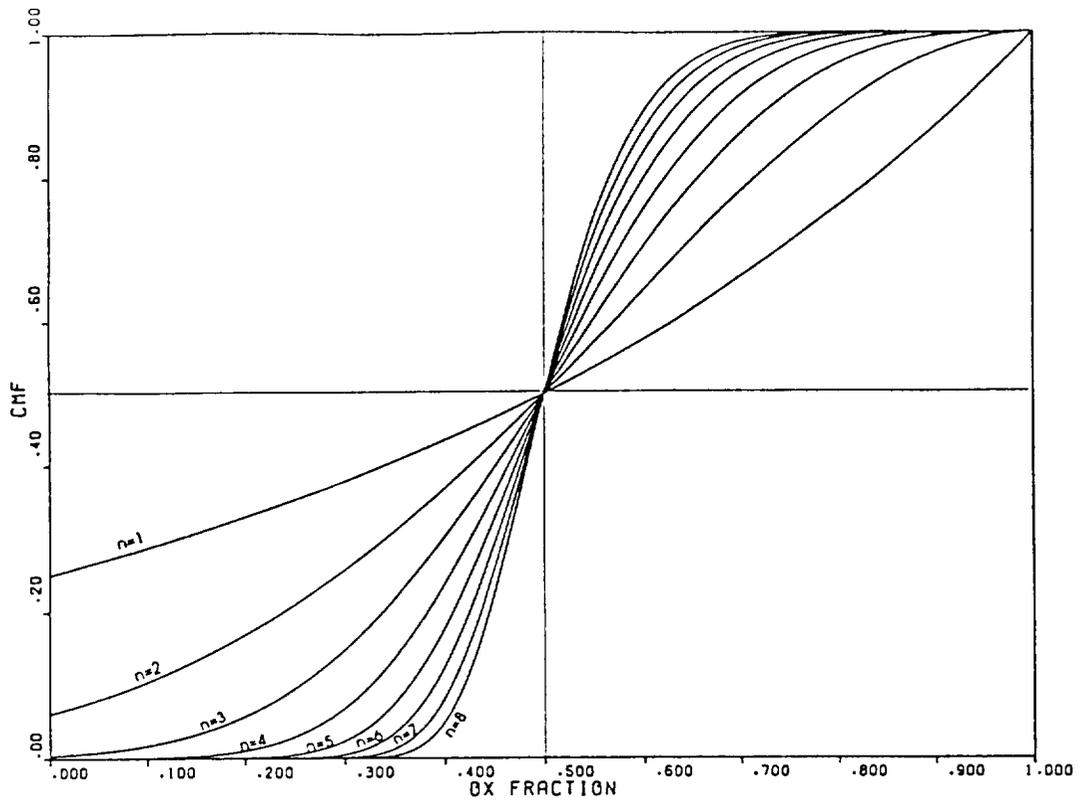
Figure 10. Mass Distribution Function vs r for n ≤ 8, R=0.5
(i.e. MR = 1, typical of Fuel Rich LOX/H2
Gas Generators and Preburners)
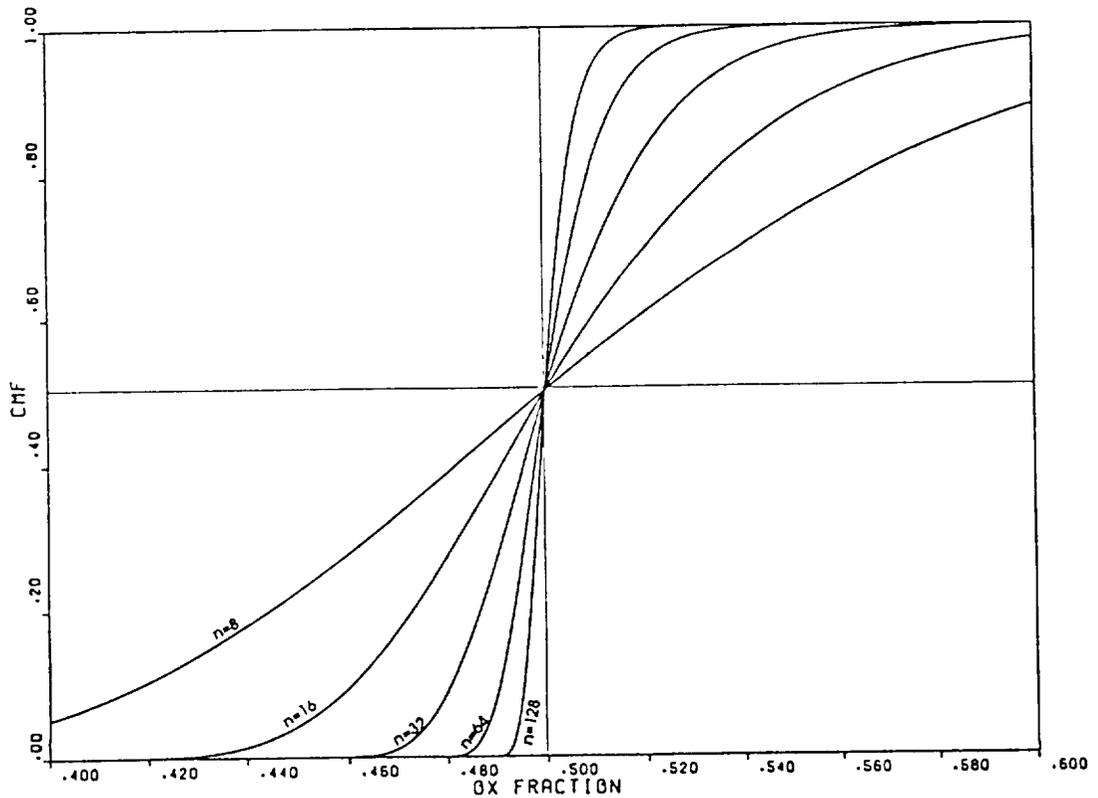
Figure 11. Mass Distribution Function vs r for n ≥ 8, R = 0.5
(i.e. MR = 1, typical of Fuel Rich LOX/H2
Gas Generators and Preburners)

C-15   C-2
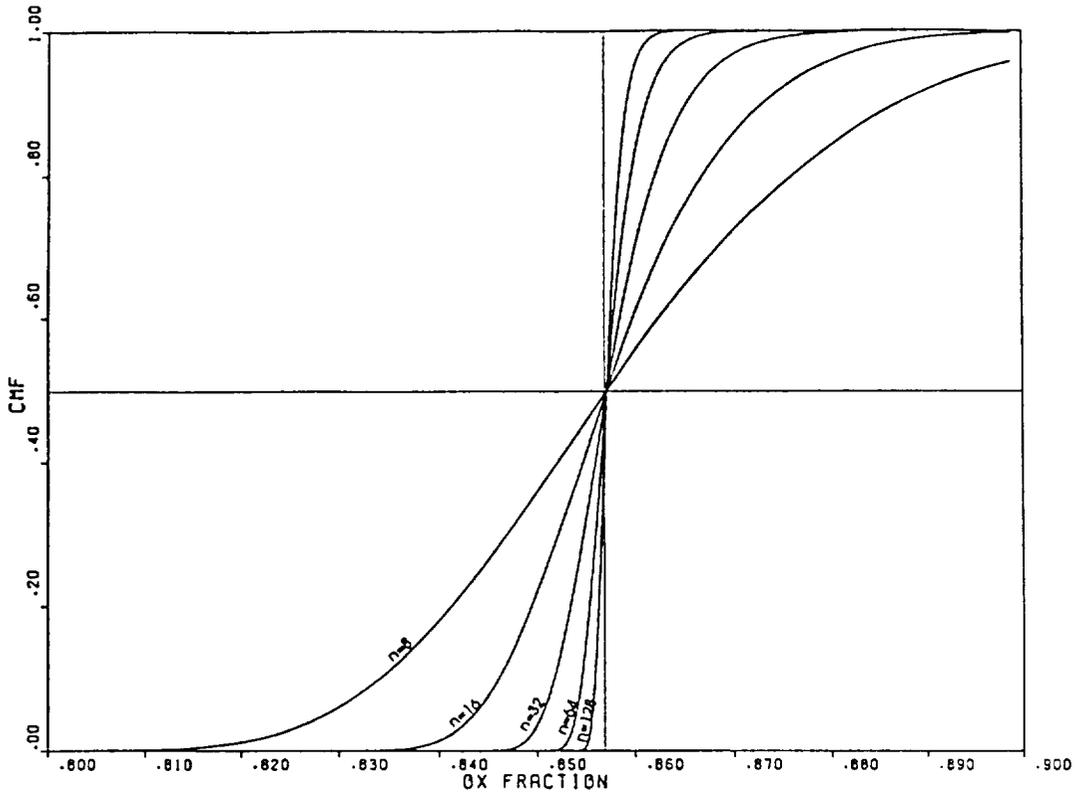
Figure 12. Mass Distribution Function vs r for n > 8, R=.857
(i.e. MR = 6, typical of LOX/H2
Primary Combustion Chambers)
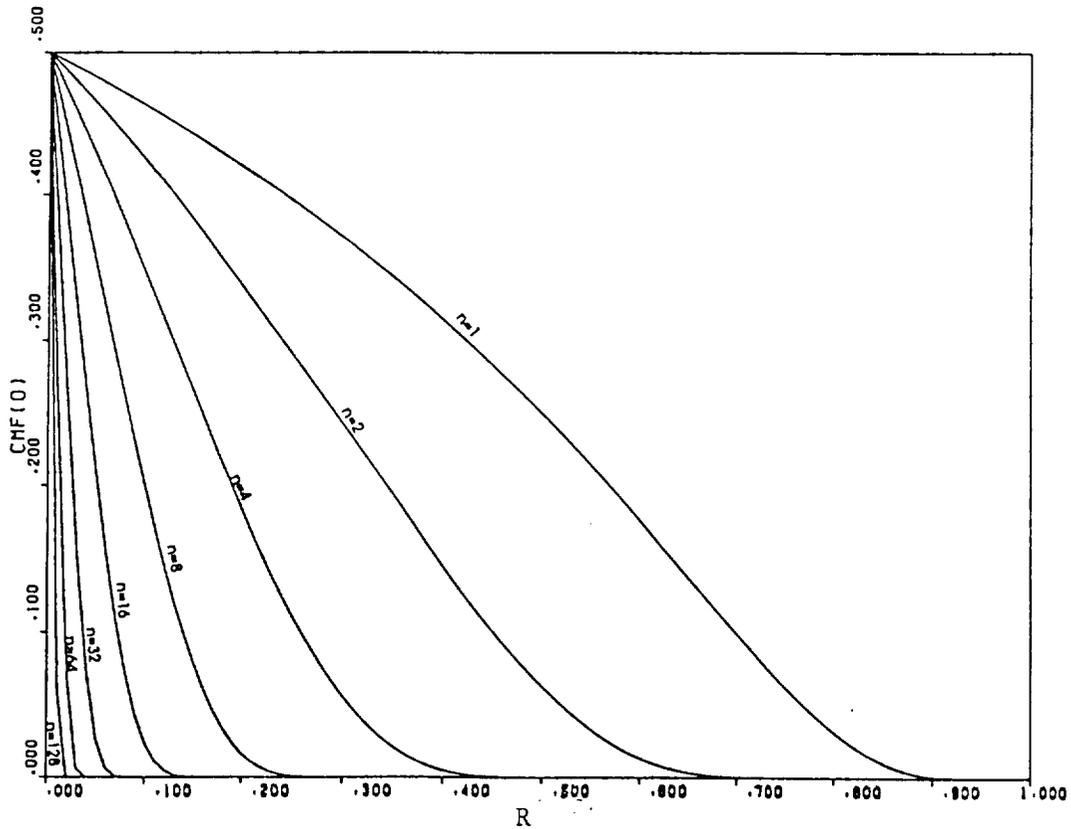
Figure 13. Cumulative Mass Fraction at the r = 0 Point vs R.

Report Documentation Page

NASA
National Aeronautics and
Space Administration

1. Report No.	2. Government Accession No.	3. Recipient's Catalog No.

4. Title and Subtitle	5. Report Date
Research Study Entitled "TDK/BLM/MABL Technical Support"	19 March 1993
	6. Performing Organization Code

7. Author(s)	8. Performing Organization Report No.
Stuart S. Dunn	
	10. Work Unit No.

9. Performing Organization Name and Address	11. Contract or Grant No.
Software & Engineering Associates, Inc. 1000 E. William Street, Suite 200 Carson City, NV 89701	NAS8-39048
	13. Type of Report and Period Covered

12. Sponsoring Agency Name and Address	Final
George C. Marshall Space Flight Center NASA Marshall Space Flight Center, AL 35812	14. Sponsoring Agency Code

15. Supplementary Notes

16. Abstract

The Two-Dimensional Kinetics (TDK) computer program is a large software package oriented to predict the performance of a liquid rocket thrust chamber. Many options are available for a variety of problems, and several boundary layer modules are coupled with the code. Substantial modifications to the program have been completed recently, and a rigorous documentation set has been prepared to use this analytical capability for the development of projected future engine designs.

The contemplated effort is directed to improve some prediction features, supporting associated design elements in the thrust chamber, to provide support for the code operation on different computer systems, and to resolve difficulties occurring during program execution.

17. Key Words (Suggested by Author(s))	18. Distribution Statement
TDK, Rocket Nozzle Performance, CFD, Chemical Kinetics	Unclassified-Unlimited

19. Security Classif. (of this report)	20. Security Classif. (of this page)	21. No. of pages	22. Price
Unclassified	Unclassified	98	

NASA FORM 1626 OCT 86

The last page of a report facing the third cover is the Report Documentation Page, RDP. Information presented on this page is used in announcing and cataloging reports as well as preparing the cover and title page. Thus it is important that the information be correct. Instructions for filling in each block of the form are as follows:

Block 1. Report No. NASA report series number, if preassigned

Block 2. Government Accession No. Leave blank.

Block 3. Recipient's Catalog No. Reserved for use by each report recipient.

Block 4. Title and Subtitle. Typed in caps and lower case with dash or period separating subtitle from title.

Block 5. Report Date. Approximate month and year the report will be published

Block 6. Performing Organization Code. Leave blank.

Block 7. Author(s). Provide full names exactly as they are to appear on the title page. If applicable, the word editor should follow a name.

Block 8. Performing Organization Report No. NASA installation report control number and, if desired, the non-NASA performing organization report control number.

Block 9. Performing Organization Name and Address. Provide affiliation (NASA program office, NASA installation, or contractor name) of authors.

Block 10. Work Unit No. Provide Research and Technology Objectives and Plans (RTOP) number.

Block 11. Contract or Grant No. Provide when applicable.

Block 12. Sponsoring Agency Name and Address. National Aeronautics and Space Administration, Washington, D.C. 20546-0001. If contractor report, add NASA installation or HQ program office.

Block 13. Type of Report and Period Covered. NASA formal report series; for Contractor Report also list type (interim, final) and period covered when applicable.

Block 14. Sponsoring Agency Code. Leave blank.

Block 15. Supplementary Notes. Information not included elsewhere; affiliation of authors if additional space is re-

quired for block 9; notice of work sponsored by another agency, monitor of contract, information about supplements (film, data tapes, etc.), meeting site and date for presented papers, journal to which an article has been submitted, note of a report made from a thesis, appendix by author other than shown in block 7.

Block 16. Abstract. The abstract should be informative rather than descriptive and should state the objectives of the investigation, the methods employed (e.g., simulation, experiment, or remote sensing), the results obtained, and the conclusions reached.

Block 17. Key Words. Identifying words or phrases to be used in cataloging the report.

Block 18. Distribution Statement. Indicate whether report is available to public or not. If not to be controlled, use "Unclassified-Unlimited." If controlled availability is required, list the category approved on the Document Availability Authorization Form (see NHB 2200.2, Form FF427). Also specify subject category (see "Table of Contents" in a current issue of STAR), in which report is to be distributed.

Block 19. Security Classification (of this report). Self-explanatory.

Block 20. Security Classification (of this page). Self-explanatory.

Block 21. No. of Pages. Count front matter pages beginning with iii, text pages including internal blank pages, and the RDP, but not the title page or the back of the title page.

Block 22. Price Code. If block 18 shows "Unclassified-Unlimited," provide the NTIS price code (see "NTIS Price Schedules" in a current issue of STAR) and at the bottom of the form add either "For sale by the National Technical Information Service, Springfield, VA 22161-2171" or "For sale by the Superintendent of Documents, U.S. Government Printing Office, Washington, DC 20402-0001," whichever is appropriate.